

EM Scattering from Perforated Films:
Transmission and Resonance

by

Aaron D. Jackson

Department of Mathematics
Duke University

Date: _____

Approved:

Stephanos Venakides, Supervisor

J. Thomas Beale

Jim Nolen

Daniel J. Gauthier

Dissertation submitted in partial fulfillment of the requirements for the degree of
Doctor of Philosophy in the Department of Mathematics
in the Graduate School of Duke University
2012

ABSTRACT

EM Scattering from Perforated Films: Transmission and
Resonance

by

Aaron D. Jackson

Department of Mathematics
Duke University

Date: _____

Approved:

Stephanos Venakides, Supervisor

J. Thomas Beale

Jim Nolen

Daniel J. Gauthier

An abstract of a dissertation submitted in partial fulfillment of the requirements for
the degree of Doctor of Philosophy in the Department of Mathematics
in the Graduate School of Duke University
2012

Copyright © 2012 by Aaron D. Jackson
All rights reserved except the rights granted by the
Creative Commons Attribution-Noncommercial Licence

Abstract

We calculate electromagnetic transmission through periodic gratings using a mode-matching method for solving Maxwell's equations. We record the derivation of the equations involved for several variations of the problem, including one- and two-dimensionally periodic films, one-sided films, films with complicated periodicity, and a simpler formula for the case of a single contributing waveguide mode. We demonstrate the effects of the Rayleigh anomaly, which causes energy transmission to be very low compared to nearby frequencies, and the associated transmission maxima which may be as high as 100% for certain energy frequencies. Finally we present further variations of the model to account for the effects of conductivity, finite hole arrays, and collimation. We find that assuming the film is perfectly conducting with infinite periodicity does not change the transmission sufficiently to explain the difference between experimental and theoretical results. However, removing the assumption that the incident radiation is in the form of a plane wave brings the transmission much more in agreement with experimental results.

Contents

Abstract	iv
List of Figures	viii
List of Abbreviations and Symbols	x
Acknowledgements	xii
1 Introduction	1
2 Basic Formulae	4
2.1 Derivation of the Matrix Equations	4
2.1.1 Maxwell's Equations and Matching Conditions	4
2.1.2 Bloch Theory and the Field Outside the Film	6
2.1.3 Waveguide Modes Inside the Holes	9
2.1.4 Properties of Plane Waves and Waveguide Modes	9
2.1.5 Field Expressions in Terms of Basis Elements	10
2.1.6 Applying the Matching Conditions at the Hole Openings	11
2.1.7 Defining the Final Matrix Equations and Calculating Transmission	13
2.2 Explicit Waveguide Mode and Plane Wave Expressions in the 2-dimensionally Periodic System	15
2.2.1 Plane Waves for the 2-dimensionally Periodic System	16
2.2.2 Waveguide Modes in a Rectangular Waveguide	19
2.2.3 Waveguide Modes in a Circular Waveguide	21

2.3	Explicit Waveguide Modes and Plane Waves for the 1-dimensionally Periodic System	25
2.3.1	Plane Waves for the 1-dimensionally Periodic System	26
2.3.2	Waveguide Modes for the 1-dimensionally Periodic System	27
2.4	Structure of the Matrix Equation and Alternate Formulations	30
2.4.1	An Equivalent Matrix Formulation	31
2.4.2	The One-sided Film	32
3	Rayleigh Anomalies and Transmission Maxima	34
3.1	Incidence at an Angle and the Rayleigh Anomaly	37
3.2	Supercells	38
3.2.1	Alterations to the Matrix Equation	39
3.2.2	Examples: Rectangular, Triangular, and Hexagonal Arrays	41
3.3	Transmission Maxima and the Single Mode Calculation	44
3.3.1	Matrix Equation and Transmission Formula for One Waveguide Mode	44
3.3.2	Maximizing Transmission	46
3.3.3	Comparison with the Full Simulation	49
3.4	Resonance and the Null Space of the Matrix Equation	50
4	Simulating Real Experiments	52
4.1	Finite Conductivity	53
4.1.1	Explicit Expressions for the Waveguide Modes	54
4.1.2	Asymptotic Expression for the Propagation Constant	58
4.1.3	Remaining Changes to the Matching Procedure	64
4.1.4	Results, and Comparison with Other Numerical Techniques	66
4.2	Finite Hole Arrays	68
4.3	Imperfect Collimation	69

5	Summary and Discussion	73
A	Explicit Waveguide Mode-Plane Wave Inner Products	75
A.1	2-dimensionally Periodic Rectangular Waveguide	76
A.2	1-dimensionally Periodic Slit Waveguide	82
B	Asymptotic Expression for the Propagation Constant of a Circular Waveguide Mode Bounded by an Imperfect Conductor	84
B.1	Derivation	84
B.2	Final simplified form of asymptotic expansions	103
C	A Theoretical Formula for Bound States in 3D	105
	Bibliography	112
	Biography	114

List of Figures

2.1	A two-dimensionally periodic film with array parameters.	5
2.2	Definition of the metal film and surrounding regions.	7
3.1	Transmission profile for a normally incident plane wave on 2-dimensionally periodic and 1-dimensionally periodic hole arrays.	36
3.2	EM field cross section for the 1-dimensionally periodic film at a transmission resonance, illuminated from below.	37
3.3	Transmission profile for a 2-dimensionally periodic array with $\theta_x = 2, \theta_y = 0$ and $\theta_x = 2, \theta_y = 1$	39
3.4	The shifting transmission profile for a 2-dimensionally periodic array of holes as space is gradually introduced after every 2 holes in the y -direction.	42
3.5	Supercell and transmission profile for a triangular array of holes illuminated by a plane wave at normal incidence.	43
3.6	Supercell and transmission profile for a hexagonal array of holes illuminated by a plane wave at normal incidence.	44
3.7	Comparison of the first-order single-mode calculation to the full simulation.	49
4.1	Transmission profile for imperfectly conducting metal.	66
4.2	Simulation with imperfect conductivity performed in COMSOL Multiphysics.	67
4.3	Progressive approximations of the transmission profile for a finite array of slits.	68
4.4	Shift of the narrow maximum with a small angle change.	70

4.5	Transmission profile for a 2-dimensionally periodic array of holes with plane waves simultaneously incident at a variety of angles.	71
-----	---	----

List of Abbreviations and Symbols

Symbols

E	Electric field ($= (E_x, E_y, E_z)^T$).
H	Magnetic field ($= (H_x, H_y, H_z)^T$).
ϵ	Material dielectric constant.
μ	Material magnetic constant.
ω	Frequency.
h	Thickness of film.
L_x, L_y	Period width in the x - and y -directions, respectively.
a, b	Width of a rectangular hole in the x - and y -directions, respectively.
R	Radius of a circular hole.
H	Index of holes when multiple holes are used.
W_k	Plane wave with index k .
Y_k	Admittance of plane wave with index k .
r_k, t_k	Amplitudes of reflected and transmitted plane wave with index k , respectively.
M_α	Waveguide mode with index α .
Y_α	Admittance of waveguide mode with index α .
A_α, B_α	Amplitude at center of hole of waveguide mode of index α propagating forward and back, respectively.
E_α, E'_α	Amplitude at each hole end of waveguide mode of index α .

- J_n, K_n Bessel functions.
- $()_t$ A vector with subscript t refers to the x, y components of that vector.
- Φ, ϕ An arbitrary function; at each appearance properties are described in the text.

Acknowledgements

My advisor and I would like to thank the NSF for supporting this research under grant DMS-0707488.

I would like to thank my advisor Stephanos Venakides for making all of this possible; Dan Gauthier for a tremendous amount of help far beyond the call of duty; and Da Huang for his extensive contributions. Thanks to my committee and most of my teachers here at Duke University, and thanks to my friends and teachers at NAU for their encouragement.

I would like to thank all of my friends at Duke Math, Physics, Chemistry, Computer Science, Biology, Economics, Law, and Divinity, and my friends in and around Durham, for putting up with me, supporting me and giving me a home here. In honor of their friendship I would like to thank, in no particular order, Josie, the color red, Romania, Regina Spektor, coffee, Illuminati, Connie Willis, harps, bad movies, Shaolin, internet t-shirt companies, Sam Chin, Eve, Killer Bunnies, absorb and project, Rolf, the beach, Katamari, jumping pictures, vegemite, Evaine and I guess Tristan too, board and card games in general, Anansi and Loki, CSAs, good movies, the women's rowing teams, carrot cake, Guglhupf, Axis and Allies, awesome computers, everyone who used to be an adventurer before taking an arrow in the knee, homemade sweets, Nathan Klug who surely doesn't remember me at all, Diablo, good chinese restaurants, those conversations that transcend language barriers, Armadillo Grill, frosting, chess, good Durham restaurants in general, Teavana, my

eternally beloved soulmate Sappho, peanut butter, Edward Norton, C. S. Lewis, Bean, Tower Indian, Won Buddhism, the Magnetic Fields, rides home after 6 hours in the advisor's office, ballroom dancing, goth clubs, Dexter, kittens, burritos, Frog Juice, the Tower, orange juice, Katie Kat, Leslie, Ollie, Vincent Price, Law and Order, Japanese people in general, tofu soup, Katamari again, Netflix, Hulu, and of course Kratos for teaching me how to, well, you know.

I would like to thank Andrea at the Mad Popper, Chad at Dulce, Bean Traders, Barnes and Noble, Sitar, Udupi, Bocci, Rockfish, Vit Goal, Baba Ghannouj, Bali-Hai, Michele Pagnotta, and the one the only Tyrone at Famous Hair. I most definitely would not like to thank Time Warner Cable.

Mostly, I want to thank Sarah Schott, Anna Little, and the evervescent Mel Gratton. You are the ones who made my time here really worth it. The happiness I've found here would not have been possible without you, and I am forever in your debt.

1

Introduction

In their 1998 paper, Ebbesen et al. demonstrated experimentally that certain frequencies of light, will pass through metal gratings to a greater degree than was previously thought possible, as discussed in the earlier paper of Bethe (1944). This was particularly surprising when the wavelength of the incident light was larger than the diameter of the grating holes, and this case was called extraordinary transmission. These findings brought substantial interest to the study of light passing through gratings.

Extraordinary transmission is present to a degree in the case of a single hole in a metal film (see, for example, Nikitin et al. (2008)), but it is stronger in the case of a periodic array of holes. Mathematical theory tells us that solutions of Maxwell's equations in a periodic system must be Bloch periodic (a discussion of Bloch theory may be found in Kuchment (1993))— that is, a periodic function multiplied by an exponential. As we will discuss in Chapter 2, this begets the Rayleigh/Wood anomaly, which is a sharp decrease in transmission when the wavelength of the incoming wave is equal to certain fractions of the period width. These minima were first documented by R. W. Wood (1902) and mathematical discussion was furthered by Lord Rayleigh

(1907). Associated with each of these transmission minima may also be one or more transmission maxima that may even reach 100% transmission. Furthermore, large fields build up inside the holes at these transmission peaks.

While the Rayleigh anomaly is straightforward to predict, the location and magnitude of the transmission maxima is a very complicated problem. Theoretical models and experiments with new hole shapes and film properties are continually being explored in the literature. In this work we solve Maxwell's equations using a mode-matching method based on the techniques discussed in Martín-Moreno and García-Vidal (2008), Martín-Moreno and García-Vidal (2004), and other works of these authors: we decompose the electromagnetic (EM) field inside and outside the film into a basis of wave modes, and use the matching conditions associated with Maxwell's equations to find the modal amplitudes. Application of Bloch theory reduces the problem to an infinite matrix equation which can be truncated and solved.

This method has several advantages. First, it is common for only one or a handful of modes to significantly contribute to the EM field, and if these are separated out then it greatly reduces calculation time. Second, the separation into individual modes illuminates the Rayleigh anomaly very clearly. And finally, unlike more traditional numerical methods which may require extra computation at corners and resonances, the modal method encounters no extra difficulty.

We begin with a model that assumes the metal is perfectly conducting with a periodic array of holes, illuminated by a plane wave, as in Martín-Moreno and García-Vidal (2008). In Chapter 2 we explain the method of mode-matching in detail. In Chapter 3, we discuss the Rayleigh anomaly and the transmission maxima, including a simplified method of predicting the location and magnitude of the maxima which depends only on a single waveguide mode inside the hole. We demonstrate the increased field strength within the holes at transmission resonances. We also discuss how to simulate non-rectangular hole arrays using period supercells.

In Chapter 4, we revise the model to more closely simulate real experiments. By this time, we (as well as other modelers, for example Medina et al. (2008)) have seen that some Rayleigh anomalies are accompanied by a double transmission maximum, one narrower than the other. However, experimenters do not encounter this double peak (for example, see Ebbesen et al. (1998); Hou et al. (2006); Przybilla et al. (2008)). We first use an asymptotic formula for the propagation constant of a circular waveguide mode to show that this difference is not accounted for by allowing the film to become finitely conducting. This result is further supported by simulations in COMSOL Multiphysics and Microwave Studio. Next we find that assuming a finite array of holes does not account for the difference either, by using the supercell method introduced in Chapter 3 to create periodic arrays which become finite in limit. Lastly, however, we find that allowing for imperfect collimation – that is, assuming that the incident radiation is more complicated than a single plane wave – causes the double maximum to devolve into a single maximum of lower magnitude, and therefore is a viable reason for the discrepancy between theory and experiment.

Finally, in the Appendices we include full mathematical descriptions of the overlaps between plane waves and waveguide modes, the full derivation of the asymptotic formulae used in Chapter 4, and an extension of a related result from the literature from two dimensions to three.

2

Basic Formulae

We begin by formalizing the case of an array of holes periodic in the x - and y -directions in a perfectly conducting metal film of finite thickness in the z -direction, with radiation incident on one side of the film in the form of a plane wave. We will use Bloch theory to help us solve Maxwell's equations by reducing the problem to an infinite matrix equation, which can then be truncated and solved. The same formalism will apply to both a 2-dimensionally periodic rectangular array of holes and to a 1-dimensionally periodic array of slits. The only differences lie in the number and explicit expressions for the waveguide modes, which can be found for rectangular holes, circular holes and slits in Sec. 2.2. The derivation in Sec. 2.1 is largely drawn from the papers of Martín-Moreno and García-Vidal (2008) and Nikitin et al. (2008), and for the expressions in Sec. 2.2 we draw from Jackson (1999).

2.1 Derivation of the Matrix Equations

2.1.1 Maxwell's Equations and Matching Conditions

Our aim is to solve the time-harmonic Maxwell's equations, which result from the full Maxwell's equations by assuming time dependence of $\exp(-i\omega t)$ with constant

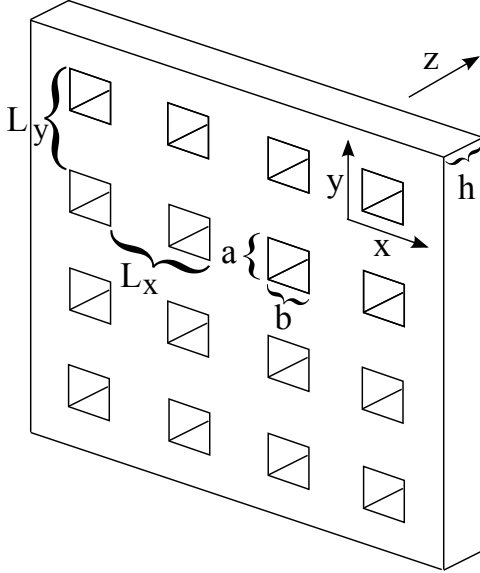


FIGURE 2.1: A sample two-dimensionally periodic film with array parameters. Here the film is periodic and extends infinitely in the x - and y -directions, and energy propagates in the z -direction. For rectangular holes, the side lengths will be denoted a and b , and the dimensions of the rectangular period cell will be denoted L_x and L_y .

frequency ω in a medium of dielectric constant ϵ (and magnetic constant $\mu = 1$),

$$\begin{aligned}
 \nabla \times \mathbf{E} &= i\omega\mathbf{H} & \nabla \cdot \mathbf{H} &= 0 \\
 \nabla \times \mathbf{H} &= -i\epsilon\omega\mathbf{E} & \nabla \cdot \mathbf{E} &= 0,
 \end{aligned}
 \tag{2.1}$$

It is helpful to note that each component of \mathbf{E} and \mathbf{H} satisfies the Helmholtz equation

$$(\Delta + \epsilon\omega^2) \psi = 0,
 \tag{2.2}$$

which we find by taking the curl again of one of the curl equations above and simplifying. When solving Maxwell's equations, our strategy is typically to solve the Helmholtz equation for one or more of the EM field components first, and then use Maxwell's equations to find the rest..

Our domain consists of the region to either side of a perfectly conducting metal film of thickness h , and inside holes through the film which are either rectangular

with side widths a and b in the x - and y -directions respectively, or circular with radius R , repeated periodically with rectangular period of side lengths L_x and L_y (see Figs. 2.1 and 2.2). Alternatively we may consider the one-dimensionally periodic case of slits in the metal instead of holes, of width a in the x -direction and infinite in the y -direction. A plane wave will be incident on the $z < 0$ side of the film. We will call the $z < 0$ side of the film the *reflection side*, and the $z > 0$ side the *transmission side*. We will assume that the film is a perfect conductor, meaning that there is no EM field inside the metal.

We will write expressions for the fields to either side of the film and inside the holes separately, and then use the matching conditions associated with Maxwell's equations to find the remaining unknown terms. In general, the matching conditions state that the components of \mathbf{E} and \mathbf{H} tangential to an interface between two materials (that is, $\mathbf{n} \times \mathbf{E}$ and $\mathbf{n} \times \mathbf{H}$ where \mathbf{n} is normal to the interface) must be continuous, as discussed in Jackson (1999). At the interface of a material with a perfect conductor, however, the magnetic field may be discontinuous; and so because the electric field is zero inside the metal, we require only

$$\mathbf{n} \times \mathbf{E} = 0 \tag{2.3}$$

at the boundary.

2.1.2 Bloch Theory and the Field Outside the Film

Outside the film, we decompose the field into a linear combination of plane waves, which form a basis for solutions of Maxwell's equations. A plane wave is the product of an exponential of the form

$$\exp i(k_x x + k_y y + k_z z), \tag{2.4}$$

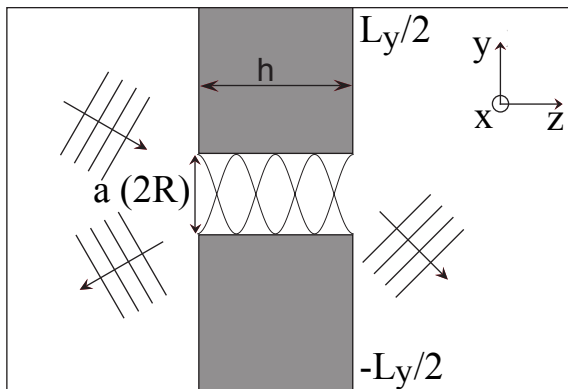


FIGURE 2.2: Cross-section of one period cell of the film. A plane wave is incident on the $z < 0$ side of a metal film of thickness h , with holes of side lengths a and b (in the case of rectangular holes) or radius R (in the case of circular holes) periodically placed with period widths L_x and L_y . Outside the film, we decompose the field into a basis of plane waves, and inside the holes, we decompose the field into a basis of waveguide modes, after which we enforce matching at the boundaries. Some of the incident energy is reflected (we will call the $z < 0$ region the *reflection side*), and some enters the hole and exits through to the other side (we will call the $z > 0$ region the *transmission side*).

and a constant vector depending on \mathbf{k} . In the regions to either side of the film we will assume that the dielectric constant is $\epsilon = 1$. Then Maxwell's equations require that the wavevector (k_x, k_y, k_z) satisfy

$$k_z^2 = \omega^2 - k_x^2 - k_y^2. \quad (2.5)$$

The number k_z is called the *propagation constant*. (The plane wave is so called because its level-sets are planes of the form $k_x x + k_y y + k_z z = b$, where b is a constant. The full expressions for the plane waves are given in Sec. 2.2.1.)

In general, an EM field is a linear combination of all plane waves satisfying (2.5). However, because our film is periodic, we may invoke Bloch theory (see Martín-Moreno and García-Vidal (2008) and Kuchment (1993)), which tells us that our EM field Ψ must be Bloch periodic, that is, in the form of a plane wave (called the *Bloch factor*) multiplying a function that has periodicity equal to that of the film,

$$\Psi(\mathbf{x}) = e^{i\mathbf{k}_0 \cdot \mathbf{x}} \psi(\mathbf{x}) \quad (2.6)$$

where ψ is periodic. Because our incident plane wave does not in general have the same periodicity as the film, it must be the Bloch factor. Furthermore, because the plane waves are a basis for solutions of Maxwell's equations, $\psi(\mathbf{x})$ may be written as a linear combination of only those plane waves which have the same periodicity as the film, of which there are only countably many. That is,

$$\Psi(\mathbf{x}) = \sum_k \mathbf{c}_k \exp(i(\mathbf{k}_0 + \mathbf{k}) \cdot \mathbf{x}), \quad (2.7)$$

where if our film has period width L_x in the x -direction, and L_y in the y -direction, then the sum is over values of \mathbf{k}_t determined by

$$\mathbf{k}_t = (k_x, k_y) = \left(\frac{2\pi j_1}{L_x}, \frac{2\pi j_2}{L_y} \right) \quad (2.8)$$

for all integers j_1, j_2 , and k_z is determined by Eq. (2.5). The resulting plane waves are orthogonal when integrated over a period cell, and we normalize them to be orthonormal. Finally, because we know the field is Bloch periodic, we only need to consider one period cell in our calculations.

It is worth noting that plane waves are not the only basis we could use outside the holes, nor are they necessarily the most useful in all circumstances. On the reflection side, it makes sense to use plane waves because experimentally, it is easier to approximate a plane wave than other types of modes. If we use plane waves on the reflection side, then using plane waves on the transmission side also allows us to reuse many calculations. However, we must account for many plane waves to get a clear picture of the reflected and transmitted fields, rarely less than 400. Choosing another basis on the transmission side might allow it to be resolved with only a

handful of basis elements. See Jackson (1999) for some discussion on different bases.

2.1.3 Waveguide Modes Inside the Holes

Meanwhile, inside the holes, we decompose the field into a linear combination of waveguide modes, which form a basis for solutions of Maxwell's equations there, as discussed in Jackson (1999). We assume that the waveguide modes, which we enumerate by α (which is a record of two or more numbers, depending on the shape of the holes— see Sec. 2.2), have exponential z -dependence $\exp ik_\alpha z$, indicating that they propagate in the z direction with propagation constant k_α . With this assumption, the Helmholtz equation (2.2) which is satisfied by each field component becomes

$$(\Delta_{x,y} + \epsilon\omega^2 - k_\alpha^2) \psi = 0. \quad (2.9)$$

We may distinguish two types of solutions to Maxwell's equations in the waveguide. The first type of mode has $E_z = 0$ and is called *transverse electric* (TE), and the second type of mode has $H_z = 0$ and is called *transverse magnetic* (TM). There are a countable number of both varieties, and properly normalized they form an orthonormal basis for solutions to Maxwell's equations inside the waveguide (Jackson (1999)).

2.1.4 Properties of Plane Waves and Waveguide Modes

We will write the EM field in terms of these basis components, and use the matching conditions to find the coefficients. We do not at this time need to write all six components of the field, however. A plane wave or waveguide mode can be fully reconstructed from only the x and y components of \mathbf{E} , as long as we also keep track of whether it propagates in the positive or negative z -direction.

The full expressions for each plane wave and waveguide mode is given in Sec. 2.2. From these we can see that each plane wave and waveguide mode also satisfies the

equation

$$\begin{pmatrix} H_y \\ -H_x \end{pmatrix} = \pm Y \begin{pmatrix} E_x \\ E_y \end{pmatrix}, \quad (2.10)$$

where the constant Y is known as the *admittance*. For each plane wave and waveguide mode the admittance is also given in Sec. 2.2; it is a ratio of the propagation constant to the frequency or vice versa (i.e., k_z/ω or ω/k_z).

2.1.5 Field Expressions in Terms of Basis Elements

Let $W_k = (E_x, E_y)^T$ represent the E_x, E_y components of the $\mathbf{k}_t = (k_x, k_y)^{th}$ plane wave outside the hole; let r_k be the amplitude of the variety that is on the reflection side of the film, and let t_k be the amplitude of the variety on the transmission side. Let W_0 represent the E_x, E_y components of the incident plane wave with wavevector k_0 ; and let Y_k and k_z be the admittance and propagation constant of W_k , respectively. Then on the reflection side of the film ($z < 0$), using Eq. (2.10) we may write

$$\begin{pmatrix} E_x \\ E_y \end{pmatrix}_{ref} = W_0 e^{ik_0(z+h/2)} + \sum_k r_k W_k e^{-ik_z(z+h/2)} \quad (2.11a)$$

$$\begin{pmatrix} H_y \\ -H_x \end{pmatrix}_{ref} = Y_{k_0} W_0 e^{ik_0(z+h/2)} - \sum_k r_k Y_k W_k e^{-ik_z(z+h/2)}. \quad (2.11b)$$

Here we explicitly write the z dependence of the exponential in order to to keep track of the direction of propagation of the plane waves. Similarly, on the transmission side of the film ($z > 0$),

$$\begin{pmatrix} E_x \\ E_y \end{pmatrix}_{trans} = \sum_k t_k W_k e^{ik_z(z-h/2)} \quad (2.12a)$$

$$\begin{pmatrix} H_y \\ -H_x \end{pmatrix}_{trans} = \sum_k t_k Y_k W_k e^{ik_z(z-h/2)}. \quad (2.12b)$$

Meanwhile, inside the holes we let $M_\alpha = (E_x, E_y)^T$ represent the E_x, E_y components of the waveguide mode of index α . Let A_α and B_α be the amplitudes of the forward- and backward-propagating varieties respectively, and let k_α be the propagation constant of the mode. (We purposefully leave the index α ambiguous at this stage. Depending on the shape of the holes it may record two, three or more variables.) Then we have

$$\begin{pmatrix} E_x \\ E_y \end{pmatrix}_{hole} = \sum_{\alpha} M_{\alpha} (A_{\alpha} e^{ik_{\alpha}z} + B_{\alpha} e^{-ik_{\alpha}z}) \quad (2.13a)$$

$$\begin{pmatrix} H_y \\ -H_x \end{pmatrix}_{hole} = \sum_{\alpha} Y_{\alpha} M_{\alpha} (A_{\alpha} e^{ik_{\alpha}z} - B_{\alpha} e^{-ik_{\alpha}z}). \quad (2.13b)$$

2.1.6 Applying the Matching Conditions at the Hole Openings

Next, we will apply the matching conditions associated with Maxwell's equations in order to find the coefficients $r_k, t_k, A_\alpha, B_\alpha$. For regions bounded by a perfect conductor, the matching conditions are that (i) the components of the electric field tangent to any interface between different material regions must be continuous; and (ii) the components of the magnetic field tangent to any interface *except* those between the perfect conductor and another material must be continuous. (If desired, the jump in the magnetic field at the interface can be used to determine the current at the surface of the metal.)

The matching on the walls of the holes will be accounted for when solving for the waveguide modes, as seen in Sec. 2.2. It remains to account for the metal surfaces at the top and bottom of the film, including at the opening of the holes: E_x and E_y must be continuous everywhere at the top and bottom of the film, while H_x and H_y must be continuous only at the hole openings. To do this, we first set Eqs. (2.11a) and (2.13a) equal at $z = -h/2$, and Eqs. (2.13a) and (2.12a) equal at $z = +h/2$. We then take the inner product of both sides of these equations with the plane wave

W_k ; since the plane waves are orthonormal, this allows us to solve for r_k and t_k in terms of A_α and B_α . In the case of a two-dimensional periodic array of holes, the inner product used here is

$$(U, V) = \int_{\text{period cell}} U_x^* V_x + U_y^* V_y dx dy, \quad (2.14)$$

where * indicates the complex conjugate, and the integration is done over one period of the film at either $z = -h/2$ on the reflection side or $z = h/2$ on the transmission side. In the case of a one-dimensionally periodic array of slits which are periodic in the x -direction and constant in the y -direction, the inner product used is

$$(U, V) = \int_{\text{period cell}} U_x^* V_x + U_y^* V_y dx. \quad (2.15)$$

Similarly, we will set Eqs. (2.11b) and (2.13b) equal at $z = -h/2$ and Eqs. (2.13b) and (2.12b) equal at $z = +h/2$, but this time we take the inner product of both sides with respect to the waveguide mode M_α instead. The waveguide mode is zero outside the hole, and thus this technique enforces equality only over the opening of the hole. In this way we obtain

$$r_k = -\delta_{k,k_0} + \sum_{\alpha} (W_k, M_\alpha) (A_\alpha e_\alpha^{-1} + B_\alpha e_\alpha) \quad (2.16a)$$

$$t_k = \sum_{\alpha} (W_k, M_\alpha) (A_\alpha e_\alpha + B_\alpha e_\alpha^{-1}) \quad (2.16b)$$

$$-\sum_k Y_k r_k(M_\alpha, W_k) = -Y_{k_0}(M_\alpha, W_{k_0}) + Y_\alpha (A_\alpha e_\alpha^{-1} - B_\alpha e_\alpha) \quad (2.17a)$$

$$\sum_k Y_k t_k(M_\alpha, W_k) = Y_\alpha (A_\alpha e_\alpha - B_\alpha e_\alpha^{-1}), \quad (2.17b)$$

where $e_\alpha = \exp ik_\alpha h/2$.

2.1.7 Defining the Final Matrix Equations and Calculating Transmission

Continuing on, we plug Eqs. (2.16a) and (2.16b) into Eqs. (2.17a) and (2.17b) (and multiply all sides by i for convenience), obtaining

$$\begin{aligned} -i \sum_k Y_k \left[-\delta_{k,k_0} + \sum_{\beta} (W_k, M_{\beta}) (A_{\beta} e_{\beta}^{-1} + B_{\beta} e_{\beta}) \right] (M_{\alpha}, W_k) = \\ = -i Y_{k_0} (M_{\alpha}, W_{k_0}) + i Y_{\alpha} (A_{\alpha} e_{\alpha}^{-1} - B_{\alpha} e_{\alpha}) \end{aligned} \quad (2.18)$$

$$i \sum_k Y_k \left[\sum_{\beta} (W_k, M_{\beta}) (A_{\beta} e_{\beta} + B_{\beta} e_{\beta}^{-1}) \right] (M_{\alpha}, W_k) = i Y_{\alpha} (A_{\alpha} e_{\alpha} - B_{\alpha} e_{\alpha}^{-1}). \quad (2.19)$$

Define the following:

$$\begin{aligned} X_{\alpha} &= A_{\alpha} e_{\alpha}^{-1} + B_{\alpha} e_{\alpha} & X'_{\alpha} &= -A_{\alpha} e_{\alpha} - B_{\alpha} e_{\alpha}^{-1} \\ G_{\alpha\beta} &= i \sum_k Y_k (M_{\alpha}, W_k) (W_k, M_{\beta}) & I_{\alpha} &= 2i Y_{k_0} (W_{k_0}, M_{\alpha}) \\ G_{\alpha}^V &= \frac{2i Y_{\alpha}}{e_{\alpha}^2 - e_{\alpha}^{-2}} & S_{\alpha} &= i Y_{\alpha} \frac{e_{\alpha}^2 + e_{\alpha}^{-2}}{e_{\alpha}^2 - e_{\alpha}^{-2}}. \end{aligned} \quad (2.20)$$

Then we may write Eqs. (2.18) and (2.19) as

$$\sum_{\beta} G_{\alpha\beta} X_{\beta} - S_{\alpha} E_{\alpha} - G_{\alpha}^V X'_{\alpha} = I_{\alpha} \quad (2.21a)$$

$$\sum_{\beta} G_{\alpha\beta} X'_{\beta} - S_{\alpha} E'_{\alpha} - G_{\alpha}^V X_{\alpha} = 0. \quad (2.21b)$$

We can also write these equations in matrix form, where G is the infinite matrix whose entries are $G_{\alpha\beta}$; E , E' , and I are the infinite vectors with entries E_{α} , E'_{α} , and

I_α ; and S and G^V are the infinite matrices with diagonal entries S_α and G_α^V and which are zero off the diagonal:

$$(G - S)X - G^V X' = I \quad (2.22a)$$

$$(G - S)X' - G^V X = 0 \quad (2.22b)$$

Finally we may write this pair of equations as a single matrix equation by defining

$$\mathbf{G} = \begin{pmatrix} G - S & -G^V \\ -G^V & G - S \end{pmatrix} \quad \mathbf{X} = \begin{pmatrix} X \\ X' \end{pmatrix} \quad \mathbf{I} = \begin{pmatrix} I \\ 0 \end{pmatrix} \quad (2.23)$$

so that

$$\mathbf{GX} = \mathbf{I}. \quad (2.24)$$

We may then truncate these matrices and solve numerically for \mathbf{X} . We choose proper truncation by using increasingly large numbers of waveguide modes and plane waves until the vector \mathbf{X} stabilizes. The structure of this matrix equation is discussed in Sec. 2.4.

Once we have \mathbf{X} , we can recover the amplitudes of all modes via

$$\begin{aligned} t_k &= - \sum_{\alpha} (W_k, M_\alpha) X'_\alpha \\ r_k &= -\delta_{k,k_0} + \sum_{\alpha} (W_k, M_\alpha) X_\alpha \\ A_\alpha &= \frac{-e_\alpha^{-1} X_\alpha - e_\alpha X'_\alpha}{e_\alpha^2 - e_\alpha^{-2}} \\ B_\alpha &= \frac{e_\alpha X_\alpha + e_\alpha^{-1} X'_\alpha}{e_\alpha^2 - e_\alpha^{-2}}. \end{aligned} \quad (2.25)$$

To find the total energy transmitted through the holes to the transmission side of the metal, we integrate the z -component of the time-averaged Poynting vector $\frac{1}{2}\Re(\mathbf{E} \times \mathbf{H}^*)$ over the basic period cell in the transmission region,

$$T = \frac{1}{2} \Re \left(\int_{\text{period cell}} \mathbf{u}_z \cdot (\mathbf{E} \times \mathbf{H}) dA \right) = \frac{1}{2} \Re \left(\int_{\text{period cell}} E_x H_y^* - E_y H_x^* dA \right). \quad (2.26)$$

Recalling that field outside the film is the sum of plane waves which are orthogonal with respect to this integral, we see that it reduces to

$$T = \sum_k \Re(Y_k) |t_k|^2 / Y_{k_0}, \quad (2.27)$$

where the denominator comes from normalization by the energy of the incident wave.

In terms of X and X' , it is equal to

$$\begin{aligned} T &= \sum_k \Im \left(i Y_k \left(\sum_{\beta} (W_k, M_{\beta}) X'_{\beta} \right) \left(\sum_{\alpha} (M_{\alpha}, W_k) X'_{\alpha} \right) \right) / Y_{k_0} \\ &= \sum_k \Im \left(i Y_k \sum_{\alpha, \beta} (W_k, M_{\beta}) (M_{\alpha}, W_k) X'_{\beta} X'_{\alpha} \right) / Y_{k_0} \end{aligned} \quad (2.28)$$

$$\begin{aligned} &= \sum_{\alpha, \beta} \Im \left(i \sum_k Y_k (M_{\alpha}, W_k) (W_k, M_{\beta}) X'_{\beta} X'_{\alpha} \right) / Y_{k_0} \\ &= \sum_{\alpha, \beta} \Im (G_{\alpha\beta} X'_{\alpha} X'_{\beta}) / Y_{k_0}. \end{aligned} \quad (2.29)$$

2.2 Explicit Waveguide Mode and Plane Wave Expressions in the 2-dimensionally Periodic System

Here we describe full plane wave and waveguide mode solutions to the time-harmonic Maxwell's equations with constant frequency ω for rectangular and circular holes. We assume that the electric and magnetic constants ϵ and μ are both equal to 1. In deriving these expressions we refer heavily to Jackson (1999).

2.2.1 Plane Waves for the 2-dimensionally Periodic System

Plane waves solutions to Maxwell's equations in free space take the form of a constant 6-vector times the exponential

$$\exp i(k_x x + k_y y + k_z z). \quad (2.30)$$

In the regions to either side of the film we will assume that the dielectric constant is $\epsilon = 1$. Then the vector (k_x, k_y, k_z) , called the wavevector, encodes the angle of incidence, and

$$k_z^2 = \omega^2 - k_x^2 - k_y^2 \quad (2.31)$$

to satisfy Maxwell's equations. We take z to be the direction of propagation, and call k_z the propagation constant. The plane wave is so called because its level-sets are planes of the form $k_x x + k_y y + k_z z = c$, and it comes in two varieties: p -polarized, which has $H_z \equiv 0$, and s -polarized, for which $E_z \equiv 0$. Properly normalized, they form an orthonormal basis for solutions of Maxwell's equations in free space (Jackson (1999)).

In the case of a two-dimensional rectangular periodic array of holes in a metal film with period width L_x in the x -direction and L_y in the y -direction, Bloch theory tells us that the solution to Maxwell's equations outside the film can be written as the sum of only a countable number of plane waves, namely, those that satisfy

$$\begin{pmatrix} k_x \\ k_y \end{pmatrix} = \begin{pmatrix} k_{0x} \\ k_{0y} \end{pmatrix} + 2\pi \begin{pmatrix} j_1/L_x \\ j_2/L_y \end{pmatrix} \quad (2.32)$$

where (k_{0x}, k_{0y}) are the x, y components of the wavevector of the arbitrary incident wave (these numbers are truly arbitrary real numbers; the propagation constant k_{0z} is given by Eq. (2.31).) and j_1, j_2 are any integers. The angle of the incident wave is given by $k_{0x} = \omega \sin(\theta_x), k_{0y} = \omega \sin(\theta_y)$. All sums over k in Sec. 2.1 are over these values of k_x, k_y ; and k_z is determined according to Eq. (2.31).

We will proceed to record the full expression for the plane waves, which are orthonormal according to the inner product

$$(U, V) = \int_{\text{period cell}} U_x^* V_x + U_y^* V_y dx dy, \quad (2.33)$$

where the integration is done over one period of the film at a single value of z . The p - and s -polarized plane waves are:

p -polarization

$$\begin{aligned} \mathbf{E} &= \frac{1}{\sqrt{L_x L_y |k_t|}} \begin{pmatrix} k_x \\ k_y \\ \mp |k_t|^2 / k_x \end{pmatrix} e^{i(k_x x + k_y y)} e^{\pm i k_z z} \\ \mathbf{H} &= \frac{\omega}{\sqrt{L_x L_y |k_t| k_z}} \begin{pmatrix} -k_y \\ k_x \\ 0 \end{pmatrix} e^{i(k_x x + k_y y)} e^{\pm i k_z z} \end{aligned} \quad (2.34)$$

where $k_t = (k_x, k_y)$, and the sign is chosen based on whether the wave is traveling in the positive (upper sign) or negative (lower sign) z -direction.

The admittance for a p -polarized plane wave is $Y = \omega / k_z$.

In Sec. 2.1 above, the terms W_k refer only to the x, y components of the electric component of the plane wave. For p -polarized waves, this is

$$W_k = \frac{1}{\sqrt{L_x L_y |k_t|}} \begin{pmatrix} k_x \\ k_y \end{pmatrix} e^{i(k_x x + k_y y)}. \quad (2.35)$$

s -polarization

$$\begin{aligned}
\mathbf{E} &= \frac{1}{\sqrt{L_x L_y} |k_t|} \begin{pmatrix} -k_y \\ k_x \\ 0 \end{pmatrix} e^{i(k_x x + k_y y)} e^{\pm i k_z z} \\
\mathbf{H} &= \frac{-k_z}{\sqrt{L_x L_y} |k_t| \omega} \begin{pmatrix} \pm k_x \\ \pm k_y \\ -|k_t|^2 / k_x \end{pmatrix} e^{i(k_x x + k_y y)} e^{\pm i k_z z}
\end{aligned} \tag{2.36}$$

where $k_t = (k_x, k_y)$, and the sign is chosen based on whether the wave is traveling in the positive (upper sign) or negative (lower sign) z -direction.

The admittance for an s -polarized plane wave is $Y = k_z / \omega$.

In Sec. 2.1 above, the terms W_k refer only x, y components of the electric component of the plane wave. For s -polarized waves, this is

$$W_k = \frac{1}{\sqrt{L_x L_y} |k_t|} \begin{pmatrix} -k_y \\ k_x \end{pmatrix} e^{i(k_x x + k_y y)}. \tag{2.37}$$

Normal Incidence

At normal incidence, when $k_x = k_y = 0$, the distinction between p - and s -polarization is arbitrary. The two varieties of normally incident plane waves are

$$\begin{aligned}
\mathbf{E} &= \frac{1}{\sqrt{L_x L_y}} \begin{pmatrix} 1 \\ 0 \\ 0 \end{pmatrix} e^{\pm i \omega z} \\
\mathbf{H} &= \frac{\pm 1}{\sqrt{L_x L_y}} \begin{pmatrix} 0 \\ 1 \\ 0 \end{pmatrix} e^{\pm i \omega z},
\end{aligned} \tag{2.38}$$

$$\begin{aligned}
\mathbf{E} &= \frac{1}{\sqrt{L_x L_y}} \begin{pmatrix} 0 \\ 1 \\ 0 \end{pmatrix} e^{\pm i \omega z} \\
\mathbf{H} &= \frac{\mp 1}{\sqrt{L_x L_y}} \begin{pmatrix} 1 \\ 0 \\ 0 \end{pmatrix} e^{\pm i \omega z},
\end{aligned} \tag{2.39}$$

where the sign is chosen based on whether the wave is traveling in the positive (upper sign) or negative (lower sign) z -direction.

The admittance of a normally incident wave is 1.

In Sec. 2.1 above, the terms W_k refer only to the x, y components of the electric component of the plane wave. For the two varieties of normally incident plane wave, this is

$$W_k = \frac{1}{\sqrt{L_x L_y}} \begin{pmatrix} 1 \\ 0 \end{pmatrix} \quad (2.40a)$$

$$W_k = \frac{1}{\sqrt{L_x L_y}} \begin{pmatrix} 0 \\ 1 \end{pmatrix}. \quad (2.40b)$$

2.2.2 Waveguide Modes in a Rectangular Waveguide

Inside the holes, waveguide modes form a basis for solutions of Maxwell's equations (Jackson (1999)). Each mode must satisfy the matching conditions associated with Maxwell's equations at the walls of the waveguide. For a perfectly conducting metal, the components of the electric field tangential to the surface must be zero. For rectangular holes, this means that $E_z \equiv 0$ on the walls, while E_x is zero on walls parallel to the x -axis and E_y is zero on walls parallel to the y -axis.

Waveguide modes in a perfect conductor, similarly to plane waves, come in two varieties: transverse electric (TE) modes, which have $E_z = 0$ everywhere, and transverse magnetic (TM) modes, which have $H_z = 0$ everywhere. For the rectangular waveguide, we will enumerate both varieties with a pair of nonnegative integers $\alpha = (m, n)$.

The inner products of the rectangular waveguide modes with the plane waves that are required in the matching procedure can be calculated by hand, and are given in Appendix A.

Let a and b be the width of the rectangular waveguide in the x - and y -directions, respectively. Then the waveguide modes are as follows (at first without normaliza-

tion, for clarity):

TE modes

$$\begin{aligned}
 E &= \frac{i\omega}{\gamma^2} \begin{pmatrix} \frac{-n\pi}{b} \cos\left(\frac{m\pi x}{a}\right) \sin\left(\frac{n\pi y}{b}\right) \\ \frac{m\pi}{a} \sin\left(\frac{m\pi x}{a}\right) \cos\left(\frac{n\pi y}{b}\right) \\ 0 \end{pmatrix} e^{\pm ik_z z} \\
 H &= \begin{pmatrix} \frac{\mp ik_z}{\gamma^2} \frac{m\pi}{a} \sin\left(\frac{m\pi x}{a}\right) \cos\left(\frac{n\pi y}{b}\right) \\ \frac{\mp ik_z}{\gamma^2} \frac{n\pi}{b} \cos\left(\frac{m\pi x}{a}\right) \sin\left(\frac{n\pi y}{b}\right) \\ \cos\left(\frac{m\pi x}{a}\right) \cos\left(\frac{n\pi y}{b}\right) \end{pmatrix} e^{\pm ik_z z},
 \end{aligned} \tag{2.41}$$

where the sign is chosen depending on whether the mode is traveling in the positive (top sign) or negative (bottom sign) z -direction; where m, n are nonnegative integers; and where γ and k_z are defined by

$$\gamma^2 = \omega^2 - k_z^2 = \pi^2 \left(\frac{m^2}{a^2} + \frac{n^2}{b^2} \right) \tag{2.42}$$

in order to satisfy Maxwell's equations. The admittance of a TE mode is $Y_{m,n} = k_z/\omega$.

In Sec. 2.1 above, the terms M_α refer only to the x, y components of the electric part of the waveguide mode. For a rectangular TE mode, this is (properly normalized according to Eq. (2.14))

$$M_{m,n} = \begin{pmatrix} (-n/b) \cos\left(\frac{m\pi}{a}(x + a/2)\right) \sin\left(\frac{n\pi}{b}(y + b/2)\right) \\ (m/a) \sin\left(\frac{m\pi}{a}(x + a/2)\right) \cos\left(\frac{n\pi}{b}(y + b/2)\right) \end{pmatrix} / \sqrt{\frac{b^2 m^2 + a^2 n^2}{4ab}}, \tag{2.43}$$

unless m or n is zero, in which case the denominator in the square root is $2ab$ instead of $4ab$. (This is only true for TE modes.)

TM modes

$$\begin{aligned}
E &= \begin{pmatrix} \frac{ik_z}{\gamma^2} \frac{m\pi}{a} \cos\left(\frac{m\pi x}{a}\right) \sin\left(\frac{n\pi y}{b}\right) \\ \frac{ik_z}{\gamma^2} \frac{n\pi}{b} \sin\left(\frac{m\pi x}{a}\right) \cos\left(\frac{n\pi y}{b}\right) \\ \pm \sin\left(\frac{m\pi x}{a}\right) \sin\left(\frac{n\pi y}{b}\right) \end{pmatrix} e^{\pm ik_z z} \\
H &= \frac{i\omega}{\gamma^2} \begin{pmatrix} \mp \frac{n\pi}{b} \sin\left(\frac{m\pi x}{a}\right) \cos\left(\frac{n\pi y}{b}\right) \\ \pm \frac{m\pi}{a} \cos\left(\frac{m\pi x}{a}\right) \sin\left(\frac{n\pi y}{b}\right) \\ 0 \end{pmatrix} e^{\pm ik_z z},
\end{aligned} \tag{2.44}$$

where the sign is chosen depending on whether the mode is traveling in the positive (top sign) or negative (bottom sign) z -direction; where m, n are nonnegative integers; and where γ and k_z are defined by

$$\gamma^2 = \omega^2 - k_z^2 = \pi^2 \left(\frac{m^2}{a^2} + \frac{n^2}{b^2} \right) \tag{2.45}$$

in order to satisfy Maxwell's equations. The admittance of a TE mode is $Y_{m,n} = \omega/k_z$.

In Sec. 2.1 above, the terms M_α refer only to the x, y components of the electric part of the waveguide mode. For a rectangular TM mode, this is (properly normalized according to Eq. (2.14))

$$M_{m,n} = \begin{pmatrix} (m/a) \cos\left(\frac{m\pi}{a}(x + a/2)\right) \sin\left(\frac{n\pi}{b}(y + b/2)\right) \\ (n/b) \sin\left(\frac{m\pi}{a}(x + a/2)\right) \cos\left(\frac{n\pi}{b}(y + b/2)\right) \end{pmatrix} / \sqrt{\frac{b^2 m^2 + a^2 n^2}{4ab}}. \tag{2.46}$$

(The change in this expression listed above for $m = 0$ or $n = 0$ is only necessary for TE modes, not for TM modes.)

2.2.3 Waveguide Modes in a Circular Waveguide

To find the waveguide modes for a circular waveguide, we convert the Helmholtz equation (2.9) for E_z (for the TM waves) or H_z (for the TE waves) to its polar form

$$\psi_{rr} + \frac{1}{r}\psi_r + \frac{1}{r^2}\psi_{\theta\theta} + \gamma^2\psi = 0 \tag{2.47}$$

where here $\gamma^2 = \epsilon\omega^2 - k_z^2$. We separate variables by writing $\psi = \Theta(\theta)\rho(r)$ and multiply by $r^2/\Theta\rho$ to find

$$r^2\frac{\rho''}{\rho} + r\frac{\rho'}{\rho} + \gamma^2r^2 = -\frac{\Theta''}{\Theta} = A^2 \quad (2.48)$$

for arbitrary constant A . There are two independent solutions to the Θ equation, which we choose to be $\sin(A\theta)$ and $\cos(A\theta)$, while the equation for ρ is the Bessel equation with solution $J_A(\gamma r)$. (The Bessel functions of the second kind Y_A are not allowed since they diverge at zero.) The fields must match (and be differentiable) at $\theta = 0$ and $\theta = 2\pi$, so A must be an integer, hereafter called n .

Suppose that the hole is centered at $x = y = 0$ and has radius R . The matching condition that the tangential components of E must be zero at the surface of the hole implies that the Bessel function $J_n(\gamma R)$ for TM modes or $J'_n(\gamma R)$ for TE modes (see explanation below Eq. (2.51)) must be zero. This means that γR may take on only a countable number of values defined by the zeroes of J_n ; these zeroes will be enumerated by the positive integer m .

Once we have the z -component of the waveguide modes, the x, y components may be recovered for TM modes via (see Jackson (1999))

$$\mathbf{E}_t = \frac{ik_z}{\gamma^2}\nabla_t E_z, \quad \mathbf{H}_t = \frac{\epsilon\omega}{k_z}\mathbf{e}_3 \times \mathbf{E}_t, \quad (2.49)$$

where $\mathbf{E}_t = (E_x, E_y)$, $\mathbf{H}_t = (H_x, H_y)$, and $\mathbf{e}_3 = (0, 0, 1)$; and for TE modes,

$$\mathbf{H}_t = \frac{ik_z}{\gamma^2}\nabla_t H_z, \quad \mathbf{E}_t = \frac{-\omega}{k_z}\mathbf{e}_3 \times \mathbf{H}_t. \quad (2.50)$$

Alternatively, we may solve for the modes in cylindrical component form with \mathbf{E}, \mathbf{H} with (see Snitzer (1961))

$$\begin{aligned}
E_r &= \frac{ik_z}{\gamma^2} \left[\frac{\partial E_z}{\partial r} + \left(\frac{\omega}{rk_z} \right) \frac{\partial H_z}{\partial \theta} \right] \\
E_\theta &= \frac{ik_z}{\gamma^2} \left[\left(\frac{1}{r} \right) \frac{\partial E_z}{\partial \theta} - \left(\frac{\omega}{k_z} \right) \frac{\partial H_z}{\partial r} \right] \\
H_r &= \frac{ik_z}{\gamma^2} \left[- \left(\frac{\epsilon\omega}{rk_z} \right) \frac{\partial E_z}{\partial \theta} + \frac{\partial H_z}{\partial r} \right] \\
H_\theta &= \frac{ik_z}{\gamma^2} \left[\left(\frac{\epsilon\omega}{k_z} \right) \frac{\partial E_z}{\partial r} + \left(\frac{1}{r} \right) \frac{\partial H_z}{\partial \theta} \right].
\end{aligned} \tag{2.51}$$

From these equations and the above discussion we see that for a TM mode, which has $H_z = 0$, the radial component of \mathbf{E} has r -dependence $J_n(\gamma r)$. Because the components of \mathbf{E} tangential to the walls of the waveguide are the r - and z -components which must be zero at $r = R$, we require for TM modes that $J_n(\gamma R)$ is zero. However, for a TE mode which has $E_z = 0$, the radial component of \mathbf{E} has r -dependence $J'_n(\gamma r)$ instead. Therefore a TM mode requires that $J'_n(\gamma R)$ is zero.

The conversion between Cartesian and cylindrical coordinate systems for a vector \mathbf{U} is

$$\begin{aligned}
U_x &= U_r \cos(\theta) - U_\theta \sin(\theta), \\
U_y &= U_r \sin(\theta) + U_\theta \cos(\theta),
\end{aligned} \tag{2.52}$$

with $x = r \cos(\theta)$ and $y = r \sin(\theta)$. The inner products required for the matching procedure can be computed in either coordinate system.

Modes inside a circular waveguide, therefore, are identified by whether they are TE or TM modes; by whether the θ dependence is sine or cosine; by the nonnegative integer index of the Bessel function J_n ; and by the location of a root of J_n for TM modes or J'_n for TE modes. The normalized modes are orthonormal and form a basis for solutions of the Helmholtz equation inside the waveguide.

Here we present the waveguide modes in polar coordinates. The Cartesian forms may be found using Eq. (2.52). The full vector expressions for the waveguide modes (without normalization, which must be done by numerical integration) are:

TM modes (*cosine variety*)

$$\begin{aligned}
E_z &= \cos(n\theta)J_n(\gamma r)e^{ik_z z} & H_z &= 0 \\
E_r &= \frac{ik_z}{\gamma^2} \cos(n\theta)J'_n(\gamma r)e^{ik_z z} & H_r &= \frac{in\epsilon\omega}{r\gamma^2} \sin(n\theta)J_n(\gamma r)e^{ik_z z} \\
E_\theta &= \frac{-ink_z}{r\gamma^2} \sin(n\theta)J_n(\gamma r)e^{ik_z z} & H_\theta &= \frac{i\epsilon\omega}{\gamma} \cos(n\theta)J'_n(\gamma r)e^{ik_z z}
\end{aligned} \tag{2.53}$$

where the derivatives are with respect to the arguments of the function J_n , where

$$\gamma = \gamma_{mn} = \sqrt{\omega^2 - k_z^2} = u_{mn}/R, \tag{2.54}$$

and where u_{mn} is the m^{th} root of the Bessel function J_n . The admittance of a TM mode is $Y_{mn} = \omega/k_z$.

TM modes (*sine variety*)

$$\begin{aligned}
E_z &= \sin(n\theta)J_n(\gamma r)e^{ik_z z} & H_z &= 0 \\
E_r &= \frac{ik_z}{\gamma^2} \sin(n\theta)J'_n(\gamma r)e^{ik_z z} & H_r &= \frac{-in\epsilon\omega}{r\gamma^2} \cos(n\theta)J_n(\gamma r)e^{ik_z z} \\
E_\theta &= \frac{ink_z}{r\gamma^2} \cos(n\theta)J_n(\gamma r) & H_\theta &= \frac{i\epsilon\omega}{\gamma} \sin(n\theta)J'_n(\gamma r),
\end{aligned} \tag{2.55}$$

with the same admittance and values of γ , k_z and u_{mn} as in the TM cosine variety.

TE modes (*cosine variety*)

$$\begin{aligned}
E_z &= 0 & H_z &= \cos(n\theta)J_n(\gamma r)e^{ik_z z} \\
E_r &= \frac{-in\omega}{\gamma^2 r} \sin(n\theta)J_n(\gamma r)e^{ik_z z} & H_r &= \frac{ik_z}{\gamma^2} \cos(n\theta)J'_n(\gamma r)e^{ik_z z} \\
E_\theta &= \frac{-i\omega}{\gamma^2} \cos(n\theta)J'_n(\gamma r)e^{ik_z z} & H_\theta &= \frac{-ink_z}{\gamma^2 r} \sin(n\theta)J_n(\gamma r)e^{ik_z z}
\end{aligned} \tag{2.56}$$

where the derivatives are with respect to the arguments of the function J_n , where

$$\gamma = \gamma_{mn} = \sqrt{\omega^2 - k_z^2} = u_{mn}/R, \tag{2.57}$$

and where u_{mn} is the m^{th} root of the Bessel function J'_n . The admittance of a TE mode is $Y_{mn} = k_z/\omega$,

TE modes (*sine variety*)

$$\begin{aligned}
E_z &= 0 & H_z &= \sin(n\theta)J_n(\gamma r)e^{ik_z z} \\
E_r &= \frac{i\omega}{\gamma^2 r} \cos(n\theta)J_n(\gamma r)e^{ik_z z} & H_r &= \frac{ik_z}{\gamma^2} \sin(n\theta)J'_n(\gamma r)e^{ik_z z} \\
E_\theta &= \frac{-i\omega}{\gamma^2} \sin(n\theta)J'_n(\gamma r)e^{ik_z z} & H_\theta &= \frac{ink_z}{\gamma^2 r} \cos(n\theta)J_n(\gamma r)e^{ik_z z},
\end{aligned} \tag{2.58}$$

with the same admittance and values of γ , k_z and u_{mn} as in the TE cosine variety.

2.3 Explicit Waveguide Modes and Plane Waves for the 1-dimensionally Periodic System

We may apply the same techniques to a system that is constant in one direction (here, y) and periodic in the other (x) to simulate transmission through an array of infinite bars and slits. The incident wave is assumed constant in the y -direction also, and therefore all waveguide modes and reflected and transmitted waves will be as well. Therefore the field is truly 2-dimensional. The formulae are the same except for the expressions for the plane waves and waveguide modes, which we list here.

2.3.1 Plane Waves for the 1-dimensionally Periodic System

Because the system is constant in the y -direction, there is only one degree of freedom in the angle of each plane wave instead of two. Plane waves still, however, come in p - and s - polarized varieties. Let L_x be the period width in the x -direction. Then the allowed wave vectors are

$$k_x = k_{x0} + \frac{2\pi j_1}{L_x}, \quad (2.59)$$

with $k_y = 0$ and $k_z^2 = \omega^2 - k_x^2$. The explicit expressions for the plane waves, properly normalized according to Eq. (2.15), are:

p -polarization

$$W_k = \begin{pmatrix} k_x \\ 0 \end{pmatrix} \frac{e^{ik_x x}}{\sqrt{L_x |k_x|}}. \quad (2.60)$$

The admittance of a p -polarized plane wave is $Y_k = \omega/k_z$, where $k_z^2 = \omega^2 - k_x^2$.

s -polarization

$$W_k = \begin{pmatrix} 0 \\ k_x \end{pmatrix} \frac{e^{ik_x x}}{\sqrt{L_x |k_x|}}. \quad (2.61)$$

The admittance of a s -polarized plane wave is $Y_k = k_z/\omega$, where $k_z^2 = \omega^2 - k_x^2$.

Normal Incidence

For normally incident plane waves with $k_x = 0$, the distinction between p - and s -polarization is arbitrary. However, unlike the case of 2-dimensional periodicity, the two types of normally incident plane waves cause very different behavior. We name them x - and y -polarized after the component of \mathbf{E} which is nonzero:

$$W_k = \begin{pmatrix} 1 \\ 0 \end{pmatrix} \frac{1}{\sqrt{L_x}} \quad (2.62)$$

$$W_k = \begin{pmatrix} 0 \\ 1 \end{pmatrix} \frac{1}{\sqrt{L_x}}. \quad (2.63)$$

The admittance of a normally incident plane wave is 1, and $k_z = \omega$.

2.3.2 Waveguide Modes for the 1-dimensionally Periodic System

If we assume that the film and the field are constant in the y -direction, then we may remove the ∂_y terms in Maxwell's equations, which causes them to decouple into two sets, one involving E_y, H_x, H_z ,

$$\begin{aligned} -\partial_z E_y &= i\omega H_x \\ \partial_x E_y &= i\omega H_z \\ \partial_z H_x - \partial_x H_z &= -i\epsilon\omega E_y \end{aligned} \quad (2.64)$$

and the other involving E_x, E_z, H_y ,

$$\begin{aligned} -\partial_z H_y &= -i\epsilon\omega E_x \\ \partial_x H_y &= -i\epsilon\omega E_z \\ \partial_z E_x - \partial_x E_z &= i\omega H_y. \end{aligned} \quad (2.65)$$

Assuming z -dependence of $\exp(ik_z z)$, each field component must satisfy the Helmholtz equation

$$(\partial_x^2 + \epsilon\omega^2 - k_z^2) \psi = 0. \quad (2.66)$$

Waveguide mode solutions to these equations still divide into TE and TM varieties, and in addition there is a TEM mode which has both E_z and H_z equal to zero.

The inner products according to Eq. (2.15) of the plane waves with the waveguide modes can be calculated by hand, and are given in Appendix A.

Let a be the width of the slits in the x -direction. The waveguide modes will be enumerated by $\alpha = m$ for integers $m \geq 0$. Their full expressions for the waveguide modes are as follows.

TE modes

$$\begin{aligned}
 E_y &= \sqrt{\frac{2}{a}} \sin\left(\frac{m\pi(x+a/2)}{a}\right) e^{\pm ik_z z} \\
 H_x &= \sqrt{\frac{2}{a}} \frac{\pm k_z}{\omega} \sin\left(\frac{m\pi(x+a/2)}{a}\right) e^{\pm ik_z z} \\
 H_z &= \sqrt{\frac{2}{a}} \frac{im\pi}{\omega a} \cos\left(\frac{m\pi(x+a/2)}{a}\right) e^{\pm ik_z z} \\
 E_z &= E_z = H_y = 0,
 \end{aligned} \tag{2.67}$$

where m is any nonnegative integer. The admittance of a TE mode is $Y_m = k_z/\omega$, where

$$k_z^2 = \omega^2 - \frac{m^2\pi^2}{a^2}. \tag{2.68}$$

In Sec. 2.1 above, the terms M_α refer only to the x, y components of the electric part of the waveguide mode. For a TE mode in an infinite slit, this is (properly normalized according to Eq. (2.15))

$$M_m = \sqrt{\frac{2}{a}} \left(\begin{array}{c} 0 \\ \sin\left(\frac{m\pi(x+a/2)}{a}\right) \end{array} \right). \tag{2.69}$$

TM modes

$$\begin{aligned}
E_x &= \sqrt{\frac{2}{a}} \cos\left(\frac{m\pi(x+a/2)}{a}\right) e^{\pm ik_z z} \\
E_z &= \sqrt{\frac{2}{a}} \frac{\mp im\pi}{k_z a} \sin\left(\frac{m\pi(x+a/2)}{a}\right) e^{\pm ik_z z} \\
H_y &= \sqrt{\frac{2}{a}} \frac{\mp \omega}{k_z} \cos\left(\frac{m\pi(x+a/2)}{a}\right) e^{\pm ik_z z} \\
E_y &= H_x = H_z = 0,
\end{aligned} \tag{2.70}$$

where m is any *positive* integer. The admittance of a TM mode is $Y_m = \omega/k_z$, where

$$k_z^2 = \omega^2 - \frac{m^2\pi^2}{a^2}. \tag{2.71}$$

In Sec. 2.1 above, the terms M_α refer only to the x, y components of the electric part of the waveguide mode. For a TM mode in an infinite slit, this is (properly normalized according to Eq. (2.15))

$$M_m = \sqrt{\frac{2}{a}} \begin{pmatrix} \cos\left(\frac{m\pi(x+a/2)}{a}\right) \\ 0 \end{pmatrix}. \tag{2.72}$$

TEM mode

$$\begin{aligned}
E_x &= \frac{e^{\pm i\omega z}}{\sqrt{a}} \\
H_y &= \mp \frac{e^{\pm ik_z z}}{\sqrt{a}} \\
E_y &= E_z = H_x = H_z = 0.
\end{aligned} \tag{2.73}$$

The admittance of this mode is $Y = 1$, and $k_z = \omega$.

In Sec. 2.1 above, the terms M_α refer only to the x, y components of the electric part of the waveguide mode. For a TEM mode in an infinite slit, this is (properly normalized according to Eq. (2.15))

$$M_m = \sqrt{\frac{1}{a}} \begin{pmatrix} 1 \\ 0 \end{pmatrix}. \quad (2.74)$$

2.4 Structure of the Matrix Equation and Alternate Formulations

We return for a moment to discuss the structure of the final matrix equation (2.25), (2.24) developed in Sec. 2.1,

$$\begin{pmatrix} G - S & -G^V \\ -G^V & G - S \end{pmatrix} \begin{pmatrix} X \\ X' \end{pmatrix} = \begin{pmatrix} I \\ 0 \end{pmatrix}, \quad (2.75)$$

where the matrix \mathbf{G} on the left and the vector $\mathbf{I} = (I, 0)^T$ are determined by the geometry and the incident plane wave, and the solution vector $\mathbf{X} = (X, X')^T$ yields the modal amplitudes

The entries of these matrices are defined in Eq. (2.20),

$$\begin{aligned} G_{\alpha\beta} &= i \sum_k Y_k(M_\alpha, W_k)(W_k, M_\beta) & I_\alpha &= 2iY_{k_0}(W_{k_0}, M_\alpha) \\ G_\alpha^V &= \frac{2iY_\alpha}{e_\alpha^2 - e_\alpha^{-2}} & S_\alpha &= iY_\alpha \frac{e_\alpha^2 + e_\alpha^{-2}}{e_\alpha^2 - e_\alpha^{-2}}, \end{aligned} \quad (2.76)$$

where the inner products (M_α, W_k) and (W_k, M_β) depend on the shape of the holes, and are given for rectangular holes and infinite slits in Appendix A.

The matrices S and G^V are diagonal. The matrix G has some interesting symmetry as well. Note that the inner products have the property that

$$(M_\alpha, W_k) = (W_k, M_\alpha)^*, \quad (2.77)$$

while the number Y_k is real for some values of k and purely imaginary for other values of k . Thus if Y_k is imaginary, then $iY_k(M_\alpha, W_k)(W_k, M_\beta) = [iY_k(M_\beta, W_k)(W_k, M_\alpha)]^*$. On the other hand, if Y_k is real, then $iY_k(M_\alpha, W_k)(W_k, M_\beta) = -[iY_k(M_\beta, W_k)(W_k, M_\alpha)]^*$. So the matrix G is neither Hermitian nor anti-Hermitian; however, its division into a sum of Hermitian and anti-Hermitian matrices is very clear and natural.

Unfortunately, we have not found that the matrix \mathbf{G} is compact, normal, Fredholm of the second kind, or regular in other well-known ways. For future efforts in this direction we will record here an alternate, equivalent formulation of the matrix equation, and the matrix equation for a one-sided film. In addition, after introduction to the concepts in Chap. 3, we will briefly discuss the null space of \mathbf{G} in Sec. 3.4.

2.4.1 An Equivalent Matrix Formulation

Returning to Eqs. (2.16), (2.17), we can obtain an different but equivalent matrix equation.

$$r_k = -\delta_{k,k_0} + \sum_{\alpha} (W_k, M_\alpha) (A_\alpha e_\alpha^{-1} + B_\alpha e_\alpha) \quad (2.78a)$$

$$t_k = \sum_{\alpha} (W_k, M_\alpha) (A_\alpha e_\alpha + B_\alpha e_\alpha^{-1}) \quad (2.78b)$$

$$-\sum_k Y_k r_k(M_\alpha, W_k) = -Y_{k_0}(M_\alpha, W_{k_0}) + Y_\alpha (A_\alpha e_\alpha^{-1} - B_\alpha e_\alpha) \quad (2.79a)$$

$$\sum_k Y_k t_k(M_\alpha, W_k) = Y_\alpha (A_\alpha e_\alpha - B_\alpha e_\alpha^{-1}). \quad (2.79b)$$

Previously, we proceeded to insert the expressions (2.78) for t_k and r_k into Eqs. (2.79). We can instead, however, solve Eqs. (2.79) for the terms A_α and B_α and insert these expressions into Eqs. (2.78). If we define

$$\begin{aligned}
Q_{kl} &= \sum_{\alpha} \left(\frac{e_{\alpha}^2 + e_{\alpha}^{-2}}{e_{\alpha}^2 - e_{\alpha}^{-2}} \right) \frac{(W_k, M_{\alpha})Y_l(M_{\alpha}, W_l)}{Y_{\alpha}} \\
P_{kl} &= \sum_{\alpha} \left(\frac{2}{e_{\alpha}^2 - e_{\alpha}^{-2}} \right) \frac{(W_k, M_{\alpha})Y_l(M_{\alpha}, W_l)}{Y_{\alpha}},
\end{aligned} \tag{2.80}$$

where k, l each enumerate the plane waves and α enumerates the waveguide modes as usual; and if we let \mathbf{r} and \mathbf{t} denote the vectors with entries r_k and t_k respectively, and I_{k_0} be the vector with the number 1 in the k_0^{th} entry and zeroes otherwise, and I be the identity matrix; then we obtain the matrix equation

$$\begin{bmatrix} Q - I & P \\ P & Q - I \end{bmatrix} \begin{bmatrix} \mathbf{r} - I_{k_0} \\ \mathbf{t} \end{bmatrix} = \begin{bmatrix} 2I_{k_0} \\ 0 \end{bmatrix}. \tag{2.81}$$

Here the rows and columns of the matrix on the left, and the vectors in the middle and right, are enumerated by the plane waves, instead of being enumerated by the waveguide modes as the previous matrix equation was.

One advantage of this formulation is the simplicity of the vector on the right side, which contains only a single nonzero number. A disadvantage, however, is that the near-symmetry of the matrix on the left is lost, because of the presence of the term Y_l in the definition of Q_{kl} and P_{kl} that in general does not have any relation to Y_k .

2.4.2 The One-sided Film

The same method can be used to calculate reflection and transmission of energy when the metal and holes are infinite in depth, and there is no transmission region. In this case the waveguide modes will only propagate in one direction. Using the same techniques we find that Eqs. (2.16), (2.17) become

$$r_k = -\delta_{k,k_0} + \sum_{\alpha} (W_k, M_{\alpha}) (A_{\alpha} e_{\alpha}^{-1}) \quad (2.82)$$

$$-\sum_k Y_k r_k(M_{\alpha}, W_k) = -Y_{k_0}(M_{\alpha}, W_{k_0}) + Y_{\alpha} (A_{\alpha} e_{\alpha}^{-1}). \quad (2.83)$$

If we let the matrix G and the vectors X and I have entries

$$\begin{aligned} X_{\alpha} &= A_{\alpha} e_{\alpha}^{-1} \\ I_{\alpha} &= 2iY_{k_0}(W_{k_0}, M_{\alpha}) \\ G_{\alpha\beta} &= i \sum_k Y_k(M_{\alpha}, W_k)(W_k, M_{\beta}), \end{aligned} \quad (2.84)$$

and let the matrix Y be the diagonal matrix with entries Y_{α} , then we obtain the matrix equation

$$(G + iY) X = I. \quad (2.85)$$

Rayleigh Anomalies and Transmission Maxima

The role of periodicity in our metal film is twofold. In the previous chapter, periodicity allowed us to invoke Bloch theory, which ensured that only countably many plane waves were needed to construct the solution to Maxwell's equations outside the film, and that matching needed be enforced over only a single period cell.

Periodicity also causes the phenomenon known as the Rayleigh anomaly. When the direction of propagation of one of the potential reflected plane waves outside the film becomes close to parallel to the surface of the metal, the transmission of energy into and through the holes is significantly reduced. The condition for a plane wave to propagate parallel to the surface of the metal is $k_z = 0$, or equivalently (see Eq. (2.31)),

$$k_x^2 + k_y^2 = \omega^2. \quad (3.1)$$

(For the 1-dimensionally periodic case, the condition is $k_x^2 = \omega^2$.) When this occurs, the admittance $Y_k = \omega/k_z$ of the p -polarized ($H_z = 0$) plane wave variety becomes infinite. This causes every nonzero element of the matrix G defined in Eq. (2.20)

to become infinite, and so upon solving the matrix equation $\mathbf{GX} = \mathbf{I}$ (2.24) in a neighborhood of a frequency satisfying this condition, the solution \mathbf{X} must be small.

For example, a plane wave normally incident on a two-dimensionally square-periodic array of square holes has $k_{0x} = k_{0y} = 0$ and $L = L_x = L_y$, and so the allowable reflected and transmitted plane waves have wavevector (see Eq. (2.32))

$$\begin{pmatrix} k_x \\ k_y \end{pmatrix} = \frac{2\pi}{L} \begin{pmatrix} j_1 \\ j_2 \end{pmatrix}, \quad (3.2)$$

where j_1, j_2 are any integers. Therefore, we expect Rayleigh anomalies to appear at

$$\omega = \frac{2\pi}{L}, \quad \frac{2\pi}{L}\sqrt{2}, \quad \frac{2\pi}{L}2, \quad \frac{2\pi}{L}\sqrt{5}, \quad \frac{2\pi}{L}\sqrt{8}, \quad (3.3)$$

etc.. Define $\lambda = 2\pi/\omega$. A plot of transmission against λ/L is shown in Fig. 3.1a for square and circular holes. As expected, the transmission near $\lambda/L = 1, 1/\sqrt{2}, 1/2,$ and $1/\sqrt{5}$ experiences sharp dips, becoming essentially zero.

The transmission minima that occur at the frequencies of the Rayleigh anomalies are often associated with nearby transmission maxima as well. These also appear in Fig. 3.1. Close to the primary Rayleigh anomaly that occurs when the frequency is equal to the period width, there are two transmission maxima, one narrower than the other, which both reach 100% transmission. There is also a less prominent double peak near $\lambda = L/\sqrt{2}$.

The one-dimensionally periodic case is similar, as seen in the right-side picture in Fig. 3.1. The Rayleigh anomaly is seen at $\lambda/L = 1, 1/2, 1/3, 1/4,$ etc.. There is only one transmission maximum near $\lambda = L$ instead of two, however, and the other Rayleigh anomalies do not reach down to zero transmission.

At the location of the transmission maxima, all of the energy from the reflected side of the film must travel through the holes to the transmitted side. Because of

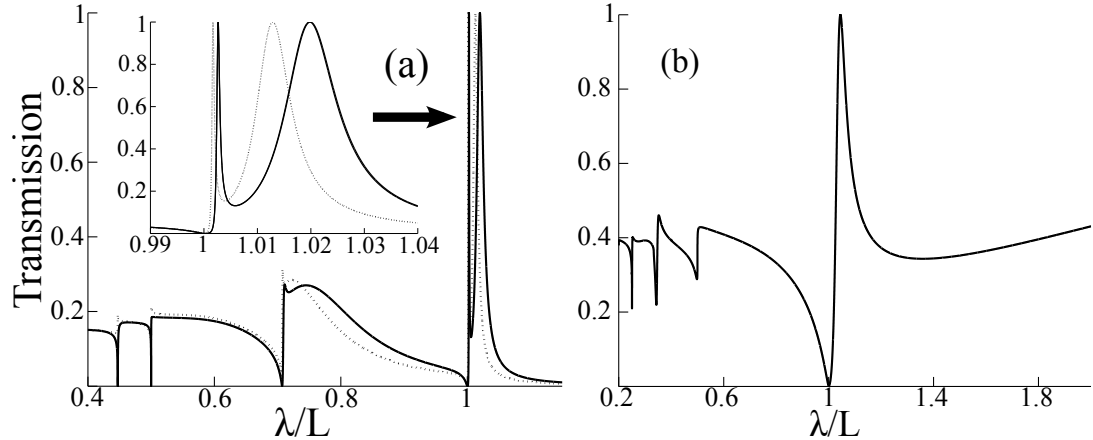


FIGURE 3.1: (a) Transmission profile, calculated using Eq. (2.27) for a range of wavelengths λ , for a normally incident plane wave on a 2-dimensionally periodic array of square holes. The period lattice is square with side length L , and the thickness of the slab is $h = 0.2L$. The solid line is for square holes with side length $a = 0.4L$, and the dotted line is for circular holes of the same area. Inset: Closeup of the twin maximum near $\lambda/L = 1$. (b) Transmission profile for a normally incident x -polarized plane wave on a 1-dimensionally periodic array of slits. The width of the hole is $a = 0.39L$; and the thickness of the slab is $h = 0.2L$, where L is the period width.

this, large energy fields can build up inside the holes. See Fig. 3.2, which displays $\Re(E_x)$ in a cross section of the infinite slits in a one-dimensionally periodic film. Large concentrations of energy exist inside the holes, concentrated at the corners. This suggests practical applications for energy collection. (The sharp corners of the holes are discussed briefly in the introduction to Chap. 4.)

The locations of the Rayleigh anomalies are easily predicted by Eq. (3.1). They change with the angle of the incident plane wave, as we will discuss in Sec. 3.1, and with the alteration of the hole arrangements as we will discuss in Sec. 3.2. The location and behavior of the transmission maxima are less straightforward to predict, but one method for doing so is discussed in Sec. 3.3.

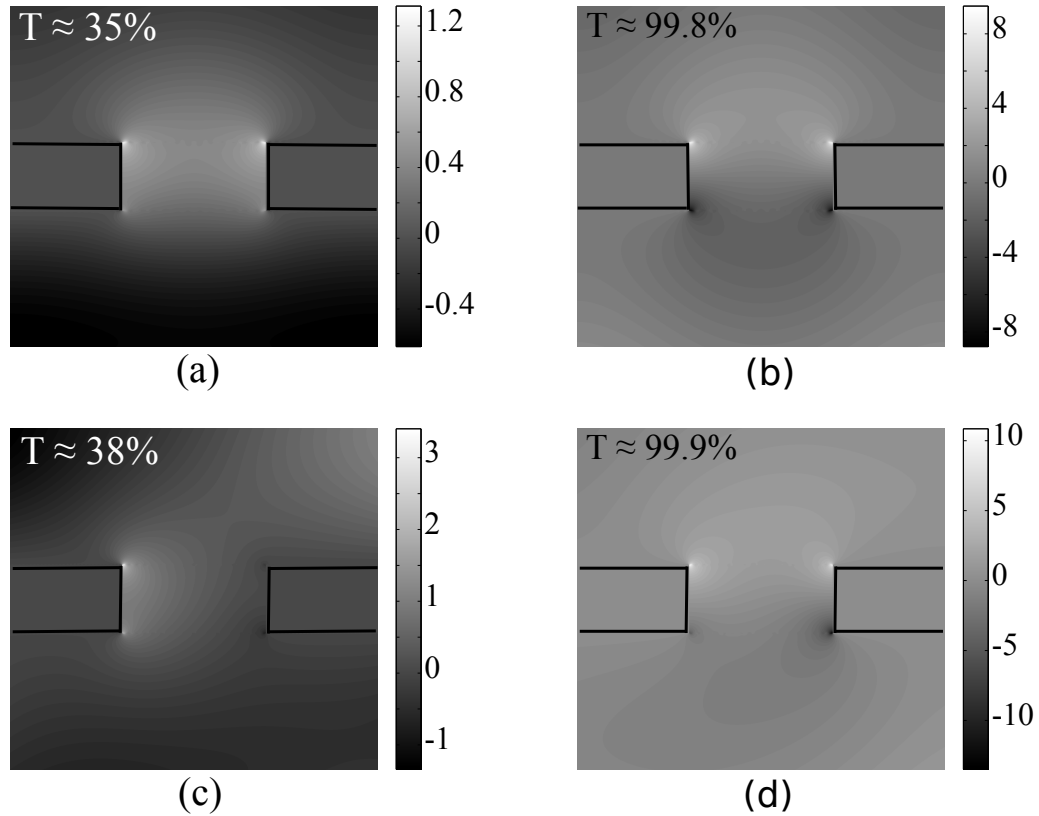


FIGURE 3.2: Cross section of $\Re(E_x)$ for a 1-dimensionally periodic film, calculated by summing modes from Secs. 2.3.1, 2.3.2 with amplitudes determined by Eqs. (2.25). (For the illustrated cases E_y is negligible.) Hole width is $a = 0.39L$, and the thickness of the film is $h = 0.2L$, for period width L . (a) Normal incidence with wavelength $\lambda = 1.4L$. The transmission is $T \approx 35\%$. (b) Normal incidence with $\lambda = 1.043L$, for which $T \approx 99.8\%$. Note higher field strengths associated with the extraordinary transmission, especially at the hole corners. (c) 20° incidence with $\lambda = 1.5L$, for which $T \approx 38\%$. (d) 20° incidence with $\lambda = 1.3475L$, for which $T \approx 99.9\%$.

3.1 Incidence at an Angle and the Rayleigh Anomaly

Each of the Rayleigh anomalies in Fig. 3.1a may be properly thought of as the intersection of at least four Rayleigh anomalies. At $\lambda = L$, for example, there are four different potential reflected plane waves which are simultaneously parallel to the surface of the metal, those with $(k_x, k_y) = (\pm 2\pi/L, 0)$ and $(0, \pm 2\pi/L)$. We will call this a fourth degree Rayleigh anomaly. At $\lambda = L/\sqrt{5}$, there is an eighth degree

Rayleigh anomaly.

As the angle of the incident plane wave changes, these Rayleigh anomalies bifurcate. For example, if the angle shifts slightly in the x -direction ($\theta_x > 0, \theta_y = 0$), there will be three anomalies near $\lambda = L$: a second-degree anomaly caused by the plane waves with $(k_x, k_y) = (\omega \sin(\theta_x), \pm 2\pi/L)$ at $\lambda = L\sqrt{1 - \sin^2(\theta_x)}$; a first-degree anomaly caused by the plane wave with $(k_x, k_y) = (\omega \sin(\theta_x) + 2\pi/L, 0)$ at $\lambda = L(1 - \sin(\theta_x))$; and a first-degree anomaly caused by the plane wave with $(k_x, k_y) = (\omega \sin(\theta_x) - 2\pi/L, 0)$ at $\lambda = L(1 + \sin(\theta_x))$. This may be seen in Fig. 3.3a.

Similarly, the anomaly at $\lambda = L/\sqrt{2}$ divides into two second-degree anomalies, and as the angle increases, eventually the one with larger value of λ joins with the first-order anomaly at $\lambda = L(1 - \sin(\theta_x))$ described above.

As another example, if the angle of incidence changes equally in the x - and y -directions, then the fourth-degree anomaly at $\lambda = L$ will divide into two second-degree anomalies; and if the angle of incidence changes by different amounts in the x - and y -directions, then it will divide instead into four first-degree anomalies. The latter case is seen in Fig. 3.3b.

Changing the period cell from square to rectangular (so that $L_x \neq L_y$) has a similar effect. Changing the shape of the holes, however, alters the shape of the curve but not the location of the Rayleigh anomalies. Further changes to the locations of the Rayleigh anomalies can be effected by creating supercells, which are the topic of the next section.

3.2 Supercells

Besides changing the angle of the incident plane wave and the dimensions of the period cell, another way to change the location of the Rayleigh anomaly is to allow our period cell to contain multiple holes in whatever arrangement we like, which we

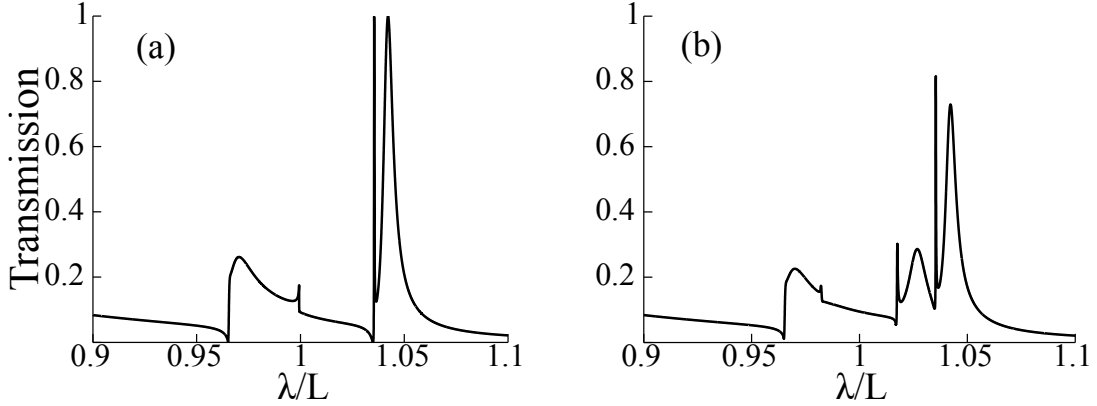


FIGURE 3.3: Transmission profile for a 2-dimensionally periodic slab with square period of side length L , with square holes of side width $a = 0.4L$, with film thickness $h = 0.2L$, and with angles of incidence (a) $\theta_x = 2^\circ, \theta_y = 0^\circ$ and (b) $\theta_x = 2^\circ, \theta_y = 1^\circ$.

call a *supercell*. This procedure will also allow us to create triangular, hexagonal and other hole arrangements within the confines of our rectangular-periodic system.

3.2.1 Alterations to the Matrix Equation

The alterations to the derivation in Chap. 2 are minimal. Define a rectangular period cell with dimensions L_x, L_y . Because we only need to enforce the matching over a single period cell, the basic cell may be centered wherever we like. Place within it any number of holes, which we will enumerate by the letter H . We must calculate all of the waveguide modes in each of the holes separately. If the holes are all the same shape, then the explicit expressions for the waveguide modes will be the same in each hole, save that they will be shifted to the proper location. For example, the normalized expression for a TE mode in a rectangular hole of side lengths a, b centered at x_H, y_H is given by (compare Eq. (2.43))

$$M_{m,n,H} = \frac{\begin{pmatrix} (-n/b) \cos\left(\frac{m\pi}{a}(x + a/2 - x_H)\right) \sin\left(\frac{m\pi}{b}(y + b/2 - y_H)\right) \\ (m/a) \sin\left(\frac{m\pi}{a}(x + a/2 - x_H)\right) \cos\left(\frac{n\pi}{b}(y + b/2 - y_H)\right) \end{pmatrix}}{\sqrt{\frac{b^2 m^2 + a^2 n^2}{4ab}}}. \quad (3.4)$$

In general the holes in the supercell may all have different shapes. Meanwhile, however, the expressions for the plane waves require no alteration.

Only a few more alterations to the calculations in Chap. 2 are needed. First, all terms which are enumerated by α , i.e., $Y_\alpha, A_\alpha, B_\alpha$, etc., must be enumerated by H as well in the sense that they become $Y_{\alpha,H}$, etc., and all sums over α become sums over α and H , referring to the α^{th} mode in hole H . For example, Eqs. (2.16), (2.17) become

$$r_k = -\delta_{k,k_0} + \sum_{\alpha,H} (W_k, M_{\alpha,H}) (A_{\alpha,H} e_{\alpha,H}^{-1} + B_{\alpha,H} e_{\alpha,H}) \quad (3.5a)$$

$$t_k = \sum_{\alpha,H} (W_k, M_{\alpha,H}) (A_{\alpha,H} e_{\alpha,H} + B_{\alpha,H} e_{\alpha,H}^{-1}) \quad (3.5b)$$

$$-\sum_k Y_k r_k(M_{\alpha,H}, W_k) = -Y_{k_0}(M_{\alpha,H}, W_{k_0}) + Y_{\alpha,H} (A_{\alpha,H} e_{\alpha,H}^{-1} - B_{\alpha,H} e_{\alpha,H}) \quad (3.6a)$$

$$\sum_k Y_k t_k(M_{\alpha,H}, W_k) = Y_{\alpha,H} (A_{\alpha,H} e_{\alpha,H} - B_{\alpha,H} e_{\alpha,H}^{-1}). \quad (3.6b)$$

Then, if we define

$$\begin{aligned} X_{\alpha,H} &= A_{\alpha,H} e_{\alpha,H}^{-1} + B_{\alpha,H} e_{\alpha,H} & X'_{\alpha,H} &= -A_{\alpha,H} e_{\alpha,H} - B_{\alpha,H} e_{\alpha,H}^{-1} \\ G_{\alpha,H;\beta,H'} &= i \sum_k Y_k (M_{\alpha,H}, W_k) (W_k, M_{\beta,H'}) \\ I_{\alpha,H} &= 2i Y_{k_0} (W_{k_0}, M_{\alpha,H}) \end{aligned} \quad (3.7)$$

$$G_{\alpha,H}^V = \frac{2i Y_{\alpha,H}}{e_{\alpha,H}^2 - e_{\alpha,H}^{-2}} \quad S_{\alpha,H} = i Y_{\alpha,H} \frac{e_{\alpha,H}^2 + e_{\alpha,H}^{-2}}{e_{\alpha,H}^2 - e_{\alpha,H}^{-2}},$$

we have the same matrix equation

$$\begin{aligned} (G - S)X - G_V X' &= I \\ (G - S)X' - G_V X &= 0, \end{aligned} \quad (3.8)$$

except that this time the size of the vectors and the side lengths of the matrix G are – though they were already infinite – now larger by a factor equal to the number of holes per period cell. The inner products are computed over each hole opening separately by

$$(M_{\alpha,H}, W_k) = \int_{\text{area of hole } H} M_{\alpha,H;x}^* W_{k;x} + M_{\alpha,H;y}^* W_{k;y} \, dx \, dy. \quad (3.9)$$

If the holes are all the same shape, then we need only compute this inner product for a single hole of that shape centered at zero, and then we may use the formula

$$(M_{\alpha,H}, W_k) = (M_{\alpha,H_0}, W_k) \times \exp(-i(x_H k_x + y_H k_y)) \quad (3.10)$$

where H is a hole centered at (x_H, y_H) and H_0 is a hole of the same shape centered at zero.

3.2.2 Examples: Rectangular, Triangular, and Hexagonal Arrays

An example of the use of this method is seen in Fig. 3.4. Here, we begin with a 2-dimensionally periodic array of supercells containing 2 holes. The basic supercell has holes centered at $(0, 0)$ and $(0, 1)$. At first we use $L_x = 1, L_y = 2$, which duplicates the array used in Fig. 3.1. Thereafter, we introduce space between holes after every 2 holes in the y -direction: first $L_y = 2.2$, then $L_y = 2.4$, and then $L_y = 3$. The overall transmission decreases with the ratio of hole area to period area, but more importantly, new Rayleigh anomalies begin to appear.

A similar method can also be used to create non-rectangular arrangements of holes. Two examples follow.

An equilaterally triangular array of holes may be created by using a supercell of size $L_x = 1$ and $L_y = \sqrt{3}$ with two holes: one at $(0, 0)$, and another at $(1/2, \sqrt{3}/2)$. This procedure is depicted in Fig. 3.5, as well as the resulting transmission profile

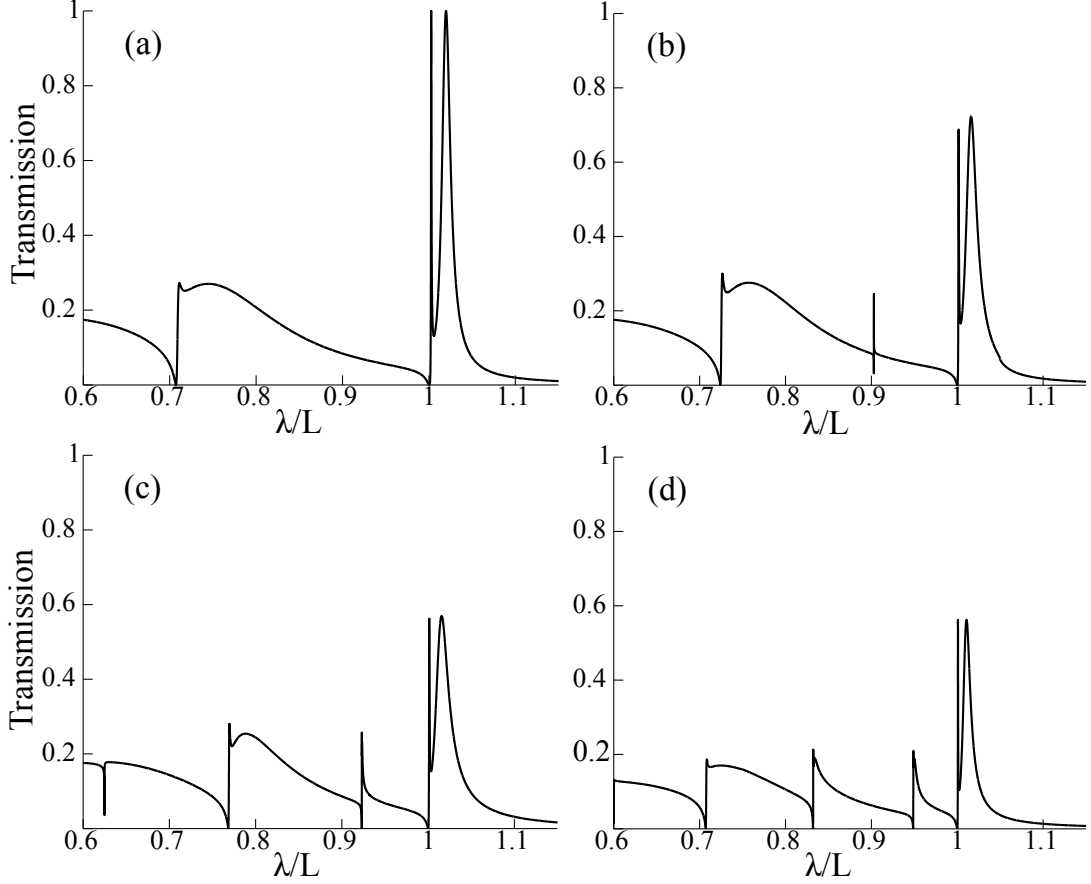


FIGURE 3.4: Transmission profiles for a 2-dimensionally periodic array of supercells containing 2 holes. The basic supercell has holes centered at $(0,0)$ and $(0,1)$. (a) At first we use $L_x = 1, L_y = 2$, which duplicates the array used in Fig. 3.1. (b) Here we use $L_x = 1, L_y = 2.2$, thereby adding a little space after every 2 holes in the y -direction. Note the birth of a new Rayleigh anomaly. (c) Here $L_x = 1, L_y = 2.4$; (d) here $L_x = 1, L_y = 3$.

for a normally incident plane wave. The holes are square with side widths $a = .0192^{1/4} \approx 0.372$ in order to preserve the same ratio of hole area to period area as in Fig. 3.1 for comparison. The twin peaks appear here near $\lambda = L_y/2$, the y -distance between holes, and the second Rayleigh anomaly does not appear until $\lambda = L_x/2$, the x -distance between holes. (This does not violate symmetry, because switching the x - and y - dimensions would result in the same behavior.)

A regular hexagonal array of holes may be created by using a supercell with four

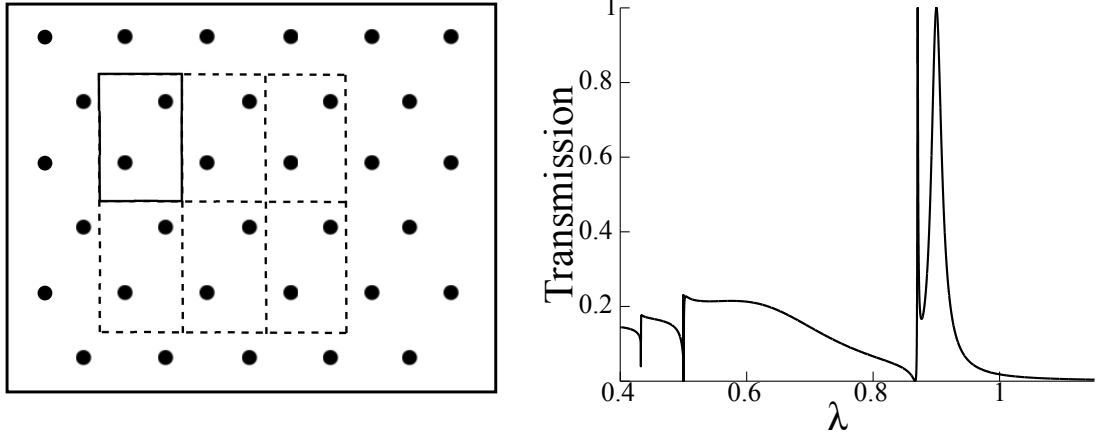


FIGURE 3.5: Left: The supercell for a triangular array of holes. Right: Transmission profile for a plane wave normally incident on the triangular array. The holes are square, and their area is chosen to retain the same ratio of hole area to period area as in Fig. 3.1. The basic period cell has holes located at $(0, 0), (1/2, \sqrt{3}/2)$. For clarity the wavelength is not normalized by the period; the length scale remains arbitrary.

holes at $(0, 0), (1/2, \sqrt{3}/2), (3/2, \sqrt{3}/2), (2, 0)$. This procedure is depicted in Fig. 3.6, as well as the resulting transmission profile for a normally incident plane wave. The holes are square with side widths $a = .0432^{1/4} \approx 0.456$ in order to preserve the same ratio of hole area to period area as in Fig. 3.1 for comparison. The usual twin peaks appear here at $\lambda = 3/2$, half the period in the x -direction, and the second Rayleigh anomaly appears at $\lambda = \sqrt{3}/2$, half the period in the y -direction and the y -distance between holes.

Unlike the case of a square array of holes in Fig. 3.1, for the case of a triangular array it may be that square holes produce qualitatively different results than circular holes. We have not yet investigated this issue. In addition, an alternative to our supercell procedure can be used in the case of a triangular array of holes, or other arrays which have symmetry in two non-orthogonal directions, by defining new coordinates in those two directions. For some discussion of this tactic see for example Chen (1970, 1971, 1973). This would save a large amount of calculation expense, as

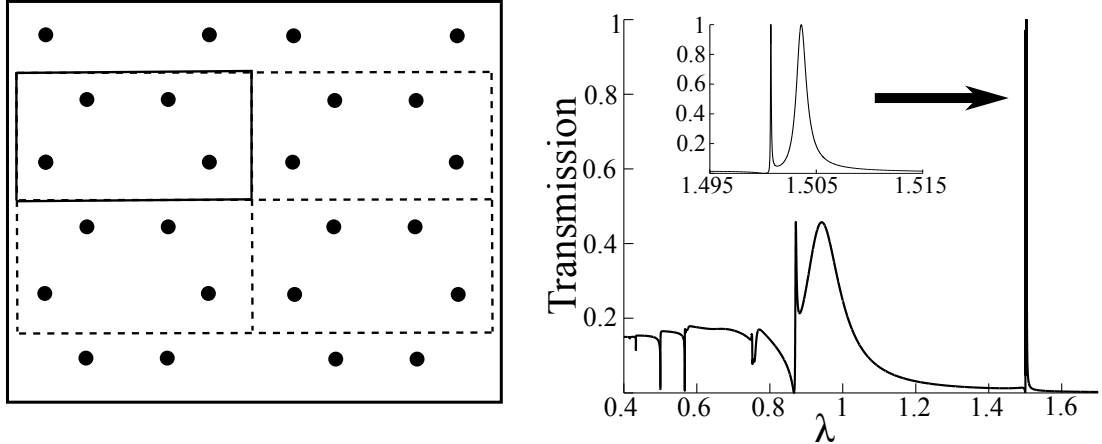


FIGURE 3.6: Left: The supercell for a hexagonal array of holes. Right: Transmission profile for a plane wave normally incident on the hexagonal array. The holes are square, and their area is chosen to retain the same ratio of hole area to period area as in Fig. 3.1. The basic period cell has holes located at $(0, 0)$, $(1/2, \sqrt{3}/2)$, $(3/2, \sqrt{3}/2)$, $(2, 0)$. For clarity the wavelength is not normalized by the period; the length scale remains arbitrary. Inset: Closeup of the twin transmission maxima that occur near $\lambda = 3/2$.

the sizes of the resulting matrices would be smaller. However, the inner products of the plane waves with the waveguide modes would be more difficult to calculate.

3.3 Transmission Maxima and the Single Mode Calculation

Unlike the minima associated with the Rayleigh anomalies, which are very easy to predict, we do not have a straightforward calculation for predicting the location and height of the associated transmission maxima. However, in some circumstances we can approximate them well with a first-order formula that clearly illustrates the connection between the Rayleigh anomaly and the associated transmission peaks.

3.3.1 Matrix Equation and Transmission Formula for One Waveguide Mode

For a plane wave normally incident on a rectangular array of rectangular holes illuminated by a p -polarized plane wave incident at any angle θ_x with $\theta_y = 0$, only a single waveguide mode contributes to the transmission of energy through the holes:

the TE mode with $m = 0, n = 1$,

$$M_{0,1} = \begin{pmatrix} 1 \\ 0 \end{pmatrix} \sqrt{\frac{2}{ab}} \sin\left(\frac{\pi}{b}(y + b/2)\right). \quad (3.11)$$

Therefore, returning to the derivations of Sec. 2.1, each of the sums over α need only contain a single term. Say that A, B are the amplitudes of this mode M as it travels forward and backward, that the scalar G is given by $G = i \sum_k Y_k(M, W_k)(W_k, M) = i \sum_k Y_k |(M, W_k)|^2$, that the scalars S and G^V are defined analogously as in the previous sections, that e_h is the single value of e_α , and that Y_h is the admittance of the single waveguide mode. Then from Eq. (2.23), we have

$$\begin{aligned} X &= \frac{(G - S)I}{(G - S)^2 - (G^V)^2} \\ X' &= \frac{G^V I}{(G - S)^2 - (G^V)^2} \end{aligned} \quad (3.12)$$

so that, from Eq. (2.25),

$$\begin{aligned} A &= \frac{1}{e_h^2 - e_h^{-2}} \frac{(-e_h^{-1}(G - S) - e_h G^V)I}{(G - S)^2 - (G^V)^2} = \frac{(e_h^{-1}(G + iY_h)I}{(e_h^{-1}(G + iY_h))^2 - (e_h(G - iY_h))^2} \\ B &= \frac{1}{e_h^2 - e_h^{-2}} \frac{(e_h(G - S) + e_h^{-1}G^V)I}{(G - S)^2 - (G^V)^2} = \frac{-e_h(G - iY_h)I}{(e_h^{-1}(G + iY_h))^2 - (e_h(G - iY_h))^2} \end{aligned} \quad (3.13)$$

If we set $\Gamma = e_h^{-1}(G + iY_h)$ and $\Delta = e_h(G - iY_h)$, then these expressions have the form

$$A = \frac{\Gamma}{\Gamma^2 - \Delta^2} I \quad B = \frac{-\Delta}{\Gamma^2 - \Delta^2} I, \quad (3.14)$$

as recognized by Martín-Moreno and García-Vidal (2008).

Meanwhile, under the single-mode calculation, the expression (2.27) becomes

$$\begin{aligned}
T &= \sum_k \Im(iY_k) |t_k|^2 / Y_{k_0} \\
&= \sum_k \Im(iY_k) |(Ae_h + Be_h^{-1})(W_k, M)|^2 / Y_{k_0} \\
&= \sum_k \Im(iY_k) \left| \left(\frac{\Gamma I}{\Gamma^2 - \Delta^2} e_h - \frac{\Delta I}{\Gamma^2 - \Delta^2} e_h^{-1} \right) (W_k, M) \right|^2 / Y_{k_0} \quad (3.15) \\
&= \sum_k \Im(iY_k) |(W_k, M)|^2 \left| \frac{2iY_h I}{\Gamma^2 - \Delta^2} \right|^2 / Y_{k_0} \\
&= \left| \frac{2iY_h I}{\Gamma^2 - \Delta^2} \right|^2 \frac{\Im(G)}{Y_{k_0}}.
\end{aligned}$$

At the Rayleigh anomaly, the number G becomes infinite. Both Γ and Δ in the denominator contain G , so the term $\Im(G)$ in the numerator is eclipsed by the order G^4 term in the denominator, which clearly illustrates the emergence of the downward transmission spike.

3.3.2 Maximizing Transmission

We may now proceed to locate the transmission maxima within the single-waveguide mode approximation by minimizing the denominator $|\Gamma^2 - \Delta^2|^2$. To do this we use a first-order calculation which singles out the link between the Rayleigh anomaly and the maxima. In a small region about the Rayleigh anomaly, the admittance Y_k of one or more of the plane waves is rapidly changing with respect to ω and approaching infinity. This admittance appears in one or more terms of the sum defining G ; so to first order, we will assume that the other terms of G are constant, retaining the value that they have at the frequency of the Rayleigh anomaly. The terms Y_h, Y_{k_0}, e_h , and I are also changing relatively slowly, so we will take them to be constant as well.

The terms Y_k which are infinite at the frequency of the Rayleigh anomaly are imaginary for lower values of ω and real for higher values of ω . Because, as we have

seen, the transmission maxima occur at values of ω lower than the frequency of the Rayleigh anomaly, we will focus on this region and assume that it is the imaginary part of $G = G_r + iG_i$ which is rapidly changing. The admittance Y_h of the waveguide mode (3.11) is

$$Y_h = \frac{k_z}{\omega} = \frac{\sqrt{\omega^2 - \pi^2/a^2}}{\omega}. \quad (3.16)$$

For now we will restrict ourselves to the situation of Fig. 3.1 of a plane wave normally incident on a perfectly conducting slab with a square-periodic array of period width L of square holes with side length $a/L = 0.4$ and film thickness $h/L = 0.2$, at the primary Rayleigh anomaly $\lambda = L$, which has the associated double transmission maxima of unit height. For this Rayleigh anomaly, Y_h is imaginary. This also implies that e_h is real with $0 < e_h < 1$. For convenience, define $y = -iY_h > 0$.

Therefore we may write

$$\begin{aligned} & |\Gamma^2 - \Delta^2|^2 \\ &= |e_h^2(G_r + iG_i - y)^2 - e_h^{-2}(G_r + iG_i + y)^2|^2 \\ &= [e_h^2(G_r^2 + 2G_r y + y^2 - G_i^2) - e_h^{-2}(G_r^2 - 2G_r y + y^2 - G_i^2)]^2 + \\ &+ [e_h^2(2G_r G_i + 2yG_i) - e_h^{-2}(2G_r G_i - 2yG_i)]^2. \end{aligned} \quad (3.17)$$

Set $u = e_h^{-2} - e_h^2 > 0$, $v = e_h^{-2} + e_h^2 > 0$, and $\nu = v/u > 1$. Then the above is equal to

$$\begin{aligned} &= [-u(G_r^2 + y^2 - G_i^2) + v(2G_r y)]^2 + 4[-u(G_r G_i) + v(yG_i)]^2 \\ &= u^2[(G_r^2 + y^2 - G_i^2) - 2\nu G_r y]^2 + 4s^2[G_r - \nu y]^2 G_i^2 \\ &= u^2[(G_r - \nu y)^2 - G_i^2 - (\nu^2 - 1)y^2]^2 + 4s^2[G_r - \nu y]^2 G_i^2. \end{aligned} \quad (3.18)$$

Set $Z = (G_r - \nu y)^2$. Then this is

$$\begin{aligned}
&= u^2 ([Z^2 - G_i^2 - (\nu^2 - 1)y^2]^2 + 4ZG_i^2) \\
&= u^2 ((Z - G_i^2)^2 + 4ZG_i^2 - 2(Z - G_i^2)(\nu^2 - 1)y^2 + (\nu^2 - 1)^2y^4) \\
&= u^2 ((Z + G_i^2)^2 - 2(Z - G_i^2)(\nu^2 - 1)y^2 + (\nu^2 - 1)y^4) \quad (3.19) \\
&= u^2 (Z^2 + 2Z(G_i^2 - (\nu^2 - 1)y^2) + (G_i^4 + (\nu^2 - 1)^2y^4 + 2G_i^2(\nu^2 - 1)y^2)) \\
&= u^2 (Z^2 + 2Z(G_i^2 - (\nu^2 - 1)y^2) + (G_i^2 + (\nu^2 - 1)y^2)^2).
\end{aligned}$$

Completing the square gives:

$$= u^2 ((Z + (G_i^2 - (\nu^2 - 1)y^2))^2 + 4(G_i^2(\nu^2 - 1)y^2)). \quad (3.20)$$

Since Y is imaginary, G_i is real, and $\nu^2 > 1$, this is a sum of positive squares. The second term will only be zero if G is real, which is not the case in this situation (nor is it ever the case in the case of normal incidence, as the admittance of a plane wave normal to the surface is always real, which causes G to have an imaginary component). Therefore the minima of this expression will be found by setting the first term equal to zero:

$$\begin{aligned}
Z &= -G_i^2 + (\nu^2 - 1)y^2 \\
G_r &= \nu y \mu \sqrt{(\nu^2 - 1)y^2 - G_i^2}.
\end{aligned} \quad (3.21)$$

We are holding all of the terms on the right constant; now we divide the left side G_r into its constant part G_c plus the part which is approaching infinity:

$$G_r = G_c + i \frac{\omega}{\omega^2 - |k_t|^2} G_f \quad (3.22)$$

where G_f is a sum over the four plane waves which are becoming parallel to the surface of their inner products $|(M, W_k)|^2$. The value $|k_t| = \sqrt{k_x^2 + k_y^2}$ is equal to $2\pi/L$ for each of these plane waves. Therefore, solving for ω yields

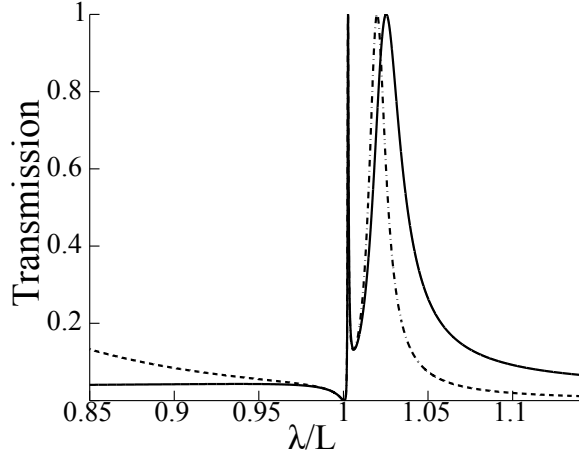


FIGURE 3.7: The dashed curve is the true transmission profile for a plane wave normally incident on a perfectly conducting metal film with square period of side width L , square holes of side lengths $a = 0.4L$, and metal thickness $h = 0.2L$. The solid curve is the first-order approximation profile created by holding all terms constant at their values at the frequency of the Rayleigh anomaly $\lambda = L$ except for the admittances of the four plane waves that are close to parallel to the film.

$$\omega = \frac{\pm \left(\nu y - G_c \pm \sqrt{(\nu^2 - 1)y^2 - G_i^2} \right) 2\pi}{\sqrt{G_f^2 + \left(\nu y - G_c \pm \sqrt{(\nu^2 - 1)y^2 - G_i^2} \right)^2} L} \quad (3.23)$$

The constant terms G_c, G_i , which we have taken to be constant with the value they attain at the frequency of the Rayleigh anomaly, must nevertheless be computed numerically. The term G_f , however, is a sum of only four terms which are listed in Appendix A.

3.3.3 Comparison with the Full Simulation

In Fig 3.7, we display the transmission curve (3.15), allowing only the admittance of the parallel plane waves to vary and holding all other terms constant, alongside the full simulation for comparison. The locations of the transmission maxima are given by Eq. (3.23). The minimum associated with the Rayleigh anomaly and the thin

peak are very well captured by our approximate formula. The second, thicker peak is captured as well, but it is shifted to a slightly higher value of λ from its correct location.

3.4 Resonance and the Null Space of the Matrix Equation

As a further investigation into the behavior of the matrix equation $\mathbf{G}\mathbf{X} = \mathbf{I}$, we will briefly discuss here the null space of the matrix \mathbf{G} .

A *bound state*, which we also call a resonance, is an EM field localized in the vicinity of the film. In our case, it would be a solution of the matrix equation $\mathbf{G}\mathbf{X} = \mathbf{0}$, that is, a solution of Maxwell's equations which exists without incident energy. In general this is likely impossible. Recall that \mathbf{G} has the form

$$\mathbf{G} = \begin{pmatrix} G - S & -G^V \\ -G^V & G - S \end{pmatrix}. \quad (3.24)$$

In the case of rectangular holes, the matrix G has a large null space, as it has infinitely many zero rows and columns (note the several zero inner products found in Appendix A). However, the diagonal matrices S and G^V are well-behaved and override the null space of G .

In the condition of a Rayleigh anomaly, however, every nonzero element of G becomes infinite; G behaves roughly as a constant matrix G_1 plus another constant matrix G_2 multiplied by an admittance term Y_k which tends to infinity. If we divide both sides of the matrix equation $\mathbf{G}\mathbf{X} = \mathbf{I}$ by this admittance Y_k , then as the frequency approaches that of the Rayleigh anomaly, the matrix equation approaches

$$\hat{\mathbf{G}}\mathbf{X} = \mathbf{0}, \quad (3.25)$$

where $\hat{\mathbf{G}}$ is given by

$$\hat{\mathbf{G}} = \begin{pmatrix} G_2 & 0 \\ 0 & G_2 \end{pmatrix}. \quad (3.26)$$

Like G , the matrix G_2 has a large null space. Therefore we may expect potential bound states to exist at the frequency of the Rayleigh anomaly.

The issue is confounded somewhat, however, by the fact that the matrix G depends on the Bloch factor, which is defined by the incident plane wave. If the incident wave is removed, it is unclear whether the matrix G is well-defined, or whether we require it to be. The methods discussed in this work would require some modification to verify these bound states and view them directly. For the moment they remain of purely theoretical interest.

Simulating Real Experiments

Our transmission simulations thus far capture the minima associated with the Rayleigh anomalies and transmission maxima at wavelengths close to where they are found in real experiments, but the sizes of these effects are out of proportion. The character of our transmission profiles is different as well— the twin maxima that we have been seeing at wavelengths close to the period width are not seen in experiments. (For example, see Ebbesen et al. (1998); Hou et al. (2006); Przybilla et al. (2008).) In this chapter we work to include the effects of finite conductivity, finite hole arrays, and incident radiation that is more complex than a plane wave, in order to discover the cause of this discrepancy.

In Sec. 4.1, we incorporate finite conductivity of the metal. We do this by use of an asymptotic calculation for the propagation constants of waveguide modes in circular holes, a quantity which cannot be solved for algebraically. The matching procedure then continues with few other changes. We find that the resulting transmission is not very much affected by this change; it is at most slightly lower than in the perfectly conducting case. This result is supported by simulations in COMSOL Multiphysics and Microwave Studio.

In Sec. 4.2, we apply the supercell technique discussed in Sec. 3.2 to approximate a finite array of holes. We again find that the transmission may be reduced by this change but otherwise it has the same behavior.

Finally in Sec. 4.3, we allow the incident energy to be more complicated than a plane wave. Thanks to Bloch theory and the orthogonality of our plane waves, only a simple averaging technique is required. We find that imperfect collimation significantly changes the character of the transmission curve, causing the minima at the Rayleigh anomalies and transmission maxima to be less pronounced and reducing the double maxima to a single maximum, as is seen in experiments.

We will take a moment to recall Fig. 3.2, depicting $\Re(E_x)$ in a cross-section of a 1-dimensionally periodic film at different angles of incidence and wavelengths. The field strengths are highest at the corners of the holes. The sharpness of the corners can also be seen as an approximation; in experimental conditions, the corners can be close to exact on the scale of a wavelength in the radio-frequency range, but as the frequencies tend towards the optical range, the corners will be more rounded. In this work, we do not study the effects of this approximation.

4.1 Finite Conductivity

An infinite conductor may not have any electric or magnetic field inside the metal, but this is not true of a finite conductor; waveguide modes from the holes extend into the walls of the waveguide, which makes explicit calculation of the waveguide modes more difficult. For rectangular holes this remains an open problem, but for a single circular hole the waveguide modes are known, except for the propagation constant which cannot be exactly solved for.

Here we derive an asymptotic formula for the propagation constant of a mode in a metal that has large but finite conductivity. Many commonly used metals are good conductors, including copper, silver and aluminum. Large conductivity ensures that

the propagation constant of each mode will be close to that of the equivalent mode in a perfect conductor. It also causes the field to decrease quickly inside the walls of the metal, which allows us to assume that a waveguide mode from one hole will not affect its neighbor.

First we will give the explicit expressions for the waveguide modes, which can also be found in Snitzer (1961) and Snyder and Love (1983). Next, we will demonstrate the derivation of the first-order terms of a novel asymptotic formula for the propagation constant. (The derivation of the second-order terms is given in Appendix B.) Finally, we will show the remaining changes needed in the matrix equations to account for finite conductivity, and discuss the results.

4.1.1 Explicit Expressions for the Waveguide Modes

Let ϵ_1 be the dielectric constant of the material in the holes (which we have thus far been taking to be air, $\epsilon_1 = 1$), and let ϵ_2 be the dielectric constant of the metal. In general both quantities may be complex, and in Sec. 4.1.2 we will be taking $|\epsilon_2|$ large, but that is not necessary for the expressions presented in this section. We assume that the magnetic constant μ has the same value in the hole and the metal.

Previously we needed the matching conditions associated with Maxwell's equations for a perfect conductor, requiring that the components of E tangent to an interface between different materials to be continuous, but there was no similar restriction on H . Now that our metal is a finite conductor, however, the tangential components of both E and H must be continuous across interfaces. Waveguide modes, with two exceptions, no longer divide into TE and TM varieties; rather, they are hybrid modes whose expressions contain elements of both. The two exceptions to this rule are the two modes corresponding to the Bessel function J_0 , of which one is a TE mode and the other TM.

The expressions in this section for the hybrid modes and the propagation constant

can also be found in Snitzer (1961) and Snyder and Love (1983). Let r, θ be the usual polar coordinates, J, K be the Bessel functions, and a be the radius of the hole. Then we have:

Inside the Hole, $n \neq 0$

$$E_z = J_n(\lambda_1 r) \cos(n\theta + \phi_n) e^{ik_z z} \quad (4.1a)$$

$$E_r = \frac{ik_z}{\lambda_1^2} \left(\frac{d}{dr}(J_n(\lambda_1 r)) - \frac{n}{r} P J_n(\lambda_1 r) \right) \cos(n\theta + \phi_n) e^{ik_z z} \quad (4.1b)$$

$$E_\theta = \frac{ik_z}{\lambda_1^2} \left(P \frac{d}{dr}(J_n(\lambda_1 r)) - \frac{n}{r} J_n(\lambda_1 r) \right) \sin(n\theta + \phi_n) e^{ik_z z} \quad (4.1c)$$

$$H_z = \frac{-k_z}{\mu\omega} P J_n(\lambda_1 r) \sin(n\theta + \phi_n) e^{ik_z z} \quad (4.1d)$$

$$H_r = \frac{-ik_1^2}{\mu\omega\lambda_1^2} \left(\frac{k_z^2}{k_1^2} P \frac{d}{dr}(J_n(\lambda_1 r)) - \frac{n}{r} J_n(\lambda_1 r) \right) \sin(n\theta + \phi_n) e^{ik_z z} \quad (4.1e)$$

$$H_\theta = \frac{ik_1^2}{\mu\omega\lambda_1^2} \left(\frac{d}{dr}(J_n(\lambda_1 r)) - \frac{k_z^2 n}{k_1^2 r} P J_n(\lambda_1 r) \right) \cos(n\theta + \phi_n) e^{ik_z z} \quad (4.1f)$$

Inside the Metal, $n \neq 0$:

$$E_z = WK_n(\lambda_2 r) \cos(n\theta + \phi_n) e^{ik_z z} \quad (4.2a)$$

$$E_r = -iW \frac{k_z}{\lambda_2^2} \left(\frac{d}{dr}(K_n(\lambda_2 r)) - \frac{n}{r} P K_n(\lambda_2 r) \right) \cos(n\theta + \phi_n) e^{ik_z z} \quad (4.2b)$$

$$E_\theta = -iW \frac{k_z}{\lambda_2^2} \left(P \frac{d}{dr}(K_n(\lambda_2 r)) - \frac{n}{r} K_n(\lambda_2 r) \right) \sin(n\theta + \phi_n) e^{ik_z z} \quad (4.2c)$$

$$H_z = -W \frac{k_z}{\mu\omega} P K_n(\lambda_2 r) \sin(n\theta + \phi_n) e^{ik_z z} \quad (4.2d)$$

$$H_r = iW \frac{k_z^2}{\mu\omega\lambda_2^2} \left(\frac{k_z^2}{k_2^2} P \frac{d}{dr}(K_n(\lambda_2 r)) - \frac{n}{r} K_n(\lambda_2 r) \right) \sin(n\theta + \phi_n) e^{ik_z z} \quad (4.2e)$$

$$H_\theta = -iW \frac{k_z^2}{\mu\omega\lambda_2^2} \left(\frac{d}{dr}(K_n(\lambda_2 r)) - \frac{k_z^2 n}{k_2^2 r} P K_n(\lambda_2 r) \right) \cos(n\theta + \phi_n) e^{ik_z z} \quad (4.2f)$$

TM, $n = 0$

$$E_z^{hole} = J_n(\lambda_1 r) e^{ik_z z} \quad (4.3a)$$

$$E_r^{hole} = \frac{ik_z}{\lambda_1^2} \left(\frac{d}{dr}(J_0(\lambda_1 r)) \right) e^{ik_z z} \quad (4.3b)$$

$$H_\theta^{hole} = \frac{ik_1^2}{\mu\omega\lambda_1^2} \left(\frac{d}{dr}(J_0(\lambda_1 r)) \right) e^{ik_z z} \quad (4.3c)$$

$$E_z^{metal} = WK_0(\lambda_2 r) e^{ik_z z} \quad (4.3d)$$

$$E_r^{metal} = -iW \frac{k_z}{\lambda_2^2} \left(\frac{d}{dr}(K_0(\lambda_2 r)) \right) \quad (4.3e)$$

$$H_\theta^{metal} = -iW \frac{k_1^2}{\mu\omega\lambda_2^2} \left(\frac{d}{dr}(K_0(\lambda_2 r)) \right) \quad (4.3f)$$

$$E_\theta = H_z = H_r = 0 \quad (4.3g)$$

TE, $n = 0$

$$H_z^{hole} = \frac{-k_z}{\mu\omega} P J_0(\lambda_1 r) e^{ik_z z} \quad (4.4a)$$

$$H_r^{hole} = \frac{-ik_z^2}{\mu\omega\lambda_1^2} \left(P \frac{d}{dr} (J_0(\lambda_1 r)) \right) e^{ik_z z} \quad (4.4b)$$

$$E_\theta^{hole} = \left(P \frac{d}{dr} (J_0(\lambda_1 r)) \right) e^{ik_z z} \quad (4.4c)$$

$$H_z^{metal} = -W \frac{k_z}{\mu\omega} P K_0(\lambda_2 r) e^{ik_z z} \quad (4.4d)$$

$$H_r^{metal} = iW \frac{k_z^2}{\mu\omega\lambda_2^2} \left(P \frac{d}{dr} (K_0(\lambda_2 r)) \right) e^{ik_z z} \quad (4.4e)$$

$$E_\theta^{metal} = -iW \frac{k_z}{\lambda_2^2} \left(P \frac{d}{dr} (K_0(\lambda_2 r)) \right) \quad (4.4f)$$

$$E_z = E_r = H_\theta = 0 \quad (4.4g)$$

where k_z is the propagation constant to be determined in Sec. 4.1.2; and further,

$$k_1^2 = \omega^2 \mu \epsilon_1 \quad \lambda_1^2 = k_1^2 - k_z^2 \quad (4.5a)$$

$$k_2^2 = \omega^2 \mu \epsilon_2 \quad \lambda_2^2 = k_2^2 - k_z^2 \quad (4.5b)$$

$$W = \frac{J_n(\lambda_1 a)}{K_n(\lambda_2 a)} \quad (4.5c)$$

$$P = \frac{n \left(\frac{1}{(\lambda_1 a)^2} + \frac{1}{(\lambda_2 a)^2} \right)}{\frac{J'_n(\lambda_1 a)}{\lambda_1 a J_n(\lambda_1 a)} + \frac{K'_n(\lambda_2 a)}{\lambda_2 a K_n(\lambda_2 a)}}; \quad (4.5d)$$

and ϕ_n is arbitrary. As with the waveguide modes inside the circular waveguides surrounded by a perfect conductor, the modes here are enumerated in part by n , the index of the Bessel function J_n . They are also enumerated by the infinitely many allowable propagation constants; and we may choose two values of ϕ_n to form a basis, usually $\phi_n = 0$ and $\pi/2$. For large values of ϵ_2 modes may be “TE-like” and “TM-

like” modes, depending on whether the term P is large or small, respectively (for example, set $P = 0$ and compare with the waveguide modes in a perfect conductor).

The inner products (M_α, W_k) must be calculated numerically. Therefore we must either convert these expressions to Cartesian coordinates or convert the plane wave expressions to cylindrical, using the conversion $E_x = E_r \cos(\theta) - E_\theta \sin(\theta)$, $E_y = E_r \sin(\theta) + E_\theta \cos(\theta)$. The second way is generally preferable since it avoids the awkward conversion $\theta = \arctan_2(y/x)$.

Finally, the propagation constant k_z is determined by the equation (Snitzer (1961))

$$\left(\frac{J'_n(\lambda_1 a)}{\lambda_1 a J_n(\lambda_1 a)} + \frac{K'_n(\lambda_2 a)}{\lambda_2 a K_n(\lambda_2 a)} \right) \left(k_1^2 \frac{J'_n(\lambda_1 a)}{\lambda_1 a J_n(\lambda_1 a)} + k_2^2 \frac{K'_n(\lambda_2 a)}{\lambda_2 a K_n(\lambda_2 a)} \right) = n^2 k_z^2 \left(\frac{1}{(\lambda_1 a)^2} + \frac{1}{(\lambda_2 a)^2} \right)^2, \quad (4.6)$$

which in general has infinitely many solutions which will be discussed in the next section.

4.1.2 Asymptotic Expression for the Propagation Constant

The equation (4.6) for the propagation constant of the hybrid mode cannot be solved analytically, but it may be solved asymptotically. Most commonly used metals are good conductors, meaning that the dielectric constant ϵ_2 is very large in magnitude. Hybrid modes surrounded by a good conductor are very similar to the waveguide modes constrained by a perfect conductor; as $|\epsilon_2| \rightarrow \infty$, the propagation constant of the hybrid mode approaches that of a TE/TM mode. Therefore we take $1/\epsilon_2$ and the deviation of the propagation constant from its limiting TE/TM mode to be approaching zero in our asymptotic calculations.

In this section we derive the first-order term of the asymptotic expansion. The calculation of the second-order term will be relegated to Appendix B.

Equation (4.6) has infinitely many solutions. We may enumerate them by three values: an integer $n \geq 0$, the order of the Bessel functions; whether the mode is TM-like or TE-like; and an integer $m > 0$, which orders the zeroes of J_n if the mode is TM-like or J'_n if the mode is TE-like. For brevity we will not explicitly write this dependence; the two cases will be identified verbally. Accordingly, we define u_0 to be the m^{th} zero of J_n or J'_n , depending on the case. Define h_0 by $u_0 = a\sqrt{\epsilon_1\mu\omega^2 - h_0^2}$, so that h_0 is the propagation constant of the limiting TE/TM mode of a perfect conductor.

Define

$$u = \lambda_1 a \qquad w = \lambda_2 a \qquad (4.7a)$$

$$\eta_1 = \frac{J'_n(u)}{uJ_n(u)} \qquad \eta_2 = \frac{K'_n(w)}{wK_n(w)}. \qquad (4.7b)$$

Then equation (4.6) becomes

$$(\eta_1 + \eta_2)(k_1^2\eta_1 + k_2^2\eta_2) = n^2k_z^2 \left(\frac{1}{u^2} + \frac{1}{w^2} \right)^2. \qquad (4.8)$$

Divide both sides of this equation by k_1^2 and set $\epsilon = \epsilon_2/\epsilon_1$. Then

$$\eta_1^2 + (1 + \epsilon)\eta_1\eta_2 + \epsilon\eta_2^2 = \frac{n^2k_z^2}{\omega^2\mu\epsilon_1} \left(\frac{1}{u^2} + \frac{1}{w^2} \right)^2. \qquad (4.9)$$

We will examine the behavior of each term separately. In the limiting case of a perfect conductor, the propagation constant k_z is equal to the number h_0 defined above: that is, $u = u_0$ is a zero of J_n in the case of a TM mode, and $u = u_0$ is a zero of J'_n in the case of a TE mode. Therefore, in the limit of a perfect conductor, the term η_1 will approach infinity or zero, respectively.

The term η_2 is less troublesome. The asymptotic expansions of K_n and K'_n are

given in Abramowitz and Stegun (1964),

$$K_n(z) \sim \sqrt{\frac{\pi}{2z}} e^{-z} \left(1 + \frac{4n^2 - 1}{8z} + \frac{(4n^2 - 1)(4n^2 - 9)}{2!(8z)^2} + \dots \right) \quad (4.10a)$$

$$K'_n(z) \sim -\sqrt{\frac{\pi}{2z}} e^{-z} \left(1 + \frac{4n^2 + 3}{8z} + \frac{(4n^2 - 1)(4n^2 + 15)}{2!(8z)^2} + \dots \right), \quad (4.10b)$$

so that to first order we have

$$\eta_2 \sim -1/w = -1/(a\sqrt{k_z^2 - \omega^2\mu\epsilon_2}), \quad (4.11)$$

which tends to zero as $|\epsilon_2| \rightarrow \infty$ at the rate of $\epsilon_2^{-1/2}$.

The remaining terms become neither very large nor very small as $|\epsilon_2| \rightarrow \infty$. Therefore we will solve Eq. (4.9) for η_1 , obtaining

$$2\eta_1 = -(1 + \epsilon)\eta_2 \pm (1 - \epsilon)\eta_2 \sqrt{1 + \frac{\frac{4n^2 k_z^2}{\omega^2 \mu \epsilon_1} \left(\frac{1}{u^2} + \frac{1}{w^2}\right)^2}{(1 - \epsilon)^2 \eta_2^2}}. \quad (4.12)$$

As $|\epsilon| \rightarrow \infty$, the denominator inside the square root tends to ∞ , as the ϵ^2 term dominates the η_2^2 term. Therefore to first order, the two solutions to this equation appear to be

$$\eta_1 = -\epsilon\eta_2 \quad (4.13)$$

$$\eta_1 = -\eta_2. \quad (4.14)$$

We will soon find, however, that Eq. (4.14) is not sufficient to provide the first-order term of the asymptotic series; we will in fact have to incorporate the first correction term from under the square root. For now note that the right side of Eq. (4.13) which tends to infinity, implying that the denominator of η_1 must be tending to zero. Therefore hybrid modes whose propagation constant satisfies Eq. (4.13) converge

to TM modes. Similarly, hybrid modes whose propagation constant satisfies the corrected Eq. (4.14) converge to TE modes.

We already have a first-order expansion for η_1 , so we must now find the same for η_2 . This term does not depend on ϵ_2 , so we expand instead in terms of the deviation of the propagation constant from its $|\epsilon_2| \rightarrow \infty$ limit. Let $k_z = h_0 + h_s$, where h_0 is the propagation constant of the limiting TM/TE waveguide mode. We will replace J_n and J'_n by the first nonzero terms of their Taylor series about the point $u_0 = a\sqrt{k_1^2 - h_0^2}$.

For the case of a limiting TM wave, u_0 is a zero of J_n , so we will have

$$\eta_1 \sim \frac{J'_n(u_0)}{uJ'_n(u_0)(u - u_0)} = \frac{1}{u(u - u_0)}. \quad (4.15)$$

Expanding the denominator,

$$u - u_0 = a\sqrt{k_1^2 - (h_0 + h_s)^2} - a\sqrt{k_1^2 - h_0^2} \sim -h_s \frac{ah_0}{\sqrt{k_1^2 - h_0^2}}. \quad (4.16)$$

The single term u has a constant first order expansion $u \sim a\sqrt{k_1^2 - h_0^2}$, so

$$\frac{1}{u(u - u_0)} \sim -h_s^{-1} \frac{1}{a^2 h_0}. \quad (4.17)$$

Returning for a moment to Eq. (4.11), the dependence of η_2 on h_s is negligible, so combining all of this with Eq. (4.13) yields

$$h_s \sim -\frac{\sqrt{h_0^2 - \omega^2 \mu \epsilon_2}}{\epsilon_2 a h_0} = -\frac{1}{\epsilon_2^{1/2}} \frac{\epsilon_1 \sqrt{h_0^2 / \epsilon_2 - \omega^2 \mu}}{a h_0} \sim -\frac{1}{\epsilon_2^{1/2}} \left(\frac{\epsilon_1 \sqrt{-\omega^2 \mu}}{a h_0} \right). \quad (4.18)$$

Therefore, the propagation constant of a ‘‘TM-like’’ hybrid mode as $|\epsilon_2| \rightarrow \infty$ is given by

$$k_z \sim h_0 - \frac{1}{\epsilon_2^{1/2}} \left(\frac{\epsilon_1 \sqrt{-\omega^2 \mu}}{ah_0} \right). \quad (4.19)$$

Now, for the case of a limiting TE wave, u_0 is instead a zero of J'_n , so the first-order approximation to η_1 is

$$\eta_1 \sim \frac{J''_n(u_0)(u - u_0)}{uJ_n(u_0)}. \quad (4.20)$$

From Eq. (4.16) and the constant limiting value for u , we obtain

$$\frac{u - u_0}{u} \sim \frac{-h_s h_0}{k_1^2 - h_0^2}. \quad (4.21)$$

Equation (4.14), however, is not sufficient to give the correct first-order term to the asymptotic expansion. We must incorporate the first correction term from the square root in Eq. (B.5):

$$2\eta_1 = -(1 + \epsilon)\eta_2 - (1 - \epsilon)\eta_2 \left[1 + \frac{4n^2 k_z^2}{\omega^2 \mu \epsilon_1} \left(\frac{1}{u^2} + \frac{1}{w^2} \right)^2 \right] = -2\eta_2 - \frac{4n^2 k_z^2}{\omega^2 \mu \epsilon_1} \left(\frac{1}{u^2} + \frac{1}{w^2} \right)^2. \quad (4.22)$$

Recall that $\eta_2 \sim -1/(a\sqrt{k_z^2 - \omega^2 \mu \epsilon_2})$; notice that the term $1/w^2$ in the numerator is negligible compared to $1/u^2$; and notice that the 1 in the denominator is negligible compared to ϵ :

$$\eta_1 = \frac{1}{a\sqrt{k_z^2 - \omega^2 \mu \epsilon_2}} - \frac{1}{\epsilon_2} \frac{n^2 k_z^2 a \sqrt{k_z^2 - \omega^2 \mu \epsilon_2}}{\omega^2 \mu u^4} \sim \frac{1}{\epsilon_2^{1/2}} \left(\frac{1}{a\sqrt{-\omega^2 \mu}} + \frac{n^2 h_0^2 a}{\sqrt{-\omega^2 \mu} u^4} \right). \quad (4.23)$$

Finally, accounting for the expression for η_1 in Eq. (4.21), we have

$$h_s \sim -\frac{1}{\epsilon_2^{1/2}} \frac{J_n(u_0)(k_1^2 - h_0^2)}{J_n''(u_0)h_0a\sqrt{-\omega^2\mu}} \left(1 + \frac{n^2h_0^2}{a^2(k_1^2 - h_0^2)^2}\right). \quad (4.24)$$

Therefore, the propagation constant of a ‘‘TE-like’’ hybrid mode as $|\epsilon_2| \rightarrow \infty$ is given by

$$k_z \sim h_0 - \frac{1}{\epsilon_1^{1/2}} \left(\frac{J_n(a\sqrt{k_1^2 - h_0^2})(k_1^2 - h_0^2)}{J_n''(a\sqrt{k_1^2 - h_0^2})h_0a\sqrt{-\omega^2\mu}} \left(1 + \frac{n^2h_0^2}{a^2(k_1^2 - h_0^2)^2}\right) \right). \quad (4.25)$$

The second-order terms for both types of modes are derived in Appendix B. For each type the asymptotic formula has the form

$$k_z \sim h_0 + \frac{C_1}{\epsilon_2^{1/2}} + \frac{C_2}{\epsilon_2}. \quad (4.26)$$

For hybrid modes approaching a TE mode, h_0 is such that $u_0 = a\sqrt{\omega^2\mu\epsilon_1 - h_0^2}$ is the m^{th} zero of J_n' , and the coefficients are given by

$$C_1^{TE} = \frac{-J_n(u_0)\alpha}{a\sqrt{-\omega^2\mu}J_n''(u_0)h_0} \left(1 + \frac{n^2h_0^2}{a^2\alpha^2}\right) \quad (4.27)$$

$$C_2^{TE} = \frac{-J_n(u_0)\alpha}{h_0J_n''(u_0)} \left(1 + \frac{n^2h_0^2}{a^2\alpha^2}\right) \left\{ \frac{1}{a^2\omega^2\mu} \left(\frac{1}{2} + \frac{n^2h_0^2}{a^2\alpha^2} + \frac{J_n(u_0)n^2}{J_n''(u_0)a^2\alpha} \left(2 + \frac{4h_0^2}{\alpha}\right) \right) \right\}, \quad (4.28)$$

where $\alpha = \omega^2\mu\epsilon_1 - h_0^2 = (u_0/a)^2$. For hybrid modes approaching a TM mode, h_0 is such that $u_0 = a\sqrt{\omega^2\mu\epsilon_1 - h_0^2}$ is the m^{th} zero of J_n , and

$$C_1^{TM} = -\frac{\epsilon_1(-\omega^2\mu)^{1/2}}{ah_0} \quad (4.29)$$

$$C_2^{TM} = \frac{\epsilon_1^2 \omega^2 \mu}{2h_0} \left(\frac{1}{a^2 h_0^2} - \frac{1}{a^2 \beta} + \frac{J_n''(u_0)}{J_n'(u_0) a \sqrt{\beta}} \right) + \frac{\epsilon_1}{2a^2 h_0}, \quad (4.30)$$

where $\beta = \omega^2 \mu \epsilon_1 - h_0^2 = (u_0/a)^2$.

4.1.3 Remaining Changes to the Matching Procedure

The remaining changes to the matching procedure for the case of finite conductivity are few. The first difference is that the matching conditions associated with Maxwell's equations now require continuity of the components tangential to each interface of both the electric and magnetic fields, rather than only the electric field. This means that the inner products of the waveguide modes with a plane wave are now done over the entire period cell, instead of only the opening of the hole. In Sec. 2.1 the formulae are already written as such, so no alteration is required.

The other more significant difference is in the admittances of the waveguide modes. Referring to the explicit expressions for the modes in Sec. 4.1.1, the r, θ components of E and H that contain the factor P will be called the *TE part* of the wave, and those without P the *TM part*. For example, for E_r inside the holes with $n = 0$, the TE part is

$$E_{r,TE} = \frac{-ik_z n}{\lambda_1^2} \frac{P}{r} J_n(\lambda_1 r) \cos(n\theta + \phi_n) e^{ik_z z}, \quad (4.31)$$

and the TM part is

$$E_{r,TM} = \frac{ik_z}{\lambda_1^2} \frac{d}{dr} (J_n(\lambda_1 r)) \cos(n\theta + \phi_n) e^{ik_z z}. \quad (4.32)$$

The reason for this division is that each hybrid mode has essentially two admittances: the TM part assumes the admittance of a TM mode as in Sec. 2.2.3, that is, $Y = \epsilon\omega/k_z$, while the TE part of the hybrid mode assumes the admittance of a TE mode,

$Y = k_z/\mu\omega$. The corrected admittance equation (compare Eq. (2.10)) for the case of finite conductivity is

$$\pm \begin{pmatrix} H_y \\ -H_x \end{pmatrix} = \frac{\epsilon_1\omega}{k_z} \begin{pmatrix} E_x \\ E_y \end{pmatrix}_{hole}^{TM} + \frac{\epsilon_2\omega}{k_z} \begin{pmatrix} E_x \\ E_y \end{pmatrix}_{metal}^{TM} + \frac{k_z}{\mu\omega} \begin{pmatrix} E_x \\ E_y \end{pmatrix}_{hole}^{TE} + \frac{k_z}{\mu\omega} \begin{pmatrix} E_x \\ E_y \end{pmatrix}_{metal}^{TE}. \quad (4.33)$$

For good conductors, the term P is very large or very small, which allows us to say the hybrid mode is TE-like or TM-like respectively.

This division of each mode into four parts, inside and outside the metal and TM/TE part, persists throughout the matrix equations. The final matrix equation retains the form

$$\begin{pmatrix} G - S & -G^V \\ -G^V & G - S \end{pmatrix} \begin{pmatrix} X \\ X' \end{pmatrix} = \begin{pmatrix} I \\ 0 \end{pmatrix}, \quad (4.34)$$

but the elements of the matrices G, S, G^V, I are now given by

$$\begin{aligned} X_\alpha &= A_\alpha e_\alpha^{-1} + B_\alpha e_\alpha & X'_\alpha &= -A_\alpha e_\alpha - B_\alpha e_\alpha^{-1} \\ G_{\alpha\beta} &= i \sum_k Y_k(M_\alpha, W_k)(W_k, M_\beta) & I_\alpha &= 2iY_{k_0}(W_{k_0}, M_\alpha) \\ G_\alpha &= \frac{2iY^\zeta}{e_\alpha^2 - e_\alpha^{-2}} & S_\alpha &= iY^\zeta \frac{e_\alpha^2 + e_\alpha^{-2}}{e_\alpha^2 - e_\alpha^{-2}} \end{aligned} \quad (4.35)$$

with Y^ζ equal to

$$Y^\zeta = \frac{\epsilon_1\omega}{k_z}(W_k, M_{\alpha,hole}^{TE}) + \frac{\epsilon_2\omega}{k_z}(W_k, M_{\alpha,metal}^{TE}) + \frac{k_z}{\mu\omega}(W_k, M_{\alpha,hole}^{TM}) + \frac{k_z}{\mu\omega}(W_k, M_{\alpha,metal}^{TM}), \quad (4.36)$$

where the term $M_{\alpha,hole}^{TE}$ is equal to the TE part of the hybrid mode inside the hole and zero outside the hole, and similarly for the other terms.

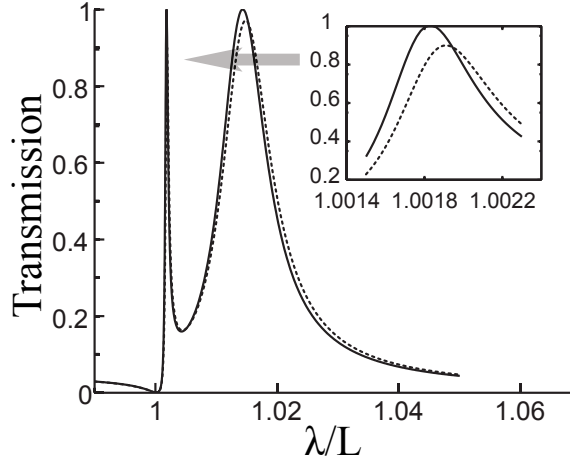


FIGURE 4.1: Transmission profile assuming an imperfectly conducting metal. The solid curve is for $\epsilon_2 = -7 \times 10^4 + i5 \times 10^7$, a typical value of the dielectric constant of copper in the microwave range (Ung and Sheng (2007)). The values for Al, Cu, and Ag do not differ enough to produce visible change in the transmission curve. The dotted line is for $\epsilon_2 = -1.7 \times 10^3 - i2 \times 10^4$, a typical value of the dielectric constant of silver in the infrared range (Ung and Sheng (2007)). Inset: Closeup of the narrow maximum.

4.1.4 Results, and Comparison with Other Numerical Techniques

Sample results of the use of this method are seen in Fig. 4.1. For good conductors in the microwave frequency range, the transmission curve is indistinguishable from the case of perfect conductivity. For the same metals in the infrared range, overall transmission is reduced in the two maxima, but the location of the Rayleigh anomaly and the location of the maxima are not changed. (In truth, the dielectric constant ϵ_2 of a metal depends on the frequency. However, for the cases under consideration, accounting for this dependence produces no visible change in the transmission.)

For comparison, performed the same simulation using COMSOL Multiphysics, a finite-element-based commercial EM software. The experimental setup is given in Fig. 4.2a. In Fig. 4.2b, the transmission curve is calculated for two different films: a perfect conductor, and Al at a frequency of 10 GHz. The simulation shows no visible difference between the perfect conductor and Al, as we have predicted. There

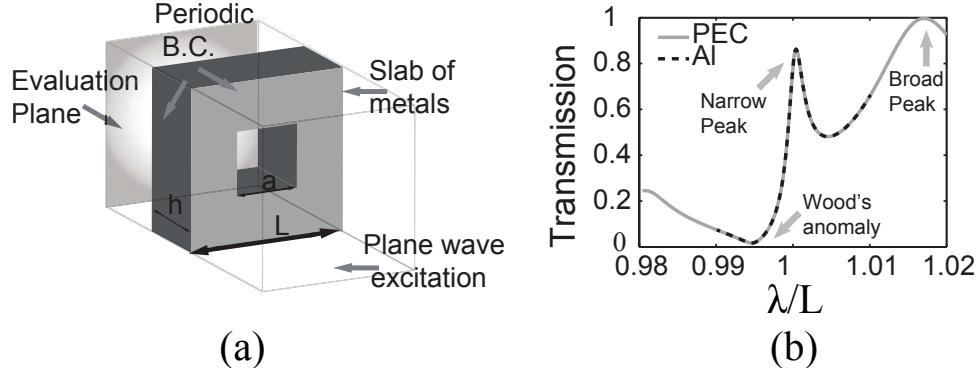


FIGURE 4.2: We simulate the same experiment using COMSOL Multiphysics. (a) The experimental setup. A plane wave is incident from one boundary plane and the transmitted energy is collected on the other. The boundary conditions are periodic, as we are assuming normal incidence. (b) Two different films are simulated: A perfect electric conductor (PEC), and Al at a frequency of 10 GHz.

is disagreement, however, between this simulation and that in Fig. 4.1 in the height of the maxima and the depth of the Rayleigh anomaly. This is due to the finite mesh and imperfect absorption at the radiation boundary plane. A denser mesh helps the numerical results to better match our prediction, at the cost of more computing resources. The mesh used to create Fig. 4.2 has more than 170,000 mesh elements and creates more than 1 million degrees of freedom, which requires more than 32GB of memory. Furthermore, the imperfect absorption at the boundary creates extra oscillations in the transmission curve which requires extra attention to eliminate. Because of this, COMSOL is not optimal software to use for this simulation.

We have also performed the simulation in Microwave Studio, in which we have better control of the reflection at the boundary. The extra oscillations are removed when the reflection at the boundary is lower than -20dB, and the Rayleigh anomaly and transmission maxima are captured more precisely. However, we have not been able to run the simulation with conditions sufficient to capture these phenomena exactly.

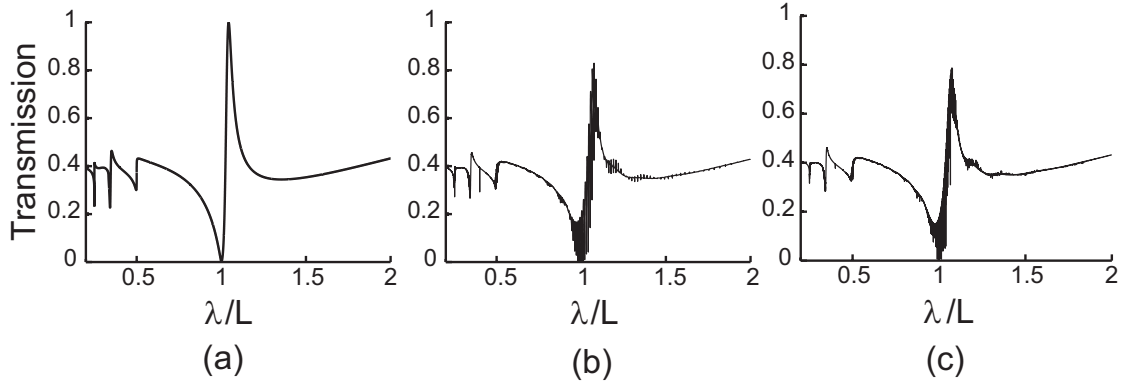


FIGURE 4.3: Approximation of a finite array for the case of a 1-dimensional array of slits. Finite arrays of 10 slits are repeated periodically with (a) no space between arrays, then (b) with distance between arrays equal to 10 times the width of each array, and finally (c) with distance between arrays equal to 50 times their width. The transmission is reduced by about 20% in total. Fabry-Perot-like oscillations appear due to the interaction between each finite array, but the location and character of the curve and the transmission anomalies remain the same.

4.2 Finite Hole Arrays

Done exactly, the calculation of transmission through a single hole would require an alteration of our method to account for the continuum of plane waves allowed outside the film; see Takakura (2001) for an explanation of this procedure. However, we can approximate the behavior of a finite array of holes by using the technique of Sec. 3.2. By defining a supercell of some number of holes followed by a large amount of space without holes, each supercell will behave as its own separate array as the amount of space tends to infinity.

Sample results of this procedure may be seen in Fig. 4.3, for the case of a 1-dimensional array of slits. A finite array of 10 slits is repeated periodically, at first with no space between them, then with distance between arrays equal to 10 times the width of each array, and finally with distance between arrays equal to 50 times their width. In total, the transmission is reduced by approximately 20%, and some Fabry-Perot-like oscillations appear due to the interaction between each finite array.

However, the character of the transmission curve remains the same, and the location and character of the Rayleigh anomalies and transmission spikes do not change.

4.3 Imperfect Collimation

In our simulations thus far, the incident energy has been perfectly collimated, meaning that it is in the form of a single plane wave. Experimenters work to be close to this ideal, and assume that their results are accurate enough to capture the important phenomena. As we began to see in Sec. 3.1, however, even small changes in the angle of incidence can significantly affect the delicate features of the transmission curve, in particular the narrow transmission maximum.

See Fig. 4.4 for further illustration of this effect. The dotted curve is for normal incidence, and the solid curve is for incidence at an angle of 0.11 degrees. With this change in angle, the narrow peak is shifted such that the portion above 50% transmission has no overlap with its previous position. In real experiments, energy is incident over a small spread of angles. This could cause the narrow peak to become more complicated or diminish in height.

We can simulate a spread of angles by solving for the field solution for each incident angle separately; by linearity of Maxwell's equations the total field is equal to the sum of the fields created by each incoming plane wave. The usual formula for transmission, Eq. (2.27)

$$T = \sum_k \Re(Y_k) |t_k|^2 / Y_{k_0}, \quad (4.37)$$

relies only on the orthogonality of the outgoing plane waves. Except in extraordinary circumstances, all outgoing plane waves created by any of the incident angles will be orthogonal, and so the formula for transmission holds without alteration, except that the sum is now over all outgoing plane waves. The end result of this is that the transmission profile for a spread of incident waves is the average of the transmission

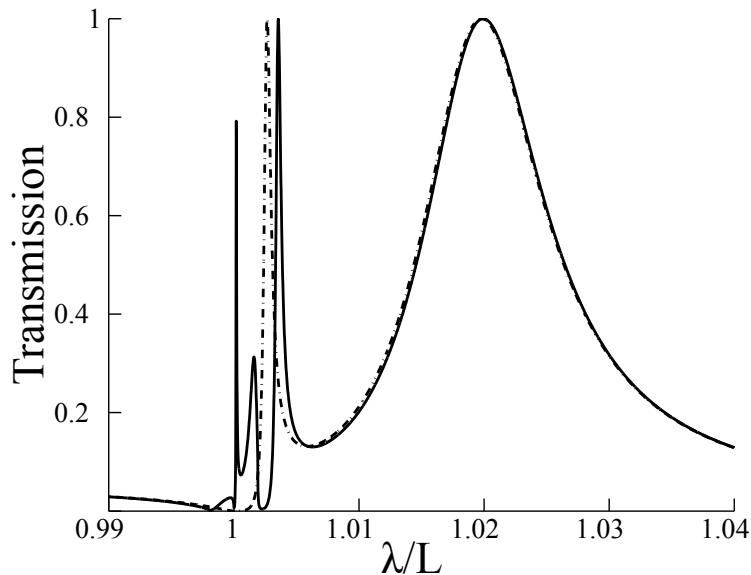


FIGURE 4.4: Transmission profile for normal incidence (dotted line) compared with incidence at 0.11 degrees (solid line). With this change in angle, the narrow peak is shifted such that its portion above 50% transmission has no overlap with its previous position.

profile for each incident wave.

(In the extraordinary circumstance that two of the incoming waves both produce the same particular outgoing wave, this formula will have to be revised. If the two incoming waves have wavevector \mathbf{k}_0 and \mathbf{l}_0 , this criterion means that for some integers j_1, j_2, j_3, j_4 ,

$$\left(k_{0x} + \frac{2\pi j_1}{L_x}, k_{0y} + \frac{2\pi j_2}{L_y} \right) = \left(l_{0x} + \frac{2\pi j_3}{L_x}, l_{0y} + \frac{2\pi j_4}{L_y} \right) \quad (4.38)$$

[see Eq. (2.8)]. This will only happen if $k_{0x} - l_{0x}$ is a multiple of $2\pi/L_x$, and similarly for the y -components. In this case all outgoing waves produced by the first angle are also produced by the second. In particular, this cannot happen if the difference between incident angles is small enough.)

See Fig. 4.5 for results of this method. We simulate incidence of a spread of angles varying within 0.1° from normal; within 0.2° of normal, and within 1° of normal. In

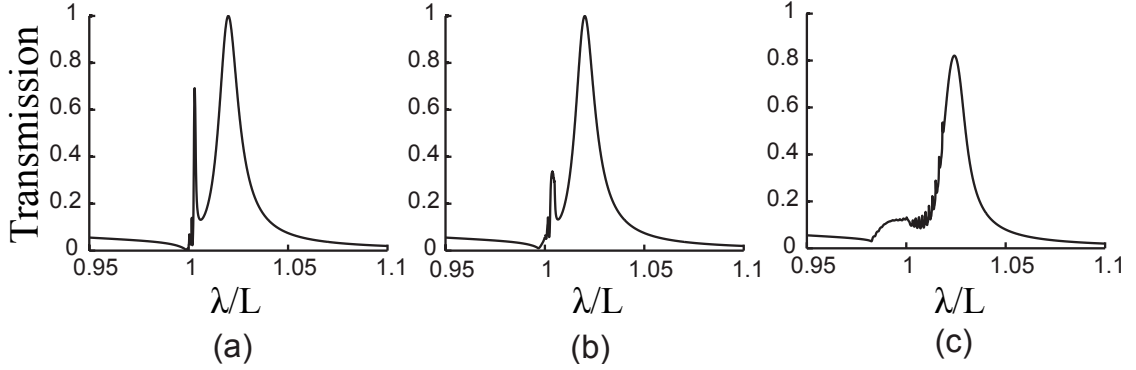


FIGURE 4.5: Transmission profile for a 2-dimensional array of holes with plane waves simultaneously incident at angles varying first (a) from -0.1° to 0.1° ; then (b) from -0.2° to 0.2° ; and finally (c) from -1° to 1° . The narrow peak lowers in height until it disappears, and then the broad peak begins to lessen more slowly. The effect of the Rayleigh anomaly is also decreased, so that there is no longer a point of zero transmission.

each case we have used 20 equally weighted incident waves at equally spaced angles between the bounds in both directions, for a total of 400 incident waves. As the spread of angles becomes larger, the narrow transmission maximum decreases in magnitude. When the incident angle varies within about 0.15 degrees of normal, the narrow maximum is reduced to 50% height, and when the angle varies within 0.3 degrees of normal, the narrow maximum disappears entirely. As the spread of angles becomes larger, the broad maximum decreases in height more slowly, and also increases in width. The minimum accompanying the Rayleigh anomaly rises from zero transmission to small positive transmission. Furthermore, the location of the broad maximum shifts to slightly higher wavelengths. (The small, fast variations in transmission seen in 4.5c are a result of using a finite number of incident waves and decrease as the number of incident waves increases.)

All of these effects are properties of experimental results. Imperfect collimation in our simulations and in experiments causes important changes in the transmission curve: the minimum occurring at the frequency of the Rayleigh anomaly and the

associated transmission maxima, as well as any other phenomena that occur over a narrow range of wavelengths, are all to varying degrees suppressed.

Summary and Discussion

To examine the phenomenon of extraordinary energy transmission through periodic gratings, we have used a mode-matching method that highlights certain features: The Rayleigh anomaly (Chapter 3), which occurs when a plane wave outside the film becomes parallel to the film, is accompanied by very low to zero energy transmission, and the wavelength at which it occurs can be controlled by altering the angle of the incoming energy and the periodic structure. It is also at times associated with large transmission maxima at nearby wavelengths. These transmission maxima are accompanied by the buildup of large energy fields inside the holes.

However, our basic model does not match experimental results very closely. These feature shallower minima at the Rayleigh anomalies and transmission maxima which are broader and lower or do not appear at all. In Sec. 4.1, we find that altering our model to allow for finite conductivity of the metal does not account for this difference: in the microwave regime the effect is negligible, while in the infrared regime the effect is a slight decrease in transmission with no other change. In Sec. 4.2, we find that allowing the array of holes to become finite reduces the transmission by a significant amount (in our example, by 20%), but the Rayleigh anomaly and

the qualitative behavior of transmission remains the same. In Sec. 4.3, however, we find that deviating from perfect collimation by even a small amount (0.1 to 1 degrees) causes significantly decreased transmission maxima and a shallower Rayleigh anomaly. Altering the collimation is the only one of these changes which creates a qualitative difference in transmission and is therefore the most important of these three effects.

We have largely come to understand the Rayleigh anomaly and its associated transmission maxima. However, transmission anomalies can occur for other reasons as well. (See, for example, Takakura (2001).) We can see these anomalies in our simulations, but our model does not lend itself to predicting or understanding them, and changing this is a likely avenue for future efforts. We would also like to examine the effects of different hole shapes, multiple films in sequence, and defects on the surface of the film. Finally, we would like to include nonlinear effects of the metal, which would mean allowing the dielectric constant to be a function of the field strength.

Appendix A

Explicit Waveguide Mode-Plane Wave Inner Products

The inner products (W_k, M_α) corresponding to the overlaps of the plane waves W_k outside the metal and the waveguide modes M_α inside the holes can be computed exactly for the case of 2-dimensionally periodic rectangular holes and 1-dimensionally periodic infinite slits. In this Appendix we list their explicit expressions.

The inner products are computed using the expressions in Sec. 2.2 and Eqs. (2.14) and (2.15). These equations imply that, in all cases, reverse inner products are complex conjugates:

$$(M_\alpha, W_k) = (W_k, M_\alpha)^*. \quad (\text{A.1})$$

For the 2-dimensional system with rectangular holes, the plane waves are enumerated by two numbers k_x, k_y which may each be any integer. The waveguide modes are enumerated by two nonnegative integers m, n . For the one-dimensional system, the plane waves are enumerated by only one integer k_x , as we take $k_y \equiv 0$; the waveguide modes are similarly enumerated by only one nonnegative integer m .

The inner products take different forms depending on whether k_x or k_y is zero and whether m, n are even, odd, or zero. They are further divided depending on whether the plane wave is p - or s -polarized, and whether the waveguide mode is a TE or TM mode.

We label the inner products by the following notation:

$$(W_k, M_\alpha) = (\textit{polarization}; \textit{properties of } k_x, k_y; \textit{TE/TM}; \textit{properties of } m, n). \quad (\text{A.2})$$

For example, the label $(p; k_x = 0, k_y \neq 0; TE; m, n \textit{ odd})$ refers to the inner product of a p -polarized plane wave with a TE mode with the listed properties of k_x, k_y, m, n .

A.1 2-dimensionally Periodic Rectangular Waveguide

Let the film be two-dimensionally periodic with period widths L_x, L_y in the x - and y -directions, respectively. Let the holes be rectangular with side widths a, b in the x - and y -directions, respectively. Finally, let $L = \sqrt{L_x L_y}$ and $|k| = \sqrt{k_x^2 + k_y^2}$. Then the inner products have the following forms:

TE mode, $k_x, k_y \neq 0, m, n \neq 0$:

$$(p; k_x, k_y \neq 0; TE; m, n \textit{ odd}) = -\frac{8i\sqrt{ab}(n^2 a^2 k_x^2 - m^2 b^2 k_y^2)\pi \cos(k_x a/2) \cos(k_y b/2)}{|k|L\sqrt{n^2 a^2 + m^2 b^2}(a^2 k_x^2 - m^2 \pi^2)(b^2 k_y^2 - n^2 \pi^2)} \quad (\text{A.3})$$

$$(p; k_x, k_y \neq 0; TE; m \textit{ odd}, n \textit{ even}) = \frac{8\sqrt{ab}(n^2 a^2 k_x^2 - m^2 b^2 k_y^2)\pi \cos(k_x a/2) \sin(k_y b/2)}{|k|L\sqrt{n^2 a^2 + m^2 b^2}(a^2 k_x^2 - m^2 \pi^2)(b^2 k_y^2 - n^2 \pi^2)} \quad (\text{A.4})$$

$$(p; k_x, k_y \neq 0; TE; m \text{ even}, n \text{ odd}) = \frac{8\sqrt{ab}(n^2a^2k_x^2 - m^2b^2k_y^2)\pi \sin(k_x a/2) \cos(k_y b/2)}{|k|L\sqrt{n^2a^2 + m^2b^2}(a^2k_x^2 - m^2\pi^2)(b^2k_y^2 - n^2\pi^2)} \quad (\text{A.5})$$

$$(p; k_x, k_y \neq 0; TE; m, n \text{ even}) = \frac{8i\sqrt{ab}(n^2a^2k_x^2 - m^2b^2k_y^2)\pi \sin(k_x a/2) \sin(k_y b/2)}{|k|L\sqrt{n^2a^2 + m^2b^2}(a^2k_x^2 - m^2\pi^2)(b^2k_y^2 - n^2\pi^2)} \quad (\text{A.6})$$

The corresponding expressions with s-polarizations are the same as above, save that the term $(n^2a^2k_x^2 - m^2b^2k_y^2)$ in each numerator is replaced with $-k_x k_y (n^2a^2 + m^2b^2)$.

TM mode, $k_x, k_y \neq 0, m, n \neq 0$:

$$(p; k_x, k_y \neq 0; TM; m, n \text{ odd}) = \frac{8imn|k|(ab)^{3/2}\pi \cos(k_x a/2) \cos(k_y b/2)}{L\sqrt{n^2a^2 + m^2b^2}(a^2k_x^2 - m^2\pi^2)(b^2k_y^2 - n^2\pi^2)} \quad (\text{A.7})$$

$$(p; k_x, k_y \neq 0; TM; m \text{ odd}, n \neq 0 \text{ even}) = -\frac{8mn|k|(ab)^{3/2}\pi \cos(k_x a/2) \sin(k_y b/2)}{L\sqrt{n^2a^2 + m^2b^2}(a^2k_x^2 - m^2\pi^2)(b^2k_y^2 - n^2\pi^2)} \quad (\text{A.8})$$

$$(p; k_x, k_y \neq 0; TM; m \neq 0 \text{ even}, n \text{ odd}) = -\frac{8mn|k|(ab)^{3/2}\pi \sin(k_x a/2) \cos(k_y b/2)}{L\sqrt{n^2a^2 + m^2b^2}(a^2k_x^2 - m^2\pi^2)(b^2k_y^2 - n^2\pi^2)} \quad (\text{A.9})$$

$$(p; k_x, k_y \neq 0; TM; m, n \neq 0 \text{ even}) = -\frac{8imn|k|(ab)^{3/2}\pi \sin(k_x a/2) \sin(k_y b/2)}{L\sqrt{n^2a^2 + m^2b^2}(a^2k_x^2 - m^2\pi^2)(b^2k_y^2 - n^2\pi^2)} \quad (\text{A.10})$$

The inner products of TM modes with s -polarized waves are zero. Furthermore, when m or n is zero, the above expressions are replaced with zero.

TE mode with either m or n zero, and $k_x, k_y \neq 0$:

$$(p; k_x, k_y \neq 0; TE; m = 0, n \text{ odd}) = -\frac{4n\pi\sqrt{2ab} \sin(k_x a/2) \cos(k_y b/2)}{L|k|a(b^2 k_y^2 - n^2 \pi^2)} \quad (\text{A.11})$$

$$(p; k_x, k_y \neq 0; TE; m \text{ odd}, n = 0) = -\frac{4m\pi\sqrt{2ab} \cos(k_x a/2) \sin(k_y b/2)}{L|k|b(a^2 k_x^2 - m^2 \pi^2)} \quad (\text{A.12})$$

$$(p; k_x, k_y \neq 0; TE; m = 0, n \text{ even}) = -\frac{4ni\pi\sqrt{2ab} \sin(k_x a/2) \sin(k_y b/2)}{L|k|a(b^2 k_y^2 - n^2 \pi^2)} \quad (\text{A.13})$$

$$(p; k_x, k_y \neq 0; TE; m \text{ even}, n = 0) = -\frac{4mi\pi\sqrt{2ab} \sin(k_x a/2) \sin(k_y b/2)}{L|k|b(a^2 k_x^2 - m^2 \pi^2)} \quad (\text{A.14})$$

To get the equivalent expressions with an s -polarized plane wave, multiply the above by $-k_y/k_x$ if $n \neq 0$, or by k_x/k_y if $m \neq 0$.

TE, $m = 0$, $n \neq 0$, one of k_x, k_y is zero:

$$(p; k_x = 0, k_y \neq 0; TE; m = 0, n \neq 0) = 0 \quad (\text{A.15})$$

$$(s; k_x = 0, k_y \neq 0; TE; m = 0, n \text{ odd}) = \frac{2n\pi\sqrt{2ab} \cos(k_y b/2) \text{sign}(k_y)}{L(b^2 k_y^2 - n^2 \pi^2)} \quad (\text{A.16})$$

$$(s; k_x = 0, k_y \neq 0; TE; m = 0, n \neq 0 \text{ even}) = \frac{2in\pi\sqrt{2ab} \sin(k_y b/2)}{L(b^2 k_y^2 - n^2 \pi^2)} \quad (\text{A.17})$$

$$(p; k_x \neq 0, k_y = 0; TE; m = 0, n \text{ odd}) = \frac{4b\sqrt{2} \sin(k_x a/2)}{L\sqrt{abk_x^2 n\pi}} \quad (\text{A.18})$$

$$(p; k_x \neq 0, k_y = 0; TE; m = 0, n \neq 0 \text{ even}) = 0 \quad (\text{A.19})$$

$$(s; k_x \neq 0, k_y = 0; TE; m = 0, n \neq 0) = 0 \quad (\text{A.20})$$

TE, $m \neq 0, n = 0$, one of k_x, k_y is zero:

$$(p; k_x = 0, k_y \neq 0; TE; m \text{ odd}, n = 0) = \frac{4a\sqrt{2} \sin(k_y b/2)}{L\sqrt{abk_y^2 m\pi}} \quad (\text{A.21})$$

$$(p; k_x = 0, k_y \neq 0; TE; m \neq 0 \text{ even}, n = 0) = 0 \quad (\text{A.22})$$

$$(s; k_x = 0, k_y \neq 0; TE; m \neq 0, n = 0) = 0 \quad (\text{A.23})$$

$$(p; k_x \neq 0, k_y = 0; TE; m \neq 0, n = 0) = 0 \quad (\text{A.24})$$

$$(s; k_x \neq 0, k_y = 0; TE; m \text{ odd}, n = 0) = -\frac{2m\pi\sqrt{2ab} \cos(k_x a/2)}{L(a^2k_x^2 - m^2\pi^2)} \quad (\text{A.25})$$

$$(s; k_x \neq 0, k_y = 0; TE; m \neq 0 \text{ even}, n = 0) = -\frac{2mi\pi\sqrt{2ab} \sin(k_x a/2)}{L(a^2k_x^2 - m^2\pi^2)} \quad (\text{A.26})$$

TE, $k_x = k_y = 0$:

$$(p; k_x = k_y = 0; TE; m = 0, n \text{ odd}) = \frac{2\sqrt{2ab}}{Ln\pi} \quad (\text{A.27})$$

$$(p; k_x = k_y = 0; TE; m = 0, n \neq 0 \text{ even}) = 0; \quad (\text{A.28})$$

$$(s; k_x = k_y = 0; TE; m = 0, n \neq 0) = 0; \quad (\text{A.29})$$

$$(p; k_x = k_y = 0; TE; m \neq 0, n = 0) = 0; \quad (\text{A.30})$$

$$(s; k_x = k_y = 0; TE; m \text{ odd}, n = 0) = \frac{2\sqrt{2ab}}{L\pi m} \quad (\text{A.31})$$

$$(s; k_x = k_y = 0; TE; m \neq 0 \text{ even}, n = 0) = 0; \quad (\text{A.32})$$

TE or TM, $k_x = k_y = 0$, $m, n \neq 0$:

$$(p \text{ or } s; k_x = k_y = 0; TE \text{ or } TM; m, n \neq 0) = 0; \quad (\text{A.33})$$

TE or TM, $m, n \neq 0$, $k_x = 0$ and $k_y \neq 0$:

$$(p; k_x = 0, k_y \neq 0; TE; m, n \text{ odd}) = -\frac{8ib^2k_y \cos(k_y b/2)}{L\pi(b^2k_y^2 - n^2\pi^2)\sqrt{n^2a/b + m^2b/a}} \quad (\text{A.34})$$

$$(p; k_x = 0, k_y \neq 0; TE; m \text{ odd}, n \neq 0 \text{ even}) = \frac{8b^2k_y \sin(k_y b/2)}{L\pi(b^2k_y^2 - n^2\pi^2)\sqrt{n^2a/b + m^2b/a}} \quad (\text{A.35})$$

$$(p; k_x = 0, k_y \neq 0; TE; m \neq 0 \text{ even}, n \neq 0) = 0 \quad (\text{A.36})$$

$$(p; k_x = 0, k_y \neq 0; TM; m, n \text{ odd}) = -\frac{8niabk_y \cos(k_y b/2)}{L\pi m(b^2 k_y^2 - n^2 \pi^2) \sqrt{n^2 a/b + m^2 b/a}} \quad (\text{A.37})$$

$$(p; k_x = 0, k_y \neq 0; TM; m \text{ odd}, n \neq 0 \text{ even}) = \frac{8nabk_y \sin(k_y b/2)}{L\pi m(b^2 k_y^2 - n^2 \pi^2) \sqrt{n^2 a/b + m^2 b/a}} \quad (\text{A.38})$$

$$(p; k_x = 0, k_y \neq 0; TM; m \neq 0 \text{ even}, n \text{ odd}) = 0 \quad (\text{A.39})$$

$$(s; k_x = 0, k_y \neq 0; TE \text{ or } TM; m, n \neq 0) = 0 \quad (\text{A.40})$$

TE or TM, $m, n \neq 0, k_x \neq 0$ and $k_y = 0$:

$$(p; k_x \neq 0, k_y = 0; TE; m, n \text{ odd}) = -\frac{8ia^2 k_x \cos(k_x a/2)}{L\pi(a^2 k_x^2 - m^2 \pi^2) \sqrt{n^2 a/b + m^2 b/a}} \quad (\text{A.41})$$

$$(p; k_x \neq 0, k_y = 0; TE; m \text{ odd}, n \neq 0 \text{ even}) = 0 \quad (\text{A.42})$$

$$(p; k_x \neq 0, k_y = 0; TE; m \neq 0 \text{ even}, n \text{ odd}) = \frac{8a^2 k_x \sin(k_x a/2)}{L\pi(a^2 k_x^2 - m^2 \pi^2) \sqrt{n^2 a/b + m^2 b/a}} \quad (\text{A.43})$$

$$(p; k_x \neq 0, k_y = 0; TE; m, n \neq 0 \text{ even}) = 0; \quad (\text{A.44})$$

$$(p; k_x \neq 0, k_y = 0; TM; m, n \text{ odd}) = \frac{8miabk_x \cos(k_x a/2)}{Ln\pi(a^2k_x^2 - n^2\pi^2)\sqrt{n^2a/b + m^2b/a}} \quad (\text{A.45})$$

$$(p; k_x \neq 0, k_y = 0; TM; m \text{ odd}, n \neq 0 \text{ even}) = 0 \quad (\text{A.46})$$

$$(p; k_x \neq 0, k_y = 0; TM; m \neq 0 \text{ even}, n \text{ odd}) = -\frac{8mabk_x \sin(k_x a/2)}{Ln\pi(a^2k_x^2 - m^2\pi^2)\sqrt{n^2a/b + m^2b/a}} \quad (\text{A.47})$$

$$(p; k_x \neq 0, k_y = 0; TM; m, n \neq 0 \text{ even}) = 0 \quad (\text{A.48})$$

$$(s; k_x \neq 0, k_y = 0; TE \text{ or } TM; m, n \neq 0) = 0; \quad (\text{A.49})$$

A.2 1-dimensionally Periodic Slit Waveguide

Let the film be periodic in the x -direction with period width $L = L_x$, and constant in the y -direction. Let the slits have width a . Then the inner products have the following forms:

$$(p; \text{any } k_x; TE; \text{any } m) = 0; \quad (\text{A.50})$$

$$(s; \text{any } k_x; TM; \text{any } m) = 0; \quad (\text{A.51})$$

$$(p; k_x \neq 0; TM; m \neq 0) = \frac{-ik_x^2\sqrt{2}}{\sqrt{L_x a}|k_x|(-k_x^2 + (m\pi/a)^2)} (e^{-ik_x a/2} \cos(m\pi) - e^{ik_x a/2}) \quad (\text{A.52})$$

$$(p; k_x = 0; TM; m \neq 0) = 0 \quad (\text{A.53})$$

$$(p; k_x \neq 0; TM; m = 0) = \frac{i}{\sqrt{L_x a} |k_x|} (e^{-ik_x a/2} - e^{ik_x a/2}) \quad (\text{A.54})$$

$$(p; k_x = 0; TM; m = 0) = \sqrt{\frac{a}{L_x}} \quad (\text{A.55})$$

$$(s; k_x \neq 0; TE; \text{any } m) = -\frac{k_x m \pi \sqrt{2}}{|k_x| a \sqrt{L_x a} (-k_x^2 + (m\pi/a)^2)} (e^{-ik_x a/2} \cos(m\pi) - e^{ik_x a/2}) \quad (\text{A.56})$$

$$(s; k_x = 0; TE; \text{any } m) = -\frac{\sqrt{2a}}{m\pi \sqrt{L_x}} (\cos(m\pi) - 1) \quad (\text{A.57})$$

Appendix B

Asymptotic Expression for the Propagation Constant of a Circular Waveguide Mode Bounded by an Imperfect Conductor

In this section we compute the first two terms of an asymptotic series for the propagation constant of a waveguide mode in a circular waveguide bounded by a metal of finite conductivity.

B.1 Derivation

Waveguide modes in a circular waveguide may be enumerated in part by an integer $n \geq 0$ denoting the index of the Bessel functions which the mode is composed of. For each n there are infinitely many modes which we enumerate with the integer $m > 0$, roughly associated with the zeroes of either the Bessel function J_n or its derivative J'_n . For each pair m, n , there are two modes, which in the perfectly conducting case are TM TE modes. (See Sec. 4.1.1 for further details.)

Suppose that the waveguide has radius a ; that it is filled with material of dielectric constant ϵ_1 and bounded by metal of dielectric constant ϵ_2 ; that the magnetic

constant μ is constant throughout both regions; and that the frequency of illumination is ω . Let k_z be the propagation constant of the mode, and define $k_1^2 = \omega^2 \mu \epsilon_1$; $k_2^2 = \omega^2 \mu \epsilon_2$; $\lambda_1^2 = k_1^2 - k_z^2$; and $\lambda_2^2 = k_2^2 - k_z^2$. Then k_z is determined by the following equation found in Snitzer (1961),

$$\left(\frac{J'_n(\lambda_1 a)}{\lambda_1 a J_n(\lambda_1 a)} + \frac{K'_n(\lambda_2 a)}{\lambda_2 a K_n(\lambda_2 a)} \right) \left(k_1^2 \frac{J'_n(\lambda_1 a)}{\lambda_1 a J_n(\lambda_1 a)} + k_2^2 \frac{K'_n(\lambda_2 a)}{\lambda_2 a K_n(\lambda_2 a)} \right) = n^2 k_z^2 \left(\frac{1}{(\lambda_1 a)^2} + \frac{1}{(\lambda_2 a)^2} \right)^2. \quad (\text{B.1})$$

Here we consider the asymptotic limit in which the metal bounding the waveguide approaches a perfect conductor, that is, $|\epsilon_2| \rightarrow \infty$. In this limit, the propagation constant k_z approaches that of a perfect conductor, that is, $k_z \rightarrow \sqrt{\omega^2 - (u_{mn}/a)^2}$, where u_{mn} is the m^{th} root of either J_n or J'_n , depending on whether the limiting mode is a TM or TE mode, respectively.

When the bounding metal is of finite conductivity, the waveguide modes are called hybrid modes, being partially composed of both TE and TM modes. When the limiting mode as $|\epsilon_2| \rightarrow \infty$ is TE, we will call the hybrid mode “TE-like”; when the limiting mode is TM, we will call the hybrid mode “TM-like.”

For brevity we will suppress the dependence of each variable on the indices m, n , as the values associated with one mode do not influence the other modes. Define h_0 to be the propagation constant of the limiting TM or TE mode. Thus h_0 is determined by the relation $u_0 = a\sqrt{\epsilon_1 \mu \omega^2 - h_0^2}$, where u_0 is a zero of the Bessel function J_n in the TM-like case, or a zero of the derivative J'_n in the TE-like case. We will solve Eq. (B.1) for k_z asymptotically under the limits $1/|\epsilon_2| \rightarrow 0$ and $h_s = k_z - h_0 \rightarrow 0$.

Set $u = a\lambda_1$, $w = a\lambda_2$, $\eta_1 = J'_n(u)/uJ_n(u)$, and $\eta_2 = K'_n(w)/wK_n(w)$. Then Eq. (B.1) becomes

$$(\eta_1 + \eta_2)(k_1^2 \eta_1 + k_2^2 \eta_2) = n^2 k_z^2 \left(\frac{1}{u^2} + \frac{1}{w^2} \right)^2. \quad (\text{B.2})$$

Divide both sides of this equation by k_1^2 and set $\epsilon = \epsilon_2/\epsilon_1$:

$$\eta_1^2 + (1 + \epsilon)\eta_1\eta_2 + \epsilon\eta_2^2 = \frac{n^2 k_z^2}{\omega^2 \mu \epsilon_1} \left(\frac{1}{u^2} + \frac{1}{w^2} \right)^2. \quad (\text{B.3})$$

We note that η_2 and w both explicitly depend on ϵ_2 , while η_1 and u do not. We solve this quadratic equation for η_1 in terms of η_2 to find

$$2\eta_1 = -(1 + \epsilon)\eta_2 \pm \sqrt{(1 + \epsilon)^2 \eta_2^2 - 4 \left(\epsilon \eta_2^2 - \frac{n^2 k_z^2}{\omega^2 \mu \epsilon_1} \left(\frac{1}{u^2} + \frac{1}{w^2} \right)^2 \right)}, \quad (\text{B.4})$$

which can be simplified and written as

$$2\eta_1 = -(1 + \epsilon)\eta_2 \pm (1 - \epsilon)\eta_2 \sqrt{1 + \frac{\frac{4n^2 k_z^2}{\omega^2 \mu \epsilon_1} \left(\frac{1}{u^2} + \frac{1}{w^2} \right)^2}{(1 - \epsilon)^2 \eta_2^2}}. \quad (\text{B.5})$$

We intend to begin by expanding η_2 , and we shall find that it is of order $1/\epsilon^{1/2}$. Thus, the denominator within the square root in Eq. (B.5) tends to infinity.

Expanding η_2

We begin by finding an expansion for η_2 . First, note that the asymptotic expansions of K_n and K'_n for large arguments z are, as found in Abramowitz and Stegun (1964),

$$K_n(z) \sim \sqrt{\frac{\pi}{2z}} e^{-z} \left(1 + \frac{4n^2 - 1}{8z} + \frac{(4n^2 - 1)(4n^2 - 9)}{2!(8z)^2} + \frac{(4n^2 - 1)(4n^2 - 9)(4n^2 - 25)}{3!(8z)^3} + \dots \right) \quad (\text{B.6})$$

$$K'_n(z) \sim -\sqrt{\frac{\pi}{2z}} e^{-z} \left(1 + \frac{4n^2 + 3}{8z} + \frac{(4n^2 - 1)(4n^2 + 15)}{2!(8z)^2} + \frac{(4n^2 - 1)(4n^2 - 9)(4n^2 + 35)}{3!(8z)^3} + \dots \right). \quad (\text{B.7})$$

The first of these equations implies via the binomial expansion that $1/K$ can be expanded as

$$\frac{1}{K_n(z)} \sim \sqrt{\frac{2z}{\pi}} e^z \left(1 - \frac{4n^2 - 1}{8z} + \frac{(4n^2 - 1)^2 - (1/2!)(4n^2 - 1)(4n^2 - 9)}{(8z)^2} + \dots \right), \quad (\text{B.8})$$

and therefore, after some simplification,

$$\frac{K'_n(z)}{zK_n(z)} \sim - \left(\frac{1}{z} + \frac{1}{2z^2} + \frac{4n^2 - 1}{8z^3} + \dots \right). \quad (\text{B.9})$$

The value of z we will be using in the above expression is of course $w = a\sqrt{k_z^2 - \omega^2\mu\epsilon_2}$.

We must expand the appropriate powers of this expression:

$$w^{-3} = \frac{1}{a^3(-\omega^2\mu\epsilon_2)^{3/2}} \times \frac{1}{1 - k_z^2/(\omega^2\mu\epsilon_2)^{3/2}} = \frac{1}{a^3(-\omega^2\mu\epsilon_2)^{3/2}} \times \left(1 + \frac{3}{2} \left(\frac{k_z^2}{\omega^2\mu\epsilon_2} \right) + \frac{15}{8} \left(\frac{k_z^2}{\omega^2\mu\epsilon_2} \right)^2 + \frac{105}{48} \left(\frac{k_z^2}{\omega^2\mu\epsilon_2} \right)^3 + \dots \right) \quad (\text{B.10})$$

$$w^{-2} = \frac{1}{a^2(-\omega^2\mu\epsilon_2)} \times \frac{1}{(1 - k_z^2/(\omega^2\mu\epsilon_2))} = \frac{1}{a^2(-\omega^2\mu\epsilon_2)} \times \left(1 + \left(\frac{k_z^2}{\omega^2\mu\epsilon_2} \right) + \left(\frac{k_z^2}{\omega^2\mu\epsilon_2} \right)^2 + \left(\frac{k_z^2}{\omega^2\mu\epsilon_2} \right)^3 + \dots \right) \quad (\text{B.11})$$

$$w^{-1} = \frac{1}{a(-\omega^2\mu\epsilon_2)^{1/2}} \times \frac{1}{(1 - k_z^2/(\omega^2\mu\epsilon_2)^{1/2})} =$$

$$\frac{1}{a(-\omega^2\mu\epsilon_2)^{1/2}} \times \left(1 + \frac{1}{2} \left(\frac{k_z^2}{\omega^2\mu\epsilon_2} \right) + \frac{3}{8} \left(\frac{k_z^2}{\omega^2\mu\epsilon_2} \right)^2 + \frac{15}{48} \left(\frac{k_z^2}{\omega^2\mu\epsilon_2} \right)^3 + \dots \right). \quad (\text{B.12})$$

Let $\delta = 1/\epsilon_2^{1/2}$. Then, incorporating the last three expressions into Eq. (B.9) along with $k_z = h_0 + h_s$, we obtain

$$\frac{K'_n(w)}{wK_n(w)} \sim -\delta \left(\frac{1}{a(-\omega^2\mu)^{1/2}} \right) - \delta^2 \left(\frac{1}{2a^2(-\omega^2\mu)} \right) - \delta^3 \left(\frac{4n^2 - 1}{8a^3(-\omega^2\mu)^{3/2}} - \frac{h_0^2}{2a(-\omega^2\mu)^{3/2}} \right) +$$

$$\delta^3 h_s \left(\frac{2h_0}{2a(-\omega^2\mu)^{3/2}} \right) + \delta^3 h_s^2 \left(\frac{1}{2a(-\omega^2\mu)^{3/2}} \right) + \dots \quad (\text{B.13})$$

correct to order 3 in δ . This is our final expansion for η_2 . For simplicity, we shall write it as

$$\eta_2 \sim A_1\delta + A_2\delta^2 + A_3\delta^3 + A_{3,1}\delta^3 h_s + A_{3,2}\delta^3 h_s^2 + \dots, \quad (\text{B.14})$$

where the values of A_1, A_2 , etc. may be read from Eq. (B.13).

Expanding the Square Root

Next, we will find an expansion for the square root term in Eq. (B.5). For the time being, call this term S :

$$S = \sqrt{1 + \frac{\frac{4n^2 k_z^2}{\omega^2 \mu \epsilon_1} \left(\frac{1}{u^2} + \frac{1}{w^2} \right)^2}{(1 - \epsilon)^2 \eta_2^2}}. \quad (\text{B.15})$$

We discovered above that η_2 decays proportionally to $1/\epsilon_2^{1/2}$, so the denominator $(1 - \epsilon^2)\eta_2^2$ inside the square root tends to infinity as $|\epsilon_2| \rightarrow \infty$. As long as the fraction is less than 1, we may write

$$S = 1 + \frac{1}{2} \left(\frac{\frac{4n^2 k_z^2}{\omega^2 \mu \epsilon_1} \left(\frac{1}{u^2} + \frac{1}{w^2} \right)^2}{(1-\epsilon)^2 \eta_2^2} \right) - \frac{1}{8} \left(\frac{\frac{4n^2 k_z^2}{\omega^2 \mu \epsilon_1} \left(\frac{1}{u^2} + \frac{1}{w^2} \right)^2}{(1-\epsilon)^2 \eta_2^2} \right)^2 + \dots \quad (\text{B.16})$$

Let us begin with the denominator:

$$\begin{aligned} [(1-\epsilon^2)\eta_2^2]^{-1} &= [(1-\epsilon)^2(A_1\delta + A_2\delta^2 + A_3\delta^3 + A_{3,1}\delta^3 h_s + A_{3,2}\delta^3 h_s^2 + \dots)]^{-1} \\ &= (A_1\delta\epsilon)^{-2} \left[\left(\frac{1}{\epsilon^2} - \frac{2}{\epsilon} + 1 \right) \left(1 + \frac{A_2}{A_1}\delta + \frac{A_3}{A_1}\delta^2 + \frac{A_{3,1}}{A_1}\delta^2 h_s + \frac{A_{3,2}}{A_1}\delta^2 h_s^2 + \dots \right)^2 \right] \\ &= \delta^2 \frac{\epsilon_1^2}{A_1^2} \left[1 + \delta \left(\frac{2A_2}{A_1} \right) + \delta^2 \left(-2\epsilon_1 + \left(\frac{A_2}{A_1} \right)^2 + 2\frac{A_3}{A_1} \right) + \right. \\ &\quad \left. \delta^2 h_s \left(\frac{2A_{3,1}}{A_1} \right) + \delta^2 h_s^2 \left(\frac{2A_{3,2}}{A_1} \right) + \dots \right]^{-1}. \end{aligned} \quad (\text{B.17})$$

The terms involving δ tend to zero, so we may use the binomial expansion and collect powers to obtain

$$\begin{aligned} &= \delta^2 \frac{\epsilon_1^2}{A_1^2} \left[1 + \delta \left(\frac{-2A_2}{A_1} \right) + \delta^2 \left(2\epsilon_1 - \left(\frac{A_2}{A_1} \right)^2 - \frac{2A_3}{A_1} + \frac{4A_2^2}{A_1^2} \right) + \right. \\ &\quad \left. \delta^2 h_s \left(-\frac{2C_{3,1}}{C_1} \right) + \delta^2 h_s^2 \left(-\frac{2A_{3,2}}{A_1} \right) + \dots \right]. \end{aligned} \quad (\text{B.18})$$

We have already expanded w^{-2} above. Incorporating $k_z = h_0 + h_s$ gives

$$\begin{aligned}
w^{-2} &= \frac{1}{a^2(-\omega^2\mu\epsilon_2)} \times \left(1 + \left(\frac{k_z^2}{\omega^2\mu\epsilon_2} \right) + \left(\frac{k_z^2}{\omega^2\mu\epsilon_2} \right)^2 + \left(\frac{k_z^2}{\omega^2\mu\epsilon_2} \right)^3 + \dots \right) \\
&= \frac{\delta^2}{-a^2\omega^2\mu} \left[1 + \delta^2 \left(\frac{h_0^2}{\omega^2\mu} \right) + \delta^2 h_s \left(\frac{2h_0}{\omega^2\mu} \right) + \delta^2 h_s^2 \left(\frac{1}{\omega^2\mu} \right) + \delta^4 \left(\frac{h_0^4}{\omega^4\mu^2} \right) + \right. \\
&\quad \left. \delta^4 h_s \left(\frac{4h_0^3}{\omega^4\mu^2} \right) + \delta^4 h_s^2 \left(\frac{6h_0^2}{\omega^4\mu^2} \right) + \delta^4 h_s^3 \left(\frac{4h_0}{\omega^4\mu^2} \right) + \delta^4 h_s^4 \left(\frac{1}{\omega^4\mu^2} \right) + \dots \right]
\end{aligned} \tag{B.19}$$

It remains to expand u^{-2} . The number u does not depend on δ , so it will have an expansion solely in terms of h_s :

$$\begin{aligned}
u^{-1} &= \left(a\sqrt{k_1^2 - k_z^2} \right)^{-1} = \left(a\sqrt{k_1^2 - (h_0 + h_s)^2} \right)^{-1} = \frac{1}{a\sqrt{k_1^2 - h_0^2}} \left(1 - \frac{2h_0h_s + h_s^2}{k_1^2 - h_0^2} \right)^{-1/2} \\
&= \frac{1}{a\sqrt{k_1^2 - h_0^2}} \left[1 + h_s \left(\frac{2h_0}{2!(k_1^2 - h_0^2)} \right) + h_s^2 \left(\frac{1}{2(k_1^2 - h_0^2)} + \frac{1 \cdot 3 \cdot 2^2 h_0^2}{2^2 \cdot 2!(k_1^2 - h_0^2)^2} \right) + \right. \\
&\quad \left. h_s^3 \left(\frac{1 \cdot 3 \cdot 4h_0}{2^2 \cdot 2!(k_1^2 - h_0^2)^2} + \frac{1 \cdot 3 \cdot 5 \cdot 2^3 h_0^3}{2^3 \cdot 3!(k_1^2 - h_0^2)^2} \right) + \right. \\
&\quad \left. h_s^4 \left(\frac{1 \cdot 3}{2^2 \cdot 2!(k_1^2 - h_0^2)^2} + \frac{1 \cdot 3 \cdot 5 \cdot 4h_0^2}{2^2 \cdot 3!(k_1^2 - h_0^2)^3} + \frac{1 \cdot 3 \cdot 5 \cdot 7 \cdot 2^4 h_0^4}{2^4 \cdot 4!(k_1^2 - h_0^2)^4} \right) + \dots \right];
\end{aligned} \tag{B.20}$$

$$\begin{aligned}
u^{-2} &= \frac{1}{a^2(k_1^2 - h_0^2)} \left[1 + h_s 2 \left(\frac{2h_0}{2(k_1^2 - h_0^2)} \right) + \right. \\
&\quad \left. h_s^2 \left\{ 2 \left(\frac{1}{2(k_1^2 - h_0^2)} + \frac{1 \cdot 3 \cdot 2^2 h_0^2}{2^2 \cdot 2!(k_1^2 - h_0^2)^2} \right) + \left(\frac{2h_0}{2(k_1^2 - h_0^2)} \right)^2 \right\} + \right. \\
&\quad \left. h_s^3 \left\{ 2 \left(\frac{1 \cdot 3 \cdot 4h_0}{2^2 \cdot 2!(k_1^2 - h_0^2)^2} + \frac{1 \cdot 3 \cdot 5 \cdot 2^3 h_0^3}{2^3 \cdot 3!(k_1^2 - h_0^2)^3} \right) + \right. \right. \\
&\quad \left. \left. 2 \left(\frac{2h_0}{2!(k_1^2 - h_0^2)} \right) \left(\frac{1}{2(k_1^2 - h_0^2)} + \frac{1 \cdot 3 \cdot 2^2 h_0^2}{2^2 \cdot 2!(k_1^2 - h_0^2)^2} \right) \right\} + \dots \right].
\end{aligned} \tag{B.21}$$

Set $D_1 = 1/(a^2(k_1^2 - h_0^2))$, and $D_2 = -1/(a^2\omega^2\mu)$. Then we can combine the last two expansions and collect powers to obtain

$$\begin{aligned} \left(\frac{1}{u^2} + \frac{1}{w^2}\right)^2 &= \mathbf{1}D_1^2 + \\ &\mathbf{h}_s D_1^2 \left(\frac{4h_0}{k_1^2 - h_0^2}\right) + \\ &\mathbf{h}_s^2 D_1^2 \left[6 \left(\frac{h_0}{k_1^2 - h_0^2}\right)^2 + \frac{2}{k_1^2 - h_0^2} + \frac{6h_0^2}{(k_1^2 - h_0^2)^2}\right] + \dots \end{aligned} \quad (\text{B.22})$$

Although further terms of this series contain powers of δ as well, we will find that only the first two terms are found in the leading two series of the final asymptotic expansion. Call the coefficients of this series B_{ij} , where i is the power of δ and j is the power of h_s . Then, correct to order δ^4 and h_s^3 ,

$$\begin{aligned} \left(\frac{1}{u^2} + \frac{1}{w^2}\right)^2 &= B_{0,0} + B_{0,1}h_s + B_{0,2}h_s^2 + B_{0,3}h_s^3 + \\ &B_{2,0}\delta^2 + B_{2,1}\delta^2h_s + B_{2,2}\delta^2h_s^2 + B_{2,3}\delta^2h_s^3 + \\ &B_{4,0}\delta^4 + B_{4,1}\delta^4h_s + B_{4,2}\delta^4h_s^2 + B_{4,3}\delta^4h_s^3. \end{aligned} \quad (\text{B.23})$$

Finally we multiply this by $(2k_z^2n^2/\omega^2\mu\epsilon_1)$ and the expansion for $[(1-\epsilon)^2\eta_2^2]^{-1}$ above, again using $k_z = h_0 + h_s$, to find

$$\begin{aligned} [(1-\epsilon)^2\eta_2^2]^{-1} \frac{2n^2k_z^2}{\omega^2\mu\epsilon_1} \left(\frac{1}{u^2} + \frac{1}{w^2}\right)^2 &= \delta^2 \left[\frac{2n^2\epsilon_1}{\omega^2\mu A_1^2} h_0^2 B_{0,0} \right] + \\ &\delta^2 \mathbf{h}_s \left[\frac{2n^2\epsilon_1}{\omega^2\mu A_1^2} (2h_0 B_{0,0} + h_0^2 B_{0,1}) \right] + \\ &\delta^2 \mathbf{h}_s^2 \left[\frac{2n^2\epsilon_1}{\omega^2\mu A_1^2} (B_{0,0} + 2h_0 B_{0,1} + h_0^2 E_{0,2}) \right] + \dots \end{aligned} \quad (\text{B.24})$$

Again, we will only end up using the first two terms of this series. For completion, we will formally continue keeping terms up to order δ^4 and h_s^3 . To do this we need the first terms of the square of the above expansion, as we see in Eq. (B.16) (this time we multiply by $-2(k_z^2 n^2 / \omega^2 \mu \epsilon_1)^2$):

$$\left\{ [(1 - \epsilon)^2 \eta_2^2]^{-1} \frac{2n^2 k_z^2}{\omega^2 \mu \epsilon_1} \left(\frac{1}{u^2} + \frac{1}{w^2} \right)^2 \right\}^2 = \delta^4 \left(\frac{-2n^4 \epsilon_1^2}{\omega^4 \mu^2 A_1^4} h_0^4 B_{0,0}^2 \right) + \delta^4 \mathbf{h}_s \left(\frac{-4n^4 \epsilon_1^2}{\omega^4 \mu^2 A_1^4} h_0^2 B_{0,0} (2h_0 B_{0,0} + h_0^2 B_{0,1}) \right) + \dots \quad (\text{B.25})$$

The final expansion of Eq. (B.16), then, is 1 plus the sum of the last two expansions. For simplicity we will write the coefficients of this sum as $C_{i,j}$, where i is the power of δ and j is the power of h_s . Then

$$S = 1 + \delta^2 C_{2,0} + \delta^2 h_s C_{2,1} + \delta^2 h_s^2 C_{2,2} + \delta^2 h_s^3 C_{2,3} + \delta^3 C_{3,0} + \delta^3 h_s C_{3,1} + \delta^3 h_s C_{3,2} + \delta^3 h_s^3 C_{3,3} + \delta^4 C_{4,0} + \delta^4 h_s C_{4,1} + \delta^4 h_s^2 C_{4,2} + \delta^4 h_s^3 C_{4,3} + \dots \quad (\text{B.26})$$

Expansion of η_1 , TE-like mode

It remains to find an expansion for the term η_1 . This will have to be done twice, once for TE-like modes and again for TM-like modes. In the limit of a TE-like hybrid mode as $|\epsilon_2| \rightarrow \infty$, the numerator of η_1 becomes zero, whereas in the limit of TM-like mode, the denominator becomes zero instead.

We begin with the TE-like mode. There is no dependence on δ of η_1 , so the expansion will depend solely on h_s . The argument $u = a\sqrt{k_1^2 - k_z^2}$ of the numerator J'_n tends towards a zero of J'_n ; we will continue to call this zero u_0 ; it is equal to

$a\sqrt{k_1^2 - h_0^2}$. Therefore, we will write a Taylor expansion for J'_n and also for the denominator J_n about this zero of J'_n :

$$J'_n(z) = J''_n(u_0)(z - u_0) + \frac{J'''_n(u_0)}{2!}(z - u_0)^2 + \frac{J_n^{(4)}(u_0)}{3!}(z - u_0)^3 + \dots \quad (\text{B.27})$$

$$J_n(z) = J_n(u_0) \left[1 + \frac{J''_n(u_0)}{2!J_n(u_0)}(z - u_0)^2 + \frac{J'''_n(u_0)}{3!J_n(u_0)}(z - u_0)^3 + \dots \right]. \quad (\text{B.28})$$

Then in the limit,

$$\begin{aligned} \frac{1}{J_n(z)} = \frac{1}{J_n(u_0)} & \left[1 + \left(\frac{-J''_n(u_0)}{2!J_n(u_0)} \right) (z - u_0)^2 + \left(\frac{-J'''_n(u_0)}{3!J_n(u_0)} \right) (z - u_0)^3 + \right. \\ & \left. \left(\frac{J''_n(u_0)^2}{2!^2 J_n(u_0)^2} - \frac{J_n^{(4)}(u_0)}{4!J_n(u_0)} \right) (z - u_0)^4 + \dots \right], \quad (\text{B.29}) \end{aligned}$$

so that taken together,

$$\begin{aligned} \frac{J'_n(z)}{J_n(z)} = \frac{1}{J_n(u_0)} & \left\{ J''_n(u_0)(z - u_0) + \frac{J'''_n(u_0)}{2!}(z - u_0)^2 + \right. \\ & \left(-J''_n(u_0) \frac{J''_n(u_0)}{2!J_n(u_0)} + \frac{J_n^{(4)}(u_0)}{3!} \right) (z - u_0)^3 + \\ & \left. \left(-J''_n(u_0) \frac{J'''_n(u_0)}{3!J_n(u_0)} - \frac{J'''_n(u_0)}{2!} \cdot \frac{J''_n(u_0)}{2!J_n(u_0)} + \frac{J_n^{(5)}(u_0)}{4!} \right) (z - u_0)^4 \right\}. \quad (\text{B.30}) \end{aligned}$$

The value of z in the above expressions will, of course, be u :

$$\begin{aligned}
u &= a\sqrt{k_1^2 - k_z^2} = a\sqrt{k_1^2 - (h_0 + h_s)^2} = a\sqrt{k_1^2 - h_0^2} \left(1 - \frac{2h_0h_s + h_s^2}{k_1^2 - h_0^2}\right)^{1/2} \\
&= u_0 \left[1 - h_s \left(\frac{h_0}{k_1^2 - h_0^2} \right) - h_s^2 \left(\frac{1}{2(k_1^2 - h_0^2)} + \frac{h_0^2}{2(k_1^2 - h_0^2)^2} \right) \right. \\
&\quad - h_s^3 \left(\frac{h_0}{2(k_1^2 - h_0^2)^2} + \frac{h_0^3}{2(k_1^2 - h_0^2)^3} \right) \\
&\quad \left. - h_s^4 \left(\frac{1}{8(k_1^2 - h_0^2)^2} + \frac{h_0^2}{4(k_1^2 - h_0^2)^3} + \frac{5h_0^4}{8(k_1^2 - h_0^2)^4} \right) + \dots \right],
\end{aligned} \tag{B.31}$$

so that $u - u_0$ has the same expansion, without the leading term. Putting this into the above expression for $J'_n(z)/J_n(z)$, we obtain

$$\begin{aligned}
\frac{J'_n(u)}{J_n(u)} &= \frac{1}{J_n(u_0)} \left[\mathbf{h}_s u_0 \left(J''_n(u_0) \frac{-h_0}{k_1^2 - h_0^2} \right) + \right. \\
&\quad \left. \mathbf{h}_s^2 \left(u_0 J''_n(u_0) \left(\frac{-1}{2(k_1^2 - h_0^2)} + \frac{-h_0^2}{2(k_1^2 - h_0^2)^2} \right) + (u_0)^2 \frac{J'''_n(u_0)}{2!} \left(\frac{h_0}{k_1^2 - h_0^2} \right)^2 \right) + \dots \right] \\
&\equiv \frac{1}{J_n(u_0)} (E_1 h_s + E_2 h_s^2 + E_3 h_s^3 + \dots).
\end{aligned} \tag{B.32}$$

Finally, we have already found the expansion of $1/u$ in Eq. (B.20). Thus,

$$\begin{aligned}
\eta_1 &= \frac{J'_n(u)}{u J_n(u)} = \frac{1}{u_0 J_n(u_0)} \left[h_s (A_1) + h_s^2 \left(E_2 + E_1 \frac{h_0}{k_1^2 - h_0^2} \right) + \right. \\
&\quad \left. h_s^3 \left(E_3 + E_2 \frac{h_0}{k_1^2 - h_0^2} + E_1 \left(\frac{1}{2(k_1^2 - h_0^2)} + \frac{3h_0^2}{2(k_1^2 - h_0^2)^2} \right) \right) + \dots \right] \\
&= F_1 h_s + F_2 h_s^2 + F_3 h_s^3 + F_4 h_s^4 + \dots
\end{aligned} \tag{B.33}$$

Solving for h_s , TE-like mode

Now we can put all of this together. Returning to the original equation (B.5),

$$2\eta_1 = -(1 + \epsilon)\eta_2 \pm (1 - \epsilon)\eta_2 \times \left[1 + \frac{1}{2} \left(\frac{\frac{4n^2 k_z^2}{\omega^2 \mu \epsilon_1} \left(\frac{1}{u^2} + \frac{1}{w^2} \right)^2}{(1 - \epsilon)^2 \eta_2^2} \right) - \frac{1}{8} \left(\frac{\frac{4n^2 k_z^2}{\omega^2 \mu \epsilon_1} \left(\frac{1}{u^2} + \frac{1}{w^2} \right)^2}{(1 - \epsilon)^2 \eta_2^2} \right)^2 + \dots \right], \quad (\text{B.34})$$

we incorporate the series expansions we found above:

$$\begin{aligned} 2(F_1 h_s + F_2 h_s^2 + F_3 h_s^3 + \dots) = & \\ & - \left(1 + \frac{\epsilon_2}{\epsilon_1} \right) (A_1 \delta + A_2 \delta^2 + A_3 \delta^3 + A_{3,1} \delta^3 h_s + A_{3,2} \delta^3 h_s^2 + \dots) \\ & \pm \left(1 - \frac{\epsilon_2}{\epsilon_1} \right) (A_1 \delta + A_2 \delta^2 + A_3 \delta^3 + A_{3,1} \delta^3 h_s + A_{3,2} \delta^3 h_s^2 + \dots) \\ & \times [1 + \delta^2 C_{2,0} + \delta^2 h_s C_{2,1} + \dots + \delta^3 h_s^3 C_{3,3} + \dots], \quad (\text{B.35}) \end{aligned}$$

where we have included terms of each series correct to order δ^3 , h_s^3 and combinations (recall that η_2 does not have a $\delta^3 h_s^3$ term).

The left side of this equation tends to zero as $h_s \rightarrow 0$, so the right side must tend to zero also. This means that we must choose the + sign. After cancellation:

$$\begin{aligned} 2(F_1 h_s + F_2 h_s^2 + F_3 h_s^3 + \dots) = & \\ & - 2(A_1 \delta + A_2 \delta^2 + A_3 \delta^3 + A_{3,1} \delta^3 h_s + A_{3,2} \delta^3 h_s^2 + \dots) \\ & - \left(1 - \frac{1}{\epsilon_1 \delta^2} \right) (A_1 \delta + A_2 \delta^2 + A_3 \delta^3 + A_{3,1} \delta^3 h_s + A_{3,2} \delta^3 h_s^2 + \dots) \\ & \times [1 + \delta^2 C_{2,0} + \delta^2 h_s C_{2,1} + \dots + \delta^3 h_s^3 C_{3,3} + \dots]. \quad (\text{B.36}) \end{aligned}$$

The largest term on the left must balance the largest term on the right. Hence to first order,

$$h_s \sim \frac{A_1}{F_1} \left(-1 + \frac{C_{2,0}}{2\epsilon_1} \right) \delta. \quad (\text{B.37})$$

Therefore, the second-order terms include the δ^2 , h_s^2 and δh_s terms:

$$2F_1 h_s + 2F_2 h_s^2 \sim - (2A_1) \delta + \left(\frac{A_1 C_{2,0}}{\epsilon_1} \right) \delta + (2A_2) \delta^2 + \left(\frac{A_2 C_{2,0}}{\epsilon_1} \right) \delta^2 + \left(\frac{A_1 C_{2,1}}{\epsilon_1} \right) \delta h_s. \quad (\text{B.38})$$

We apply the quadratic formula to solve for h_s :

$$4F_2 h_s \sim - \left(2F_1 - \frac{A_1 C_{2,1}}{\epsilon_1} \delta \right) \pm \sqrt{\left(2F_1 - \frac{A_1 C_{2,1}}{\epsilon_1} \delta \right)^2 - 4(2F_2) \left[(2A_1) \delta - \left(\frac{A_1 C_{2,0}}{\epsilon_1} \right) \delta^2 + (2A_2) \delta^2 - \left(\frac{A_2 C_{2,0}}{\epsilon_1} \right) \delta^2 \right]}. \quad (\text{B.39})$$

In order that h_s be of order δ , we must take the positive sign.

$$\begin{aligned} 4F_2 h_s &\sim - \left(2F_1 - \frac{A_1 C_{2,1}}{\epsilon_1} \delta \right) + \\ &\quad \left(2F_1 - \frac{A_1 C_{2,1}}{\epsilon_1} \delta \right) \left\{ 1 + \frac{-4(2F_2) \left[(2A_1) \delta - \left(\frac{A_1 C_{2,0}}{\epsilon_1} \right) \delta + (2A_2) \delta^2 - \left(\frac{A_2 C_{2,0}}{\epsilon_1} \right) \delta^2 \right]}{\left(2F_1 - \frac{A_1 C_{2,1}}{\epsilon_1} \delta \right)^2} \right\}^{1/2} \\ &= \left(2F_1 - \frac{A_1 C_{2,1}}{\epsilon_1} \delta \right) \times \\ &\quad \left\{ \frac{1}{2} \left(\frac{-4(2F_2) \left[(2A_1) \delta - \left(\frac{A_1 C_{2,0}}{\epsilon_1} \right) \delta + (2A_2) \delta^2 - \left(\frac{A_2 C_{2,0}}{\epsilon_1} \right) \delta^2 \right]}{\left(2F_1 - \frac{A_1 C_{2,1}}{\epsilon_1} \delta \right)^2} \right) - \frac{1}{8} (X)^2 + \dots \right\} \end{aligned} \quad (\text{B.40})$$

where the term X is the same as in the previous parentheses. We expand the denominator in powers of δ , minding that we only need to record terms of order δ^2 :

$$\begin{aligned} \left(2F_1 - \frac{A_1 C_{2,1}}{\epsilon_1} \delta\right)^{-2} &= (2F_1)^{-2} \left(1 + \frac{-A_1 C_{2,1}}{2F_1 \epsilon_1} \delta\right)^{-2} \\ &= (2F_1)^{-2} \left[1 - 2 \left(\frac{-A_1 C_{2,1}}{2C_1 \epsilon_1} \delta\right) + 3 \left(\frac{-A_1 C_{2,1}}{2F_1 \epsilon_1} \delta\right)^2 + \dots\right]. \end{aligned} \quad (\text{B.41})$$

Multiplying this by the numerator, we find

$$\begin{aligned} &\frac{-4(2F_2) \left[(2A_1)\delta - \left(\frac{A_1 C_{2,0}}{\epsilon_1}\right) \delta + (2A_2)\delta^2 - \left(\frac{A_2 C_{2,0}}{\epsilon_1}\right) \delta^2 \right]}{\left(2F_1 - \frac{A_1 C_{2,1}}{\epsilon_1} \delta\right)^2} = \\ &\delta \left[-2F_2 F_1^{-2} \left(2A_1 - \frac{A_1 C_{2,0}}{\epsilon_1}\right) \right] + \delta^2 \left[4F_2 F_1^{-2} \left(\frac{-A_1 C_{2,1}}{2F_1 \epsilon_1}\right) \left(2A_1 - \frac{A_1 C_{2,0}}{\epsilon_1}\right) \right. \\ &\quad \left. - 2F_2 F_1^{-2} \left(2A_2 - \frac{A_2 C_{2,0}}{\epsilon_1}\right) \right]. \end{aligned} \quad (\text{B.42})$$

The δ^1 term in this equation will be squared in the X^2 term of Eq. (B.40) in order to achieve all of the δ^2 terms. Finally we find that

$$\begin{aligned} h_s \sim &\delta \left\{ -\frac{A_1}{F_1} \left(1 - \frac{C_{2,0}}{2\epsilon_1}\right) \right\} + \\ &\delta^2 \left\{ \frac{C_1^2}{F_1} \left(1 - \frac{C_{2,0}}{2\epsilon_1}\right) \left[-1 + \frac{C_{2,0}}{2\epsilon_1} - \frac{C_{2,1}}{2F_1 \epsilon_1} \right] - \frac{C_2}{F_1} \left(1 - \frac{C_{2,0}}{2\epsilon_1}\right) \right\}. \end{aligned} \quad (\text{B.43})$$

Expansion of η_1 , TM-like mode

In the previous sections we saw that in the limit of a TE-like mode as $|\epsilon_2| \rightarrow \infty$, the numerator of η_1 becomes zero. In the limit of a TM-mode, however, the denominator of η_1 becomes zero instead. Therefore we must compute a new expansion of η_1 .

In the limit of a TM-like mode, the propagation constant k_z tends to a zero of the Bessel function J_n . We call this zero u_0 ; it is equal to $a\sqrt{k_1^2 - h_0^2}$, where h_0 is the propagation constant of the limiting TM mode. We begin by writings Taylor expansions for J_n and J'_n about u_0 :

$$J_n(z) = J'_n(u_0)(z - u_0) + \frac{J''_n(u_0)}{2!}(z - u_0)^2 + \frac{J'''_n(u_0)}{3!}(z - u_0)^3 + \dots \quad (\text{B.44})$$

$$J'_n(z) = J'_n(u_0) + J''_n(u_0)(z - u_0) + \frac{J'''_n(u_0)}{2!}(z - u_0)^2 + \dots \quad (\text{B.45})$$

The Bessel function J_n is in the denominator of η_1 :

$$\begin{aligned} \frac{1}{J_n(z)} &= \left[J'_n(u_0)(z - u_0) + \frac{J''_n(u_0)}{2!}(z - u_0)^2 + \dots \right]^{-1} \\ &= [J'_n(u_0)(z - u_0)]^{-1} (1 - (X) + (X)^2 - (X)^3 + \dots) \end{aligned} \quad (\text{B.46})$$

where the term X is equal to

$$X = \frac{J''_n(u_0)}{2!J'_n(u_0)}(z - u_0) + \frac{J'''_n(u_0)}{3!J'_n(u_0)}(z - u_0)^2 + \dots \quad (\text{B.47})$$

Collecting powers of $z - u_0$, we obtain

$$\begin{aligned} \frac{1}{J_n(z)} &= [J'_n(u_0)(z - u_0)]^{-1} \left[1 + (z - u_0) \left[-\frac{J''_n(u_0)}{2!J'_n(u_0)} \right] + \right. \\ &\quad (z - u_0)^2 \left(\left(\frac{J''_n(u_0)}{2!J'_n(u_0)} \right)^2 + \frac{J'''_n(u_0)}{3!J'_n(u_0)} \right) + \\ &\quad \left. (z - u_0)^3 \left[-\left(\frac{J''_n(u_0)}{2!J'_n(u_0)} \right)^3 + 2 \left(\frac{J''_n(u_0)}{2!J'_n(u_0)} \right) \left(\frac{J'''_n(u_0)}{3!J'_n(u_0)} \right) - \frac{J_n^{(4)}(u_0)}{3!J'_n(u_0)} \right]^2 + \dots \right], \end{aligned} \quad (\text{B.48})$$

and so

$$\begin{aligned} \frac{J'_n(z)}{J_n(z)} &= [J'_n(u_0)]^{-1} \{ (\mathbf{z} - \mathbf{u}_0)^{-1} J'_n(u_0) + \mathbf{1} \left(J'_n(u_0) \left(-\frac{J''_n(u_0)}{2!J'_n(u_0)} \right) + J''_n(u_0) \right) + \\ &\quad (\mathbf{z} - \mathbf{u}_0) \left(J'_n(u_0) \left[\left(\frac{J''_n(u_0)}{2!J'_n(u_0)} \right)^2 + \frac{J'''_n(u_0)}{3!J'_n(u_0)} \right] + J''_n(u_0) \left[-\frac{J''_n(u_0)}{2!J'_n(u_0)} \right] + \frac{J'''_n(u_0)}{2!} \right) + \dots \}. \end{aligned} \quad (\text{B.49})$$

As before, the value of z will be $u = a\sqrt{k_1^2 - k_z^2}$. The full expression for $u - u_0$ is the same as it was for the TE-like mode for $u - u_0$:

$$\begin{aligned}
u - u_0 = u_0 & \left[-h_s \left(\frac{h_0}{k_1^2 - h_0^2} \right) - h_s^2 \left(\frac{1}{2(k_1^2 - h_0^2)} + \frac{h_0^2}{2(k_1^2 - h_0^2)^2} \right) \right. \\
& - h_s^3 \left(\frac{h_0}{2(k_1^2 - h_0^2)^2} + \frac{h_0^3}{2(k_1^2 - h_0^2)^3} \right) \\
& \left. - h_s^4 \left(\frac{1}{8(k_1^2 - h_0^2)^2} + \frac{h_0^2}{4(k_1^2 - h_0^2)^3} + \frac{5h_0^4}{8(k_1^2 - h_0^2)^4} \right) + \dots \right].
\end{aligned} \tag{B.50}$$

This time, we also need an expansion for the inverse:

$$\begin{aligned}
(u - u_0)^{-1} & = \left(-h_s u_0 \left(\frac{h_0}{k_1^2 - h_0^2} \right) \right)^{-1} \left[1 + h_s \left(\frac{1}{2h_0} + \frac{h_0}{2!(k_1^2 - h_0^2)} \right) + \right. \\
& h_s^2 \left(\frac{1}{k_1^2 - h_0^2} + \frac{h_0^2}{2(k_1^2 - h_0^2)^2} \right) + \\
& \left. h_s^3 \left(\frac{1}{4h_0(k_1^2 - h_0^2)} + \frac{h_0}{4(k_1^2 - h_0^2)^2} + \frac{5h_0^3}{8(k_1^2 - h_0^2)^2} \right) + \dots \right]^{-1} \\
& = \left(-h_s u_0 \left(\frac{h_0}{k_1^2 - h_0^2} \right) \right)^{-1} \left[1 - (X) + (X)^2 - (X)^3 + \dots \right]
\end{aligned} \tag{B.51}$$

where X is the sum of the terms of order h_s^1 and above; collecting powers, we find

$$\begin{aligned}
(u - u_0)^{-1} &= \left(-u_0 \left(\frac{h_0}{k_1^2 - h_0^2} \right) \right)^{-1} \{ \mathbf{h}_s^{-1} + \mathbf{1} \left[-\frac{1}{2h_0} - \frac{h_0}{2(k_1^2 - h_0^2)} \right] + \\
&\quad \mathbf{h}_s \left[\left(\frac{1}{2h_0} + \frac{h_0}{2(k_1^2 - h_0^2)} \right)^2 - \left(\frac{1}{2(k_1^2 - h_0^2)} + \frac{h_0^2}{2(k_1^2 - h_0^2)} \right) \right] + \\
&\quad \mathbf{h}_s^2 \left[-\left(\frac{1}{2h_0} + \frac{h_0}{2(k_1^2 - h_0^2)} \right)^3 \right. \\
&\quad \quad \left. + 2 \left(\frac{1}{2h_0} + \frac{h_0}{2(k_1^2 - h_0^2)} \right) \left(\frac{1}{2(k_1^2 - h_0^2)} + \frac{h_0^2}{2(k_1^2 - h_0^2)} \right) \right. \\
&\quad \quad \left. - \left(\frac{1}{8h_0(k_1^2 - h_0^2)} + \frac{h_0}{4(k_1^2 - h_0^2)^2} + \frac{5h_0^3}{8(k_1^2 - h_0^2)^3} \right) \right] \} + \dots
\end{aligned} \tag{B.52}$$

Incorporating this into the expansion for J'_n/J_n , we find

$$\begin{aligned}
\frac{J'_n(u)}{J_n(u)} &= [J'_n(u_0)]^{-1} \{ \mathbf{h}_s^{-1} \left[J'_n(u_0) \left(\frac{-u_0 h_0}{k_1^2 - h_0^2} \right)^{-1} \right] + \\
&\quad \mathbf{1} \left[J'_n(u_0) \left(\frac{-u_0 h_0}{k_1^2 - h_0^2} \right)^{-1} \left(-\frac{1}{2h_0} - \frac{h_0}{2(k_1^2 - h_0^2)} \right) - J'_n(u_0) \left(\frac{J''_n(u_0)}{2J'_n(u_0)} \right) + J''_n(u_0) \right] + \\
&\quad \mathbf{h}_s [J'_n(u_0) \left[\left(\frac{1}{2h_0} + \frac{h_0}{2(k_1^2 - h_0^2)^2} \right)^2 - \left(\frac{1}{2(k_1^2 - h_0^2)} + \frac{h_0^2}{2(k_1^2 - h_0^2)^2} \right) \right] \left(\frac{-u_0 h_0}{k_1^2 - h_0^2} \right)^{-1} \\
&\quad \quad + \left(J'_n(u_0) \left[\left(\frac{J''_n(u_0)}{2J'_n(u_0)} \right)^2 + \frac{J'''_n(u_0)}{3!J'_n(u_0)} \right] - J''_n(u_0) \left[\frac{J''_n(u_0)}{2J'_n(u_0)} \right] + \frac{J'''_n(u_0)}{2} \right) \\
&\quad \quad \times \left(\frac{-u_0 h_0}{k_1^2 - h_0^2} \right)] + \dots \\
&= \frac{1}{J'_n(u_0)} (G_{-1} h_s^{-1} + G_0 + G_1 h_s + G_2 h_s^2 + \dots).
\end{aligned} \tag{B.53}$$

Finally, we already have the expansion for $1/u$ from Eq. (B.20). Incorporating this, we find

$$\begin{aligned}
\eta_1 &= \frac{J'_n(u)}{uJ_n(u)} = \frac{1}{u_0 J'_n(u_0)} [\mathbf{h}_s^{-1} G_{-1} + \mathbf{1} \left(G_0 + G_{-1} \left(\frac{h_0}{k_1^2 - h_0^2} \right) \right) + \\
&\quad \mathbf{h}_s \left(G_1 + G_0 \left(\frac{h_0}{k_1^2 - h_0^2} \right) + G_{-1} \left(\frac{1}{2(k_1^2 - h_0^2)} + \frac{3h_0^2}{2(k_1^2 - h_0^2)^2} \right) \right) + \dots \quad (\text{B.54}) \\
&= L_{-1} h_s^{-1} + L_0 + L_1 h_s + L_2 h_s^2 + \dots .
\end{aligned}$$

Solving for h_s , TM-like mode

Again we return to Eq. (B.5):

$$\begin{aligned}
2\eta_1 &= -(1 + \epsilon)\eta_2 \pm (1 - \epsilon)\eta_2 \times \\
&\quad \left[1 + \frac{1}{2} \left(\frac{4n^2 k_z^2 \left(\frac{1}{u^2} + \frac{1}{w^2} \right)^2}{\omega^2 \mu \epsilon_1 (1 - \epsilon)^2 \eta_2^2} \right) - \frac{1}{8} \left(\frac{4n^2 k_z^2 \left(\frac{1}{u^2} + \frac{1}{w^2} \right)^2}{\omega^2 \mu \epsilon_1 (1 - \epsilon)^2 \eta_2^2} \right)^2 + \dots \right]. \quad (\text{B.55})
\end{aligned}$$

We incorporate the series expansions of each term:

$$\begin{aligned}
2(L_{-1} h_s^{-1} + L_0 + L_1 h_s + L_2 h_s^2 + \dots) &= \\
&- \left(1 + \frac{\epsilon_2}{\epsilon_1} \right) (A_1 \delta + A_2 \delta^2 + A_3 \delta^3 + A_{3,1} \delta^3 h_s + A_{3,2} \delta^3 h_s + \dots) \\
&+ \left(1 - \frac{\epsilon_2}{\epsilon_1} \right) (A_1 \delta + A_2 \delta^2 + A_3 \delta^3 + A_{3,1} \delta^3 h_s + A_{3,2} \delta^3 h_s^2 + \dots) \\
&\quad \times [\delta^2 C_{2,0} + \delta^2 h_s C_{2,1} + \dots + \delta^3 h_s^2 C_{3,2}], \quad (\text{B.56})
\end{aligned}$$

correct to order δ^3 , h_s^2 and combinations. Because the left side tends to infinity, the right side must do the same, and hence we must take the + sign, which reduces this equation to

$$\begin{aligned}
2(L_{-1}h_s^{-1} + L_0 + L_1h_s + L_2h_s^2 + \dots) = & \\
& - \frac{2}{\epsilon_1} \delta^{-2} (A_1\delta + A_2\delta^2 + A_3\delta^3 + A_{3,1}\delta^3h_s + A_{3,2}\delta^3h_s^2 + \dots) \\
& + \left(1 - \frac{1}{\epsilon_1}\delta^{-2}\right) (A_1\delta + A_2\delta^2 + A_3\delta^3 + A_{3,1}\delta^3h_s + A_{3,2}\delta^3h_s^2 + \dots) \\
& \times [\delta^2C_{2,0} + \delta^2h_sC_{2,1} + \dots + \delta^3h_s^2C_{3,2} + \dots]. \quad (\text{B.57})
\end{aligned}$$

The first appearance of h_s on the right side is accompanied by δ . If we keep on the right side the three lowest-order terms, we find

$$\begin{aligned}
2(L_{-1}h_s^{-1} + L_0 + L_1h_s + L_2h_s^2 + \dots) = & \\
& \delta^{-1} \left(-\frac{2A_1}{\epsilon_1}\right) + \mathbf{1} \left(-\frac{2A_2}{\epsilon_1}\right) + \delta \left(-\frac{2A_3}{\epsilon_1} - \frac{A_1C_{2,0}}{\epsilon_1}\right) + \dots \quad (\text{B.58})
\end{aligned}$$

The terms tending to infinity on either side must balance, so we must have

$$h_s \sim \left(-\frac{L_{-1}}{A_1}\right) \delta. \quad (\text{B.59})$$

Therefore the second order terms are

$$2L_{-1}h_s^{-1} + 2L_0 = \delta^{-1} \left(-\frac{2A_1}{\epsilon_1}\right) + \left(-\frac{2A_2}{\epsilon_1}\right). \quad (\text{B.60})$$

Solving this for h_s , we obtain

$$h_s \sim -\left(\frac{L_{-1}\epsilon_1}{A_1}\right) \delta + \left(\frac{L_{-1}\epsilon_1}{A_1}\right) \left(\frac{A_2}{A_1} + \frac{L_0\epsilon_1}{A_1}\right) \delta^2. \quad (\text{B.61})$$

While it seems that we could use the quadratic formula to find a third term in the expansion, this would in fact require us to calculate several more terms in each series expansion.

B.2 Final simplified form of asymptotic expansions

To review, each waveguide mode we are considering can be identified by three values: an integer $n \geq 0$, which is the index of the Bessel functions the mode is composed of; whether the mode is TM-like or TE-like; and an integer $m > 0$ which enumerates the zeroes of J_n in the TM-like case, or the zeroes of J'_n in the TE-like case. For brevity we suppress the dependence of each term on m, n , as the values associated with one mode have no bearing on the other modes.

For the TE-like case, set u_0 to be the m^{th} zero of J'_n , and define h_0 by the relation $u_0 = a\sqrt{\epsilon_1\mu\omega^2 - h_0^2}$ (so that h_0 is the propagation constant of the limiting TE mode). Then the propagation constant of a TE-like hybrid mode is

$$k_z \sim h_0 + \frac{Q_1}{\epsilon_2^{1/2}} + \frac{Q_2}{\epsilon_2}, \quad (\text{B.62})$$

where the constant coefficients are

$$Q_1 = \frac{-J_n(u_0)(k_1^2 - h_0^2)}{ah_0(-\omega^2\mu)^{1/2}J'_n(u_0)} \left(1 + \frac{n^2h_0^2}{(k_1^2 - h_0^2)^2} \right) \quad (\text{B.63})$$

$$Q_2 = \frac{-J_n(u_0)(k_1^2 - h_0^2)}{h_0J''_n(u_0)} \left(1 + \frac{n^2h_0^2}{(k_1^2 - h_0^2)^2} \right) \times \left\{ \frac{1}{a^2\omega^2\mu} \left(\frac{1}{2} + \frac{n^2h_0^2}{(k_1^2 - h_0^2)^2} + \frac{J_n(u_0)n^2}{J''_n(u_0)(k_1^2 - h_0^2)} \left(2 + \frac{4h_0^2}{k_1^2 - h_0^2} \right) \right) \right\}. \quad (\text{B.64})$$

For the TM-like case, set u_0 to be the m^{th} zero of J_n , and define h_0 by the

relation $u_0 = a\sqrt{\epsilon_1\mu\omega^2 - h_0^2}$ (so that h_0 is the propagation constant of the limiting TM mode). Then the propagation constant of a TM-like hybrid mode is

$$k_z \sim h_0 + \frac{R_1}{\epsilon_2^{1/2}} + \frac{R_2}{\epsilon_2}, \quad (\text{B.65})$$

where the constant coefficients are given by

$$R_1 = -\frac{\epsilon_1(-\omega^2\mu)^{1/2}}{ah_0} \quad (\text{B.66})$$

$$R_2 = \frac{\epsilon_1\omega^2\mu}{2h_0} \left(\frac{1}{a^2h_0^2} - \frac{1}{u_0^2} + \frac{J_n''(u_0)}{u_0J_n'(u_0)} \right) + \frac{\epsilon_1}{2a^2h_0}. \quad (\text{B.67})$$

Appendix C

A Theoretical Formula for Bound States in 3D

In this Appendix we extend a result of Shipman and Venakides (2005) from two dimensions to three. This result is a partial formula for transmission through a periodic array of holes in a film near a *bound state*, that is, a state in which energy is localized in the vicinity of the film. In particular, we examine *nonrobust* bound states, those which disappear upon perturbation of the wave number.

(The topics discussed in this Appendix are not directly related to those found previously in this work, and follows the notation of the above cited paper.)

This formula is essentially the same as in Shipman and Venakides (2005), except that it is valid for a two-dimensionally periodic film, instead of a one-dimensionally periodic array. The bulk of what follows may be found in the reference. It is reproduced here for completeness.

We will work with Maxwell's equations at constant frequency ω . The scatterer is a sheet of finite thickness with dielectric properties that are 2-D periodic. We assume no losses in the materials that compose the sheet or in the surrounding material. Besides periodicity, our approach does not pose any additional restrictions on the

geometry of the slab.

Maxwell's equations give rise to a system of integral equations on the material interface, which we write symbolically as

$$A\psi = \phi. \tag{C.1}$$

Here ϕ and ψ take values on the material interface, and A is a bounded integral operator. ϕ is the trace of the source (incoming) electromagnetic field on the interface (a vector function with 6 components, which we will take to be a plane wave), and ψ is the trace of the total external electromagnetic field, which is the sum of the source and scattered fields.

Each component u of the electromagnetic field will, for the complex pair (κ, ω) have an expansion in Fourier harmonics away from the slab:

$$u(\mathbf{x}, z) = \sum_{m \in \mathbb{Z}^2} c_m^\pm e^{\pm i\eta_m z} e^{i(m+\kappa) \cdot \mathbf{x}}, \tag{C.2}$$

where $\eta_m^2 = \epsilon_0 \mu_0 \omega^2 - (m_1 + \kappa_1)^2 - (m_2 + \kappa_2)^2$. We require that each component also satisfies an *outgoing condition*: η_m should be chosen to be positive when it is real, and to have positive imaginary part when it is imaginary. Those finitely many m for which η_m is real are said to contribute *propagating harmonics* to the sum, while those for which η_m are imaginary contribute *decaying harmonics*. (Henceforth the dielectric and magnetic constants ϵ_0 and μ_0 will both be taken to be 1.)

For our purposes, we extend all of these notions to complex ω and κ . The outgoing condition is extended, with the exponents η_m analytically continued in ω and κ ; it remains true that all but a finite number of the harmonics will decay as $|z| \rightarrow \infty$. The operator A depends analytically on ω and κ as well.

A solution ψ of the equation $A\psi = 0$ is called a *resonance*; thus, resonances occur at values of (κ, ω) for which A has an eigenvalue $l = l(\kappa, \omega)$ that equals zero. A *bound*

state is a resonance which decays at infinity. Henceforth use the term *resonance* only when it is not a bound state. A conservation of energy argument shows that bound states can only occur at real frequencies and wave numbers. We identify two types of bound states:

(1) A *robust* bound state is one for which there are arbitrarily small real perturbations of κ that result in real perturbations of those ω at which the bound state exists; that is, we have a real local dispersion relation $\omega = W(\kappa)$. A robust bound state will only occur at values of (κ, ω) for which there are no propagating harmonics in the Fourier expansion above.

(2) At a *nonrobust* bound state, real perturbations of κ result in complex perturbations of ω . In this situation, there do exist propagating harmonics, but they attain zero coefficients c_j (often as a result of some sort of symmetry, for example, $\kappa = 0$). As κ is perturbed and ω becomes complex, the bound state devolves into a resonance.

In this Appendix we examine transmission properties at (κ, ω) close to a nonrobust bound state at $\omega = \omega_0 > 0, \kappa = \kappa_0 = 0$ where the eigenvalue l has a simple zero. We assume there is exactly one propagating harmonic, at $m = (0, 0)$, which attains a zero coefficient c_0 at (κ_0, ω_0) , and the rest of the harmonics decay. (We will write $\eta = \eta_0$.)

Choose (κ, ω) so that $l(\kappa, \omega)$ is close to but different from zero. Our source field ϕ , as input into the integral equations $A\psi = \phi$, is a plane wave, normalized by the eigenvalue l and with time dependence suppressed:

$$l\phi = l\mathbf{U}_0 e^{i(\kappa \cdot \mathbf{x} + \eta z)}, \quad (\text{C.3})$$

where $\eta = \sqrt{\omega^2 - |\kappa|^2}$, and $\mathbf{U}_0 = (\mathbf{H}_0, \mathbf{E}_0)$ is a unit vector in \mathbb{R}^6 consisting of two vectors in \mathbb{R}^3 which specify the directions of the magnetic and electric fields.

Maxwell's equations require that \mathbf{E}_0 and \mathbf{H}_0 both be perpendicular to $(\kappa_1, \kappa_2, \eta)$, and also to each other.

Solving the integral equation gives the full field which, at large $|z|$, behaves (since there is only one propagating harmonic) as

$$\psi \sim (\mathbf{U}_0 l e^{i\eta z} + \mathbf{U}_1 r e^{-i\eta z}) e^{i\kappa \cdot \mathbf{x}}, (z \rightarrow -\infty) \quad (\text{C.4})$$

$$\psi \sim \mathbf{U}_2 t e^{i\eta z} e^{i\kappa \cdot \mathbf{x}}, (z \rightarrow \infty), \quad (\text{C.5})$$

where t is the transmission amplitude and r is the reflection amplitude. The direction vector \mathbf{U}_0 may not be preserved by the actions of reflection and transmission; hence we introduce \mathbf{U}_1 and \mathbf{U}_2 which satisfy the same restrictions as did \mathbf{U}_0 .

Due to the analyticity of A , we know that l , r and t are all analytic in the variables κ, ω in a complex region of $(\kappa, \omega) = (0, \omega_0)$. Also, computation of the energy flux through the slab gives us the conservation of energy relation $|l|^2 = |r|^2 + |t|^2$ for real values of (κ, ω) . Since we have assumed that l has a simple zero at $(0, \omega_0)$, this means among other things that t and r are both also zero there. The following expression for l is then a consequence of the Weierstrauss preparation theorem:

$$l = e^{i\theta_l} [\bar{\omega} + c_1 \kappa_1 + c_2 \kappa_2 + c_{11} \kappa_1^2 + c_{12} \kappa_1 \kappa_2 + c_{22} \kappa_2^2 + H(\kappa)] [l_0 + l_1 \kappa_1 + l_2 \kappa_2 + l_3 \bar{\omega} + H(\kappa, \omega)], \quad (\text{C.6})$$

where $\bar{\omega} = \omega - \omega_0$; l_0 is positive, and H is simply a placeholder for higher order terms.

The Weierstrauss preparation theorem, in somewhat less than full detail, concerns an analytic function of several variables ($l(\kappa, \omega)$ in our case), which is zero at a certain point $((\kappa, \omega) = (\kappa_0, \omega_0))$. The function can be written as the product of (a) a polynomial in one of the variables (ω) with coefficients that depend on the

other variables (κ), that equals zero at the point in question, times (b) an analytic function which is nonzero at that point. We have assumed that l has a simple zero at (κ_0, ω_0) ; so the polynomial factor given by the Weierstrass preparation theorem can be factored into a term which is zero at that point and is linear in ω , times a term which is nonzero there. The linear term is retained and the nonzero part is absorbed into the auxiliary analytic function.

Similarly, we make the generic assumptions that $\partial t/\partial\omega(0, \omega_0), \partial r/\partial\omega(0, \omega_0)$ are both nonzero. This allows us to find similar expressions for r and t :

$$r = e^{i\theta_r} [\bar{\omega} + \rho_1\kappa_1 + \rho_2\kappa_2 + \rho_{11}\kappa_1^2 + \rho_{12}\kappa_1\kappa_2 + \rho_{22}\kappa_2^2 + H(\kappa)] [r_0 + r_1\kappa_1 + r_2\kappa_2 + r_3\bar{\omega} + H(\kappa, \omega)] \quad (\text{C.7})$$

$$t = e^{i\theta_t} [\bar{\omega} + \tau_1\kappa_1 + \tau_2\kappa_2 + \tau_{11}\kappa_1^2 + \tau_{12}\kappa_1\kappa_2 + \tau_{22}\kappa_2^2 + H(\kappa)] [t_0 + t_1\kappa_1 + t_2\kappa_2 + t_3\bar{\omega} + H(\kappa, \omega)] \quad (\text{C.8})$$

where again r_0 and t_0 are positive.

We observe several properties of the coefficients:

- (i) The coefficients obviously vary with the geometry of the scatterer.
- (ii) A pseudoperiodic (Bloch) outgoing Helmholtz field with real wavevector must have $Im(\omega) \leq 0$. Hence, for real κ near κ_0 , we have $Im(\omega) \leq 0$ whenever $l(\kappa, \omega) = 0$.
- (ii) The previous item forces c_1 and c_2 to be real, for otherwise we could easily choose real κ_j such that, in setting $l = 0$, ω must have a positive imaginary part.
- (iii) For the same reason, we must have $Im(c_{jj}) \geq 0, j = 1, 2$. The condition $Im(c_{12}) \leq 2\sqrt{Im(c_{11}c_{22})}$ is sufficient to ensure no trouble from the mixed term.

The relation $|l|^2 = |t|^2 + |r|^2$, applied to the expressions above, gives several further relationships between coefficients:

- (1) Collecting $\bar{\omega}^2$ terms give $l_0^2 = r_0^2 + t_0^2$.
- (2) The κ_j^2 terms, $j = 1, 2$, give $|c_j|^2 l_0^2 = |\rho_j|^2 r_0^2 + |\tau_j|^2 t_0^2$.
- (3) The $\bar{\omega}\kappa_j$ terms, $j = 1, 2$, give $l_0^2 \text{Re}(c_1) = r_0^2 \text{Re}(\rho_1) + t_0^2 \text{Re}(\tau_1)$.
- (4) The $\kappa_1\kappa_2$ terms give $l_0^2 \text{Re}(c_1 c_2) = r_0^2 \text{Re}(\rho_1 \rho_2) + t_0^2 \text{Re}(\tau_1 \tau_2)$.
- (5) If we allow κ, ω to tend to zero along a path on which $\kappa_2 = \kappa_1^2$, and $\omega + c_1 \kappa_1 + c_2 \kappa_2 = 0$, then the quadratic terms of $|l|^2$ disappear and what remains is $O(\kappa_1^4)$. The quadratic terms of $|r|^2$ and $|t|^2$ must also vanish, then, which requires that $\rho_1 = \tau_1 = c_1$. Performing the same manipulation with $\kappa_1 = \kappa_2^2$ instead leads to $\rho_2 = \tau_2 = c_2$.

Of course, we are also interested in the total transmission, which is defined either as the ratio

$$T = \frac{|t|}{|l|} = \frac{|t/r|}{\sqrt{1 + |t/r|^2}} \quad (\text{C.9})$$

or, in the physics literature, as the square of this quantity. Rather than including the entire expansions, we expect to get acceptably accurate results by writing

$$\left| \frac{t}{r} \right| \approx \frac{t_0 |\bar{\omega} + c_1 \kappa_1 + c_2 \kappa_2 + \tau_{11} \kappa_1^2 + \tau_{12} \kappa_1 \kappa_2 + \tau_{22} \kappa_2^2|}{r_0 |\bar{\omega} + c_1 \kappa_1 + c_2 \kappa_2 + \rho_{11} \kappa_1^2 + \rho_{12} \kappa_1 \kappa_2 + \rho_{22} \kappa_2^2|} (1 + \zeta_1 \kappa_1 + \zeta_2 \kappa_1 + \zeta_3 \bar{\omega}) \quad (\text{C.10})$$

$$=: \frac{N}{D} Q, \quad (\text{C.11})$$

where $\zeta_j = t_j - r_j$ for $j = 1, 2, 3$. Then

$$T \approx \frac{NQ}{\sqrt{N^2 Q^2 + D^2}}. \quad (\text{C.12})$$

If $\kappa_2 = 0$ identically, then this reduces to the same formula found in the two-dimensional reduction of the problem (Shipman and Venakides (2005)).

If symmetries of the problem cause some of the coefficients to have simple forms, we may find further relations between them. For example:

(6) Suppose that c_{11}, c_{12}, c_{22} are real. Then, if we allow κ, ω to tend to zero along a path on which $\kappa_2 = \kappa_1^2$, and all first- and second- order terms of l cancel (in the previous point only the first-order terms cancel), then what remains of $|l|^2$ will be $O(\kappa_1^6)$. The quadratic and quartic terms of $|r|^2$ and $|t|^2$ must also vanish, then, which requires that $\rho_{11} = \tau_{11} = c_{11}$. Repeating the process with $\kappa_1 = \kappa_2^2$, and then finally with $\kappa_1 = \kappa_2$, tells us also that $\rho_{22} = \tau_{22} = c_{22}$, and $\rho_{12} = \tau_{12} = c_{12}$.

(7) If $c_1 = c_2 = 0$, the $\bar{\omega}\kappa_j^2$ terms, $j = 1, 2$, give $Re(c_{jj})l_0^2 = Re(\rho_{jj})r_0^2 + Re(\tau_{jj})t_0^2$.

(8) If $c_1 = c_2 = 0$, the $\bar{\omega}\kappa_1\kappa_2$ terms give $Re(c_{12})l_0^2 = Re(\rho_{12})r_0^2 + Re(\tau_{12})t_0^2$.

(9) If $c_1 = 0$, the κ_1^4 terms give $|c_{11}|^2l_0^2 = |\rho_{11}|^2r_0^2 + |\tau_{11}|^2t_0^2$. The same holds replacing all 1 and 11 indices by 2 and 22.

Bibliography

- Abramowitz, M. and Stegun, I. (1964), *Handbook of mathematical functions with formulas, graphs, and mathematical tables*, Dover Publications.
- Bethe, H. A. (1944), “Theory of diffraction by small holes,” *Phys. Rev.*, 66, 163–182.
- Chen, C.-C. (1970), “Transmission through a conducting screen perforated periodically with apertures,” *IEEE Trans. on Mic. Theory and Tech.*, MTT-18, 627–632.
- Chen, C.-C. (1971), “Diffraction of electromagnetic waves by a conducting screen perforated periodically with circular holes,” *IEEE Trans. on Mic. Theory and Tech.*, MTT-19, 475–481.
- Chen, C.-C. (1973), “Transmission of microwave through perforated flat plates of finite thickness,” *IEEE Trans. on Mic. Theory and Tech.*, MTT-21, 1–6.
- Ebbesen, T. W., Lezec, H. J., Ghaemi, H. F., Thio, T., and Woff, P. A. (1998), “Extraordinary optical transmission through sub-wavelength hole arrays,” *Nature*, 391, 667–669.
- García-Vidal, F. J., Martín-Moreno, ., Moreno, E., Kumar, L. K. S., and Gordon, R. (2006), “Transmission of light through a single rectangular hole in a real metal,” *Phys. Rev. B*, 74.
- Hou, B., Hang, Z. H., Wen, W., Chan, C. T., and Sheng, P. (2006), “Microwave transmission through metallic hole arrays: Surface electric field measurements,” *App. Phys. Lett.*, 89.
- Jackson, A. D., Huang, D., Gauthier, D., and Venakides, S. (2012), “Importance of conductivity, periodicity and collimation in a model for transmission of energy through sub-wavelength, periodically arranged holes in a metal film,” *Submitted 2012*.
- Jackson, J. D. (1999), *Classical Electrodynamics*, John Wiley & Sons, Inc., New York.
- Kuchment, P. (1993), *Floquet theory for partial differential equations*, Birkhauser Verlag.

- Martín-Moreno, L. and García-Vidal, F. J. (2004), “Optical transmission through circular hole arrays in optically thick metal films,” *Opt. Express*, 12, 3619–3628.
- Martín-Moreno, L. and García-Vidal, F. J. (2008), “Minimal model for optical transmission through holey metal films,” *J. Phys.: Condens. Matter*, 78.
- Medina, F., Mesa, F., and Marques, R. (2008), “Extraordinary transmission through arrays of electrically small holes from a circuit theory perspective,” *IEEE Trans. Mic. Th. Tech.*, 56, 3108–3120.
- Nikitin, A. Y., Zueco, D., García-Vidal, F. J., and Martín-Moreno, L. (2008), “Electromagnetic wave transmission through a small hole in a perfect electric conductor of finite thickness,” *Phys. Rev. B*, 78.
- Przybilla, F., Degiron, A., Genet, C., Ebbesen, T. W., de Leon-Perez, F., Bravo-Abad, J., García-Vidal, F., and Martín-Moreno, L. (2008), “Efficiency and finite size effects in enhanced transmission through subwavelength apertures,” *Opt. Express*, 16, 9571–9579.
- Rayleigh, L. (1907), “Note on the remarkable case of diffraction spectra described by Prof. Wood,” *Phil. Mag. Series 6*, 14:79, 60–65.
- Shipman, S. P. and Venakides, S. (2005), “Resonant transmission near nonrobust periodic slab modes,” *Phys. Rev. E*, 71.
- Snitzer, E. (1961), “Cylindrical dielectric waveguide modes,” *J. Opt. Soc. Am.*, 51, 491–498.
- Snyder, A. W. and Love, J. D. (1983), *Optical Waveguide Theory*, Kluwer Academic Publishers, London.
- Takakura, Y. (2001), “Optical resonance in a narrow slit in a thick metallic screen,” *Physical Review Letters*, 86, 5601–5603.
- Ung, B. and Sheng, Y. (2007), “Interference of surface waves in a metallic nanoslit,” *Opt. Express*, 15, 1182–1190.
- Wood, R. W. (1902), “On a remarkable case of uneven distribution of light in a diffraction grating spectrum,” *Phil. Mag. Series 6*, 4:21, 396–402.

Biography

Aaron David Jackson was born November 15, 1984 in San Diego. He has earned a Bachelor of Science degree in mathematics and a Bachelor of Arts degree in music from Northern Arizona University, and a doctorate in mathematics from Duke University. He is the subject of the book *The Unauthorized Biography of a Western Superhero* by Anne McCaffrey. He currently teaches mathematics and I Liq Chuan; is in training for a professional rugby team; and is a board member along with his sister at the Lily Jackson Institute of Science.

Primary findings in this work are undergoing journal submission, reference Jackson et al. (2012).